Ababa University Office Addis of Research and Graduate Programs

College of Natural and Computational Sciences

Department of Chemistry

Syntheses of 7-fluoro-6-(thiophen-2-yl)-4H-thieno[3,2-b]indole-based polymers

By: Asaminew Yerango

Advisor: Prof. Wendimagegn Mammo

A Thesis Submitted to the Department of Chemistry, Office of Research and Graduate Programs of Addis Ababa University, in Partial Fulfillment of the Requirements for the Degree of Master of Science in Chemistry.

July 2020

Declaration

I, the undersigned, declare that this MSc thesis is my original work and has not been presented for any degree in any other university and that all sources of materials used for this project have been duly acknowledged.

Name: **Asaminew Yerango**

Signature: ——————————

This MSc. thesis has been submitted for examination with my approval as a university advisor.

Name: **Prof. Wendimagegn Mammo**

Signature: ——————————

Date and place of submission: Department of Chemistry

Addis Ababa University

June 2020

Addis Ababa University

College of Natural and Computational Sciences

Department of Chemistry

Syntheses of 7-fluoro-6-(thiophen-2-yl)-4*H*-thieno[3,2-*b*]indole-based polymers

By Asaminew Yerango

Approved by the Examining Board:	Signature	Date
1. Prof. Wendimagegn Mammo Advisor	_____	_____
2. Dr. Estifanos Ele Examiner	_____	_____
3. Dr. Mekonnen Abebayehu Examiner	_____	_____
4. Dr. Negash Getachew Chairman, Department of Chemistry	_____	_____

Acknowledgments

I thank my supervisor Prof. Wendimagegn Mammo for his wonderful advising and encouragement. I would also like to appreciate him so much for his superb knowledge, fatherly approach, kindness, great patience and excellent character.

I also thank Dr Yonas Chebude allowing me to use his Lab to run FTIR of my samples and Prof. Shimelis Admassie allowing me to run UV-Vis and CV in his lab.

I am grateful for Dr Asfaw Negash for his kindly help in running UV-Vis and CV experiment, Dr Birhan Alkadir, Melaku Assefa and Yohannis Meaza for technical, moral support and brotherly approach we had.

I appreciate the AAU (Chemistry Department) for giving chance and covering my tuition, so that I could pursue my MSc in this prestigious university.

Last but not least, my gratitude extends out to all Chemistry Department staff members for their kind encouragement and my families for their best wishes and moral support.

Table of Contents

List of Figures

List of Schemes

List of Tables

List of Appendices

List of abbreviations

D	Donor
A	Acceptor
BHJ	Bulk heterojunction
^{1}H NMR	Proton nuclear magnetic resonance
^{13}C- NMR	Carbon-13 nuclear magnetic resonance
$CDCl_3$	Deuterated chloroform
CD_2Cl_2	Deuterated dichloromethane
DCM	Dichloromethane
NBS	*N*-bromosuccinimide
o-DCB	*ortho*-dichlorobenzene
THF	Tetrahydrofuran
s	Singlet
d	Doublet
dd	Doublet of doublets
ddd	Doublet of doublet of doublets
dt	Doublet of triplets
t	Triplet
m	Multiplet
DEPT	Distortionless Enhancement by Polarization Transfer
DMF	*N*,*N*-Dimethylformamide
E_g^{opt}	Optical band gap
PCE	Power conversion efficiency
FF	Fill factor

V_{OC}	Open circuit voltage
J_{SC}	Short circuit current density
h	Hour
HOMO	Highest occupied molecular orbital
LUMO	Lowest unoccupied molecular orbital
Hz	Hertz
ppm	Parts per million
δ	Chemical shift unit
ICT	Intramolecular charge transfer
J	Coupling constant
OPV	Organic photovoltaic
OSC	Organic solar cell
P(*o*-tolyl)$_3$	Tri(*o*-tolyl)phosphine
$Pd_2(dba)_3$	Tris(dibenzylideneacetone)dipalladium(0)
rt	Room temperature
UV-Vis	Ultraviolet-visible
CV	Cyclic voltammetry

Abstract

Four high band gap donor polymers and one medium band gap terpolymer were synthesized using 2-bromo-6-(5-bromothiophen-2-yl)-4-(2-ethylhexyl)-7-fluoro-4*H*-thieno[3,2-*b*]indole (**34**), 2-bromo-6-(5-bromothiophen-2-yl)-7-fluoro-4-octyl-4*H*-thieno[3,2-*b*]indole (**36**), 2-bromo-6-(5-bromothiophen-2-yl)-4-decyl-7-fluoro-4*H*-thieno[3,2-*b*]indole (**38**), 2-bromo-6-(5-bromothiophen-2-yl)-7-fluoro-4-(2-(2-methoxyethoxy)ethyl)-4*H*-thieno[3,2-*b*]indole (**43**) , (4,8-bis(4,5-dioctylthiophen-2-yl)benzo[1,2-*b*:5,4-*b'*]dithiophene-2,6-diyl)bis(trimethyl-stannane)(**44**) as electron donors and 4,7-dibromo-5,6-difluorobenzo[*c*][1,2,5]thiadiazole (**45**) as electron acceptor, by using the Stille polymerization reaction. These polymers have good solubility in chloroform and were characterized by using UV-Vis spectroscopy and cyclic voltammetry. All monomers and intermediate compounds were characterized by using infrared and NMR spectroscopy.

1. Introduction

Fossil fuels such as coal, oil, and gas are the most used energy sources. The production and use of fossil fuels causes a number of environmental problems, besides, the fossil fuel reserves are being depleted at a very fast rate. Thus, the need to develop renewable energy sources has become urgent. The development of photovoltaic (PV) cells, which transform inexhaustible solar energy into electricity, is therefore one of the promising long term solutions for clean, renewable energy. The main limitation of the PV technology has been the high cost of silicon-based solar cells. Organic photovoltaics (OPV)s are promising cost-effective alternatives to silicon-based solar cells, and possess low cost, light weight, and flexibility advantage.[1] Currently, research in OPV is mainly focused on bulk heterojunction (BHJ)-based devices, which involve a blend layer of electron donor (polymers or small molecules) and electron acceptor (fullerene or non-fullerene derivatives) materials generally used as an active layer, that have attracted and received great attention in the scientific community.[2]

As shown in **Figure1**, the general working principle in BHJ organic solar cells first involves the photo-excitation of the donor material by the absorption of light energy to generate excitons. The excitons diffuse to the donor-acceptor (D-A) interface where exciton dissociation occurs via an electron-transfer process. The fully separated free charge carriers are transported to the respective electrodes in opposite directions with the aid of the internal electric field, which in turn generates the photocurrent and photovoltage.[3, 4]

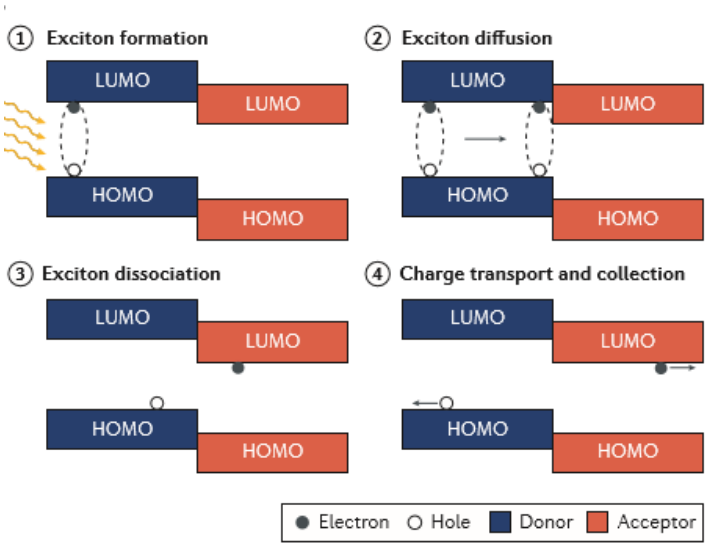

Figure 1. The working mechanism of a BHJ organic solar cell.

2. Basic Parameters Used to Characterize OPVs

The performance of a solar cell is evaluated by its power conversion efficiency (PCE) which is the product of open circuit voltage (V_{oc}), short circuit current (J_{sc}) and fill factor (FF). Open circuit voltage (V_{oc}) is related with the difference between the highest occupied molecular orbital (HOMO) of the donor polymer and lowest unoccupied molecular orbital (LUMO) of the acceptor.[5] To maximize V_{oc}, the donor molecule should have low-lying HOMO or the acceptor molecule should have high-lying LUMO. On the other hand J_{sc} is related with the absorption of the active layer (donor:acceptor) in the solar spectrum. If the active layer absorbs light broadly and intensely, J_{sc} will be high. For this purpose the donor and acceptor should absorb complementarily at longer wavelength to maximize the photons that could be harvested. This leads to achieve high J_{sc} due to high absorption ranges in the solar spectrum. In general, to increase PCE, materials should have broad and strong absorption bands for good light harvesting, favorable energy difference (band gap) between the HOMO and the LUMO for efficient charge separation, and high hole and electron mobility for efficient charge transport.

3. Literature Review

The most widely studied architecture of organic solar cells (OSCs) is the donor-acceptor BHJ structure, consisting of a photoactive conjugated polymer and a fullerene derivative.[6] In general, to produce efficient OPVs, one needs donor and acceptor materials with high charge-carrier mobility, complementary absorption bands in the Vis-NIR range, and a small energy offset to minimize voltage losses.[7] To date, PCE above 18% has been reached in single-junction OSC due to complementary absorption of donor and acceptor materials.[8] The PCEs of PSCs can be improved by synthesizing novel donor and acceptor materials with increased light absorption and optimized morphology of the active layer. The donor materials should provide broad absorption range with low band gap, deep HOMO energy level and high mobility of charge carriers.[9, 10] In accordance with the above requirements, a large number of donor materials have been developed. Donor–acceptor (D–A) conjugated polymers have dominated the library of donor materials for OSCs because their intrinsic optical and electronic properties can be readily tuned by controlling the intramolecular charge transfer (ICT) from donor unit to acceptor unit.[11] Among all the reported D–A donor materials, the

carbazole-based polymer, poly-(2,7-carbazole-*alt*-dithienylbenzothiadiazole) (PCDTBT) (**Figure 2**), is one excellent parent structure with a low-lying HOMO of –5.45 eV, showing outstanding stability against oxidation at high temperatures and feasible synthesis.[10] In 2007, Leclerc *et al.* reported that the PSCs based on a blend of PCDTBT and PCBM delivered a PCE of 3.6%.[12] Since PCDTBT suffers from large optical band gap that limits its light-harvesting ability, HXS-1 was developed by introducing octyloxy groups on the electron-withdrawing 4,7-bis(2-thienyl)-2,1,3-benzothiadiazole (DTBT) unit and exhibited a PCE of 5.4%, but had poor solubility.[13] To improve the solubility, PCDTBT-8 was synthesized by replacing the straight *N*-octyl chain on the carbazole unit with the branched heptadecyl side chain, and displayed a PCE of 4.22% despite the fact that PCDTBT-8 has a wider band gap than PCDTBT.[14]

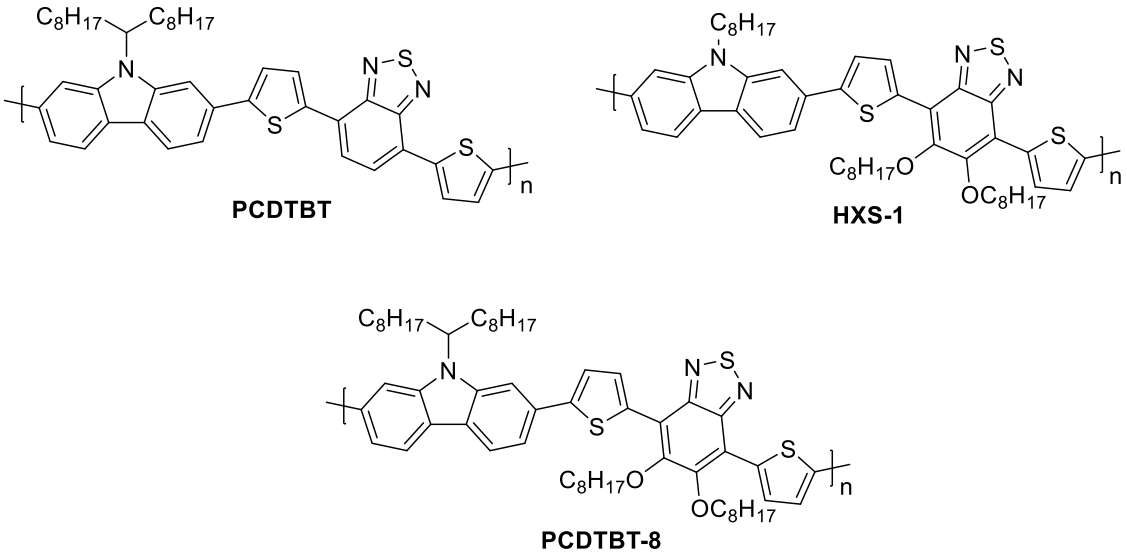

Figure 2. Chemical structures of PCDTBT and its analogues.

The inherent disadvantages of PCDTBT, such as slightly limited absorption range and relatively low carrier mobility led to mediocre J_{sc} values. In order to further optimize its light-harvesting and charge-transporting ability, various PCDTBT-based structural derivatives, such as ladder-type PCDTBT and naphthothiadiazole and selenophene analogues of PCDTBT were developed (**Figure 3**). However, the resulting polymers did not yield devices with correspondingly high performances. The introduction of fluorine atoms onto conjugated polymer backbones has been proven to be an effective way to enhance the efficiency of BHJ solar cells by lowering of the polymer HOMO energy level as well as the possible formation of the secondary bonding (C−F···H, F··· S, and C−F···πF) through inter- or intramolecular interactions.[15, 16, 20] Yang *et al.*[15] reported PCDTFBT and PCDT2FBT (**Figure 3**), variations

on PCDTBT with incorporation of F atoms on the DTBT unit, leading to high V_{oc} values yet moderate PCEs.

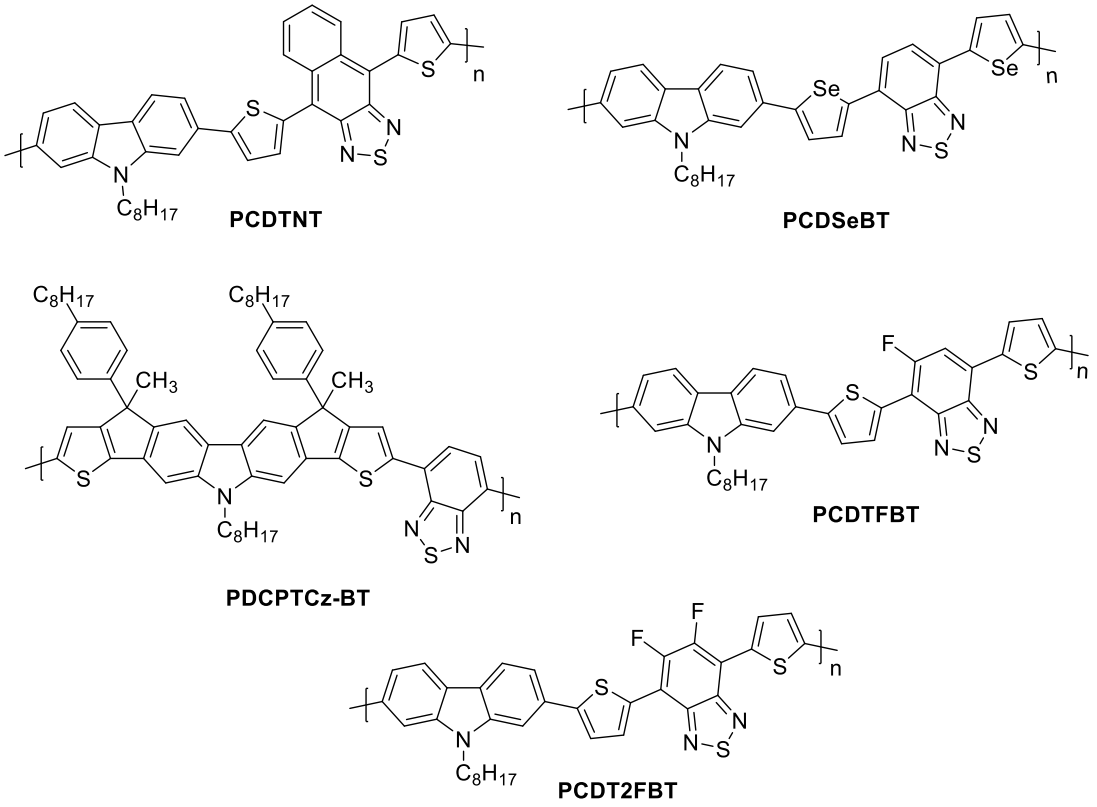

Figure 3. Chemical structures of PCDTBT-derivatives.

Inspired by the advantages of carbazole-based PCDTBT analogues and dithienopyrrole (DTP)-based polymers, Huang *et al.*[11] reported thieno[3,2-*b*]indole (TI), structurally merged by a carbazole unit and a DTP unit, for novel D–A conjugated polymers. They reported three polymers based on TI and DTBT derivatives as the structural analogues of PCDTBT (**Figure** 4). The *N*-alkyl-TI unit was copolymerized with electron-deficient DTBT to afford a new alternating D–A polymer **P1**, but with a poor solubility that led to low number average molecular weight (M_n). To further improve solubility and molecular weights, hexyl side chain was attached onto the TI moiety to produce **P2.** Furthermore, octyloxy groups were incorporated onto and the electron-deficient DTBT unit to prepare **P3**. These structural modifications resulted in profound effects on the physical properties of the polymers and their performances in solar cell devices. The optimized device based on **P3**:$PC_{71}BM$ with a relatively higher mobility gave the best photovoltaic performance with a PCE of 2.73%. These results suggest that the electron-rich TI unit is a promising donor unit for designing D–A conjugated polymers for OSCs.

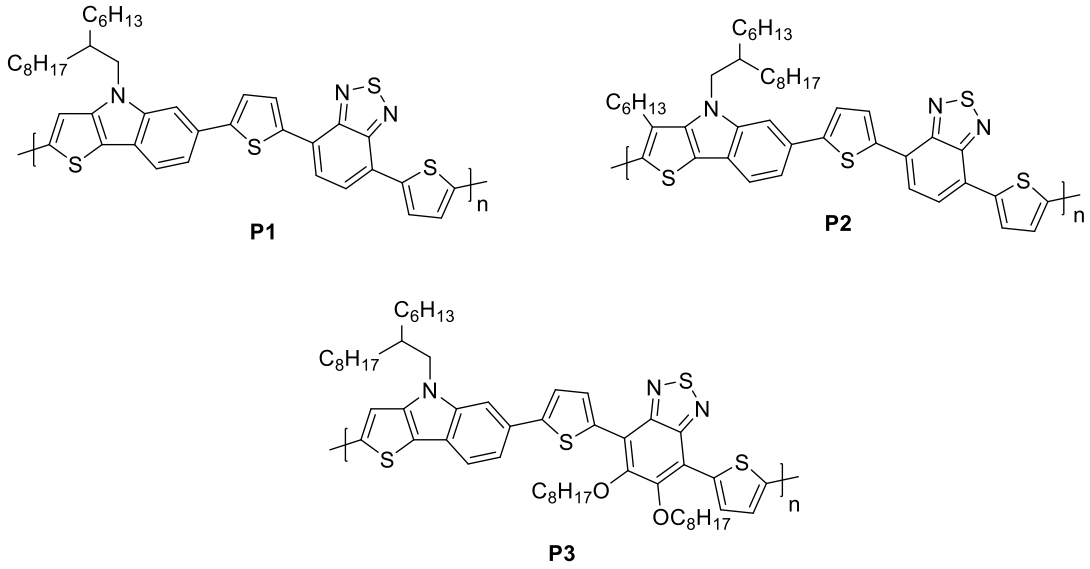

Figure 4. Chemical structures of **P1**, **P2** and **P3**.

The syntheses of TI-based monomers and polymers are depicted in **Scheme**s **1** and **2**, respectively. Both 2-(4-bromo-2-nitrophenyl)thiophene (**2**) and 2-(4-bromo-2-nitrophenyl)-4-hexylthiophene (**6**) were synthesized via Suzuki coupling reactions using $Pd(PPh_3)_4$ as catalyst in 73% and 83% yields, respectively, starting from dibromo-2-nitrobenzene (**1**). 6-Bromo-4*H*-thieno[3,2-*b*]indole (**3**) and 6-bromo-3-hexyl-4*H*-thieno[3,2-*b*]indole (**7**) were obtained through reductive Cadogan cyclization. Alkylation of compounds **3** and **7** with 1-bromo-2-hexyldecane using KOH as base, KI as catalyst and THF as the solvent, afforded 6-bromo-4-(2-hexyldecyl)-4*H*-thieno[3,2-*b*]indole (**4**) and 6-bromo-3-hexyl-4-(2-hexyldecyl)-4*H*-thieno[3,2-*b*]indole (**8**), respectively. Subsequent bromination of compounds **4** and **8** with NBS gave 2,6-dibromo-4-(2-hexyldecyl)-4*H*-thieno[3,2-*b*]indole (**5**) and 2,6-dibromo-3-hexyl-4-(2-hexyldecyl)-4*H*-thieno[3,2-*b*]indole (**M2**), respectively. 4-(2-Hexyldecyl)-2,6-bis(4,4,5,5-tetramethyl-1,3,2-dioxaborolan-2-yl)-4*H*-thieno[3,2-*b*]indole (**M1**) was synthesized from compound **5** and bis(pinacolato)diboron by using $PdCl_2$(dppf) as catalyst.

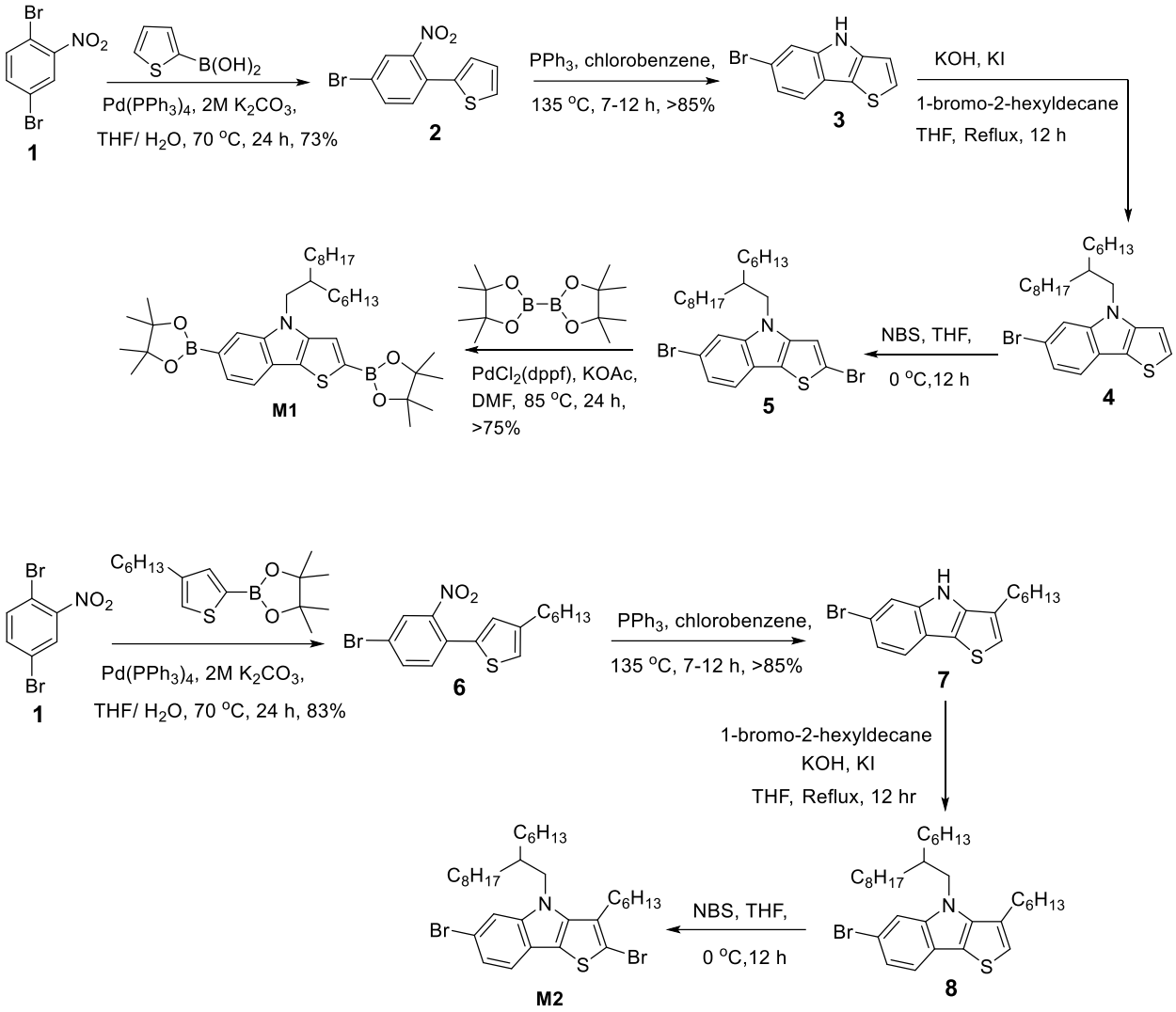

Scheme 1. Preparation of monomers **M1** and **M2**.

The polymers **P1** and **P3** were synthesized by Suzuki polycondensation reaction using $Pd(PPh_3)_4$ as the catalyst in toluene. On the other hand, the copolymer **P2** was obtained by Stille coupling polymerization using $Pd_2(dba)_3$ as catalyst and P(*o*-tolyl)$_3$ as ligand in toluene as shown in **Scheme 2** .

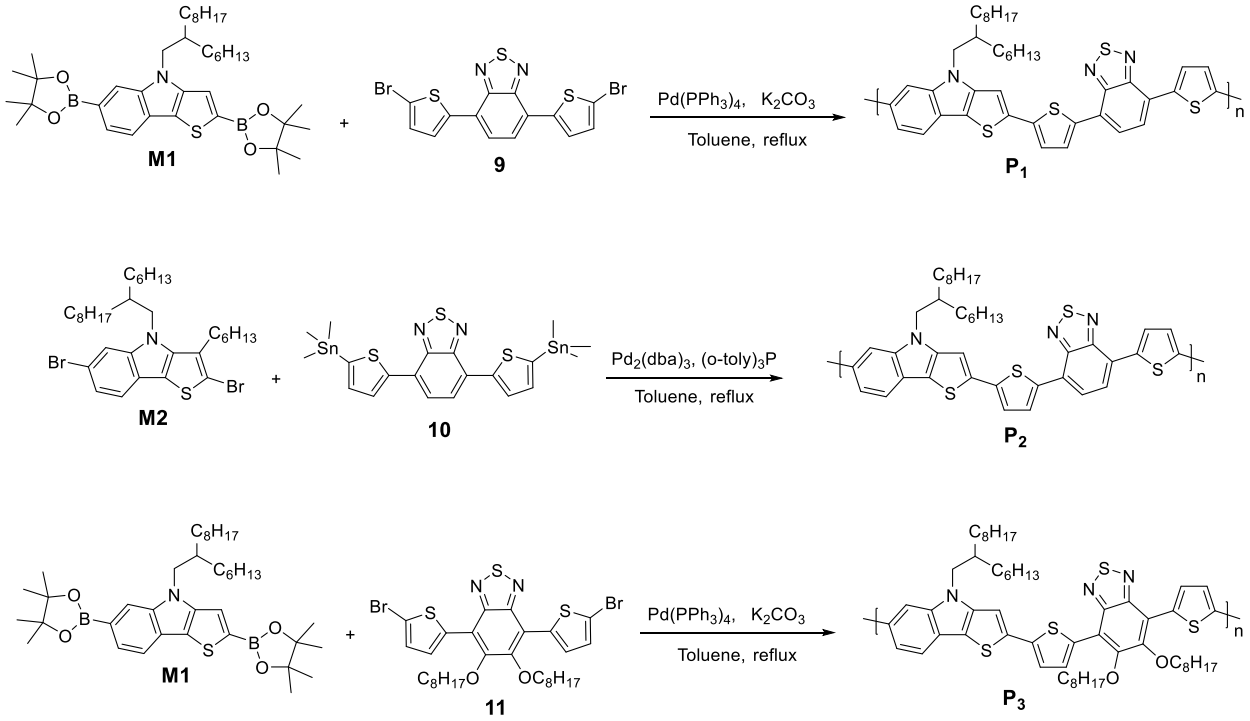

Scheme 2. Preparation of polymers **P1** – **P3**.

The normalized ultraviolet-visible (UV-Vis) absorption spectra of **P1**, **P2** and **P3** in dilute chloroform solutions (*ca* 10^{-5} M) and as thin films on glass slides were investigated. **P1** and **P2** displayed two distinct absorption maxima both in solution and in the solid state. One absorption maximum occurs at the shorter wavelength region (350–500 nm) corresponding to π–π electron transition of the donor units, and the other absorption maximum at the longer wavelength region (500–800 nm) due to ICT from the donor units to the acceptor units. The thin film absorption spectra of all polymers exhibited much red-shifted absorption maxima compared to the spectra in chloroform solution demonstrating an effective interchain π–π stacking in the solid state. The optical band gaps obtained from the onsets of absorption are 1.57, 1.70 and 1.77 eV for **P1**, P2 and **P3**, respectively.

The frontier molecular orbital energy levels of the polymers were determined by cyclic voltammetry. The onsets of oxidation (E^{ox}_{onset}) of the polymers **P1**, **P2** and **P3** were estimated to be 0.37, 0.42 and 0.52 V, corresponding to HOMO energy levels of -5.17, -5.22 and -5.32 eV, respectively, which suggests that all polymers have good air stability for applications in OSCs. The onsets of reduction (E^{red}_{onset}) of **P1**, **P2** and **P3** were estimated to be -1.08, -1.13 and -1.11 V, corresponding to LUMO energy levels of -3.72, -3.67 and -3.69 eV, respectively.

The photovoltaic performances of the polymers were investigated in BHJ devices with a conventional configuration of glass/ITO/PEDOT:PSS/polymer:$PC_{71}BM$/Ca/Al. The PCEs of the OSCs were optimized by changing the D/A ratio, thermal annealing treatment and additives. The optimized weight ratios of polymer to $PC_{71}BM$ were 1:3 for **P1**, and 1:4 for **P2** and **P3**. **P1** showed the best results when devices were annealed at 80 ^oC while polymers **P2** and **P3** offered the best PCEs when devices were annealed at 150 ^oC and 25 ^oC, respectively. Solar cells based on **P1**:$PC_{71}BM$ blend spin-coated from chlorobenzene (CB) gave a PCE of 1.79% while **P2**-based devices showed poor PV performance with a PCE of only 0.53% suggesting that the hexyl side-chains suppress inter-chain stacking and reduce the charge transport property. The best PV performances were recorded by **P3**-based solar cells where PCE of 2.7% was obtained.

In 2015 H. Suh *et al.*[30] reported 6-(2-thienyl)-4*H*-thieno[3,2-*b*]indole (TTI) as electron donating unit in D-A conjugated OSCs. They prepared conjugated copolymers **(P4-P5)** utilizing 6-(2-thienyl)-4*H*-thieno[3,2-*b*]indole (TTI) as electron donor and 4,7-bis(4-hexylthiophen-2-yl)2,1,3-benzothiadiazole (**18**) and 2-dimethyl-4,7-di(2-thienyl)2*H*-benzimidazole (**19**) as electron acceptor and studied their applications in OSCs. TTI-based compounds were prepared by incorporating thiophene onto 4*H*-thieno[3,2-*b*]indole (TI) as shown in **Scheme 3.** It was shown that the substitution of six-membered benzene ring of the carbazole with electron rich five-membered thiophene ring improved light harvesting ability and ICT and lowered the band gap of the polymers due to high planarity between electron donor and acceptor units

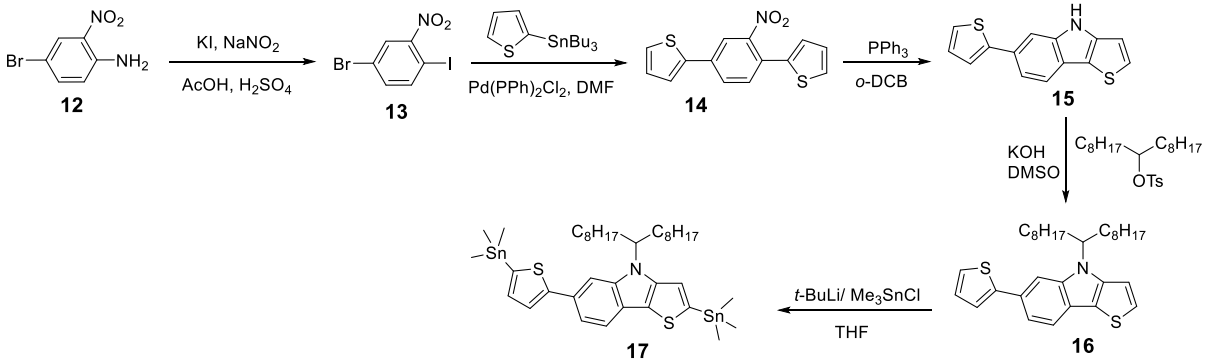

Scheme 3. Synthetic route towards monomer **17**.

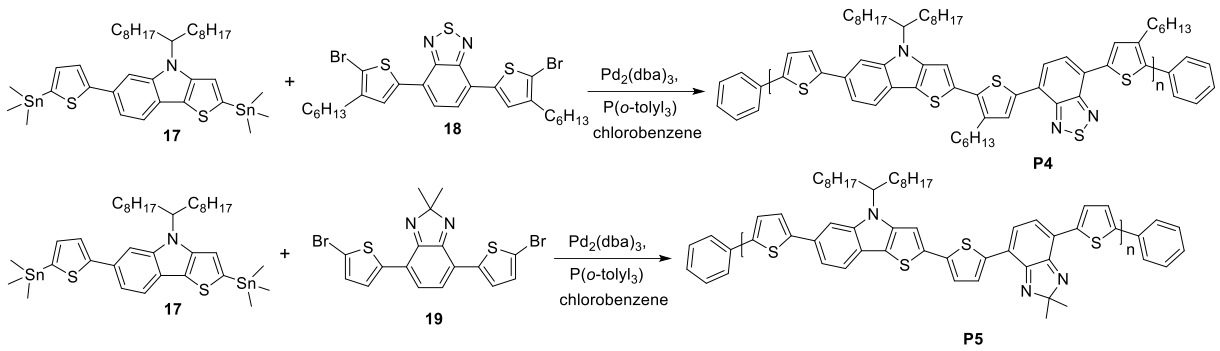

Scheme 4. Preparation of **P4** and **P5**

The UV-Vis absorption spectra of the **P4** and **P5** were recorded in chloroform solution and as thin films. The solution spectra of **P4** showed two absorption maxima at 409 and 561 nm and the thin film spectra showed two absorption maxima at 423 and 594 nm. The solution spectra of **P5** revealed two strong absorption maxima at 459 and 720 nm and thin film spectra at 446 and 682 nm. The absorptions in the short-wavelength region are due to π-π transition in the polymer main chains and the maxima in the long-wavelength range are attributed to ICT between electron donor and acceptor units. The optical band gaps obtained from the absorption onsets were 1.69 and 1.46 for **P4** and **P5**, respectively. The cyclic voltammetry was used to estimate the HOMO/LUMO energy levels of **P4** and **P5** to be -5.31/-3.66 and -5.20/-3.77, respectively. The PV performances of polymers were studied using conventional OSCs with an architecture of ITO/PEDOT**:**PSS/polymer:$PC_{71}BM$/Al with different donor: acceptor ratio in CB and *o*-DCB solution. A device made of **P4**: PC71BM (1:3) in *o*-DCB gave PCEs of 2.70% with V_{OC} of 0.79 V, J_{SC} of 7.68 mA/cm^2, and FF of 44%. When CB used as solvent, the device showed PCE of 3.14% with V_{OC} of 0.81 V, J_{SC} of 8.19 mA/cm^2, and FF of 47%. With 1,8-octanedithiol (ODT) as additive the PCE was improved to 3.35% with slightly increased FF (51%) and same V_{OC} (0.81 V) and J_{SC} (8.19 mA/cm^2) values. The device fabricated using **P5**:$PC_{71}BM$ (1:1) in CB revealed PCE of 0.76% with V_{OC} of 0.58 V, J_{SC} of 2.75 mA/cm^2 and FF of 48%. Despite the slightly lowered V_{OC} (0.57 V) and FF (40%) values, the device based on the blend of **P5**:$PC_{71}BM$ in *o*-DCB solvent showed an improved PCE (1.44%) with increased J_{SC} (6.36 mA/cm^2).

In 2016 Jeong *et al.*[9] reported copolymers (**P6**-**P7**) using 6-(2-thienyl)-4*H*-thieno[3,2-*b*]indole (TTI) as an electron-donating unit and 2,1,3-benzothiadiazole and 2,2-dimethyl-2*H*-benzimidazole as electron-withdrawing units. The TTI-based monomer **17** was copolymerized with 4,7-dibromobenzo[2,1,3]thiadiazole (**20**) and 4,7-dibromo-2,2-dimethyl-

2*H*-benzo[*d*]imidazole (**21**) as depicted in **Schemes 5**, for efficient ICT effect to generate low band gap polymers. It was rationalized that the replacement of the six-membered benzene ring in carbazole by the five-membered thiophene ring in TI will improve electron-donating ability and enhance planarity as a result of the lower steric hindrance caused by the thiophene ring. The donor-acceptor conjugated polymers **P6** and **P7** (**Scheme 5**) showed good solubility in various organic solvents.

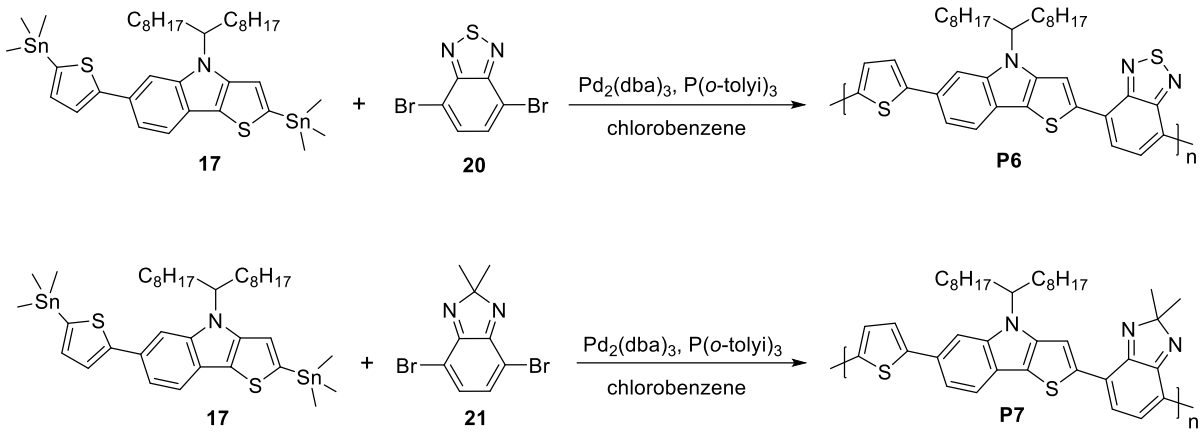

Scheme 5. Synthetic route towards the synthesis of polymers **P6** and **P7**.

The UV–Vis absorption spectra of **P6** and **P7** were recorded in *o*-dichlorobenzene (*o*-DCB) solution and as thin films. The solution spectra of **P6** and **P7** showed two major absorption maxima at 396 and 622 nm and 395 and 665 nm, respectively. The long wavelength absorption maxima in the thin film spectra of **P6** and **P7** were red–shifted to 650 and 688 nm, respectively. **P7** had a wider absorption range with a lower band gap than **P6**. The absorptions in the short-wavelength region are due to π-π transition in the polymer main chains and the maxima in the long-wavelength range are attributed to ICT between electron donor and acceptor units. The optical band gaps of **P6** and **P7** were 1.68 and 1.54, respectively, as estimated from the onsets of absorption of the thin films. Cyclic voltammetry was used to estimate the HOMO energy levels of **P6** and **P7** to be -5.32 and -5.29 eV, and LUMO energy levels to be -3.50 and -3.61, respectively. The HOMO energy levels of **P6** and **P7** have quite similar values, but the LUMO energy level of **P7** is lower than that of **P6**. The PV performances of **P6** and **P7** were investigated using conventional OSCs with an architecture of ITO/PEDOT**:**PSS/polymer:$PC_{71}BM$/Al, and maximum PCEs of 0.85 and 2.60%, respectively, were obtained.[9] **P7** has broader absorption with lower band gap for

better coverage of the solar spectrum, higher mobility to provide increased FF, and better RMS values of the morphology to improve the J_{SC}, giving a higher PCE than **P6**.[18, 19]

In 2017 Jeong *et al.*[29] prepared D-A copolymers (**P8**-**P9**) based on 6-(2-thienyl)-4*H*-thieno[3,2-*b*]indole (TTI) as an electron donor and fluorinated DTBT as an electron acceptor for OSC applications. It has been shown that the TTI moiety has good hole-transporting property, electron-donating ability and planarity and contributes to ICT effect and high J_{SC} in OSC devices.[10,11,30,31] Besides, the incorporation of the electronegative fluorine atom in polymer backbone results in lowering the energies of both the HOMO and the LUMO contributing to large *Voc* values of BHJ OSCs.[32, 33]

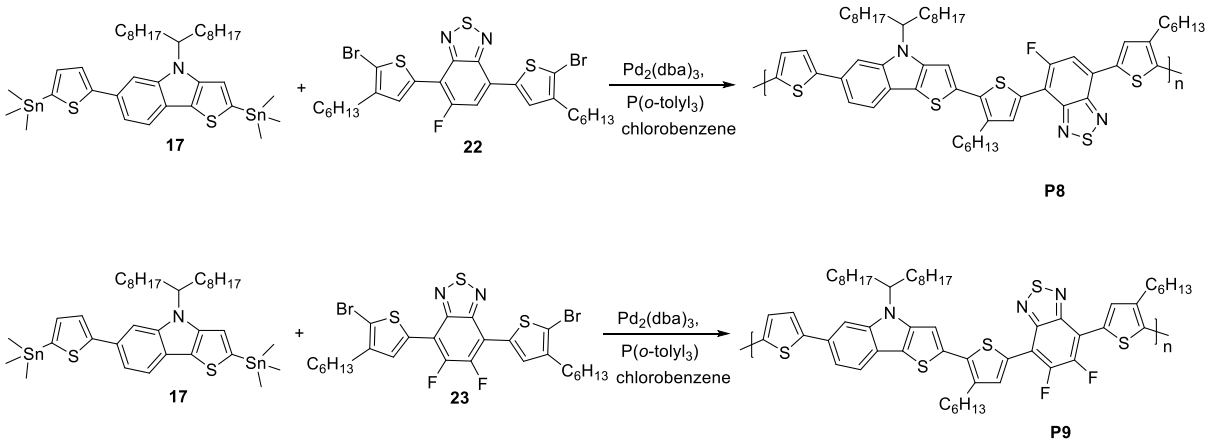

Scheme 6. Synthesis of **P8** and **P9**

Both **P8** and **P9** showed similar UV-Vis absorption spectra. The thin film absorption spectra of **P8** and **P9** showed red-shift absorption maxima compared to the spectra in solution indicating improved molecular packing and π-π stacking in the solid state. The optical band gaps calculated from the onsets of absorption of thin films of **P8** and **P9** were 1.68 and 1.66 eV, respectively. The HOMO/LUMO energy levels of **P8** and **P9**, were estimated from cyclic voltammetric studies to be -5.69/-4.01 and -5.76/-4.10 eV, respectively. The introduction of electronegative fluorine atom contributed to the deepening of the HOMO energy levels of both polymers. Fullerene-based BHJ OSCs were fabricated from **P8** and **P9** with the conventional device architecture, ITO/PEDOT:PSS/polymers:$PC_{71}BM$/Al. The OSCs were optimized by varying polymer:$PC_{71}BM$ ratios, thickness of the active layers and by using of various additives. The device based on **P8**:$PC_{71}BM$ with 1:2 ratio showed a PCE of 2.44%

with the highest V_{OC} of 0.83 V, a J_{SC} of 7.38 mA cm^{-2} and a *FF* of 40.0%. When **P8**:PC$_{71}$BM blend films were treated with additives such as DIO and CN the device performances were negatively affected. However, when 1,1-diphenylethylene (DPE) used as an additive, the PCE was increased to 2.83% with a FF of 42.4%, an increased J_{SC} of 8.33 mA cm^{-2} and a slightly decreased V_{OC} value of 0.80 V. The device fabricated from **P9**:PC$_{71}$BM with 1:1 ratio exhibited a PCE of 3.71% with a V_{OC} of 0.76 V, a J_{SC} of 8.87 mAcm^{-2} and a *FF* of 55.2%. Addition of DIO and DPE had negative effects on the device performances, but, with CN as an additive additive, the highest PCE of 4.36% was obtained with improved *FF* (57.1%) and J_{SC} (10.0 mA cm^{-2}) and a V_{OC} of 0.76 V.

In 2015 H. Suh *et al.*[30] prepared conjugated D-A copolymer utilizing 6-(2-thienyl)-4*H*-thieno[3,2-*b*]indole (TTI) as electron donor and 3,6-di(2-thienyl)-2,5dihydropyrrolo[3,4-*c*]pyrrole-1,4-dione (DPP) as electron acceptor and studied its applications in OSCs.

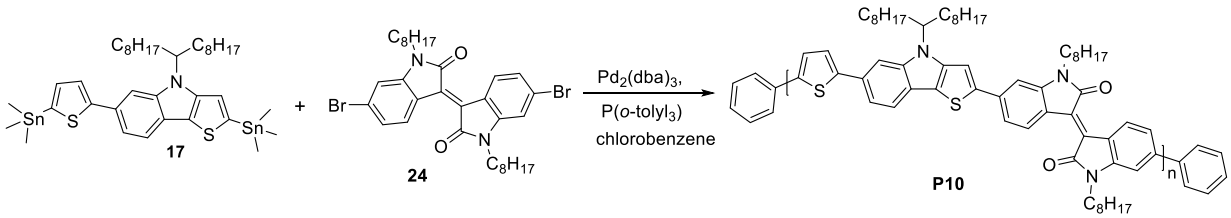

Scheme 7. Synthetic route towards polymer **P10**

The UV-Vis absorption spectrum of the **P10** was recorded in chloroform solution and as thin films. The solution absorption spectra of **P10** appeared at 418 and 697 nm and the thin films were observed at 430 and 759 nm. The optical band gap obtained from the absorption onset was 1.31. The HOMO and LUMO energy level estimated from CV analysis was -5.09 and -3.71 eV, respectively. The PV performance of the **P10** was studied using conventional OSCs with an architecture of ITO/PEDOT**:**PSS/polymer:PC$_{71}$BM/Al in CB and *o*-DCB solution. Device based on the blend of **P10**: PC71BM (1:1) in CB exhibited a PCE of 1.0% with V_{OC} of 0.49 V, J_{SC} of 4.85 mA/cm^2, and FF of 42%. When *o*-DCB used as solvent, PCE was improved to 1.30% with V_{OC} of 0.49 V, J_{SC} of 6.01 mA/cm^2, and FF of 44%. When poly difunctional polyglycidyl epoxide (DPE) is used as additive, the device gave PCE of 1.33% with V_{OC} of 0.45 V, J_{SC} of 7.08 mA/cm^2 and FF of 41%.

In 2016 Kim *et al.*[27] synthesized four conjugated copolymers (**P11** – **P14**) using 6-(2-thienyl)-4*H*-thieno[3,2-*b*]indole (TTI) as electron donor and isoindigo as electron acceptor and studied their applications in OSC devices. The high planarity and electron donating ability of TTI

resulted in efficient intramolecular charge transfer for the generation of low band gap polymers. The two conjugated carbonyls in the isoindigo unit increased the electron withdrawing ability of the acceptor and the alkyl groups on amide nitrogen enhanced the solubility and solution processablity of the polymers. The syntheses of monomer **25** and polymers **P11** – **P14** are depicted in **Scheme 8**.

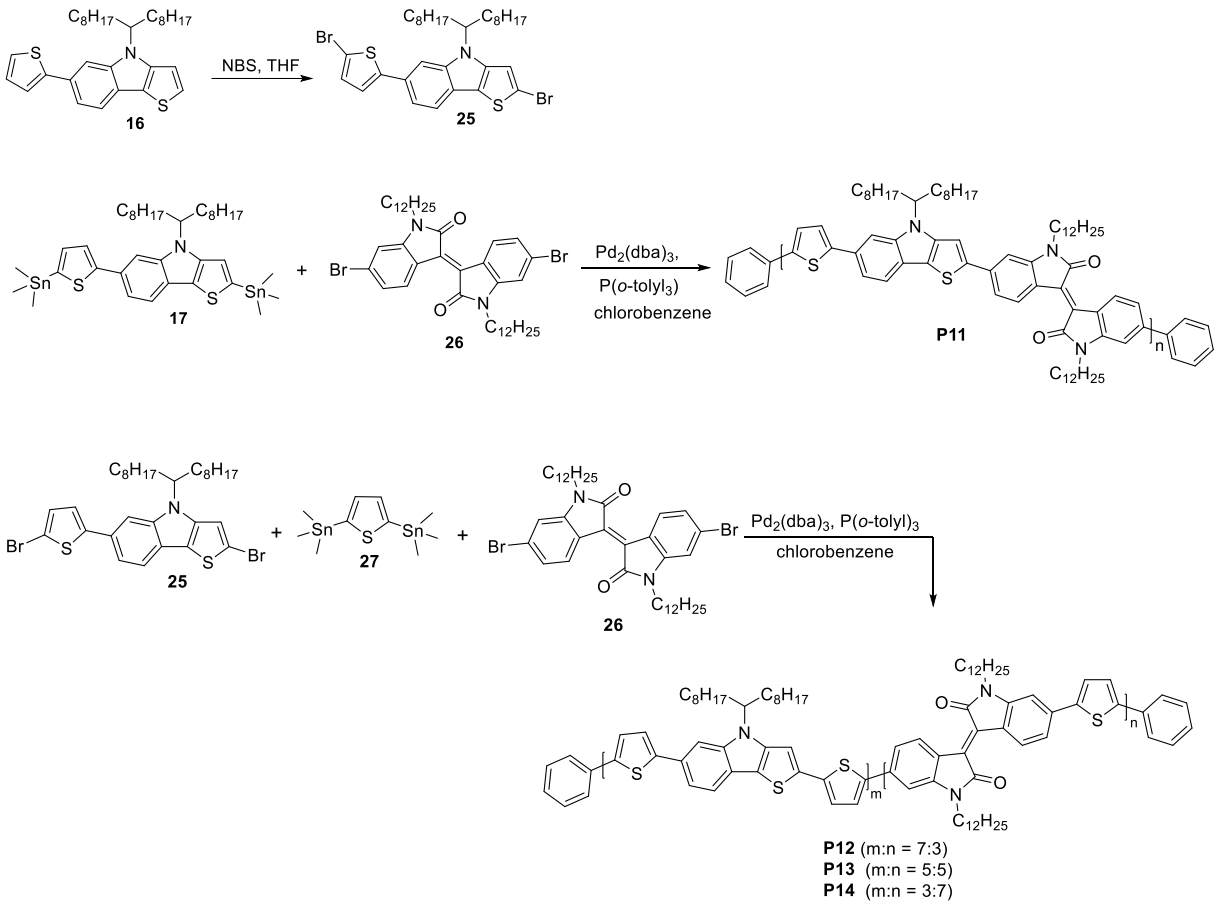

Scheme 8. Synthetic route towards monomer **25** and polymers **P11**, **P12**, **P13** and **P14**.

The optical properties of the polymers were studied in *o*-DCB solutions and as thin films by UV-Vis absorption spectroscopy. **P14** exhibited the highest molar absorption coefficient of 284,000 M^{-1} cm^{-1} at around 656 nm in *o*-DCB solution. The UV-Vis absorption spectra of the copolymers showed red-shifted absorption maxima as the amount of isoindigo increased. The optical band gaps calculated from the onsets of absorption were 1.59, 1.59, 1.57 and 1.55 eV for the **P11**, **P12, P13** and **P14**, respectively. **P14** showed a broader absorption with lower

band gap than the alternating copolymer **P11** because of a higher content of isoindigo. The HOMO energy levels of **P11**, **P12**, **P13** and **P14** determined by cyclic voltammetry were -5.45, -5.32, -5.43 and -5.50 eV and the LUMO energy levels were -3.69, -3.72, -3.86 and -3.90 eV, respectively. The photovoltaic properties of the polymers were investigated by using conventional solar cell devices with architecture of ITO/PEDOT:PSS/polymers:$PC_{71}BM$/Al. The **P14:**$PC_{71}BM$-based device without additive gave a PCE of 3.32% with a V_{OC} of 0.64 V, a J_{SC} of 10.8 mA/cm^2, and a FF of 48%. When 1-chloronaphthalene (CN) was used as an additive both the J_{SC} and *FF* improved resulting in a PCE 4.03%. The higher efficiency obtained from **P14**-based device was due to broader absorption, lower band gap and optimal mobility for effective charge transportation. Due to higher absorption coefficient around 600-780 nm, J_{SC} and V_{OC} values, the device based on **P11** gave higher PCE (3.02%) values as compared to devices based on **P12** (2.43%) and **P13** (2.31%).

In 2019 Suh *et al.*[28] synthesized four copolymers (**P15 – P18**) using 6-(2-thienyl)-4*H*-thieno[3,2-*b*]indole (TTI) as electron donor and *N*-alkyl-2,2'-bithiophene-3,3'-dicarboximide (BTI) as the electron acceptor for OSC applications by using the Stille polycondensation polymerization reaction. **Scheme 9** depicts the syntheses of these polymers.

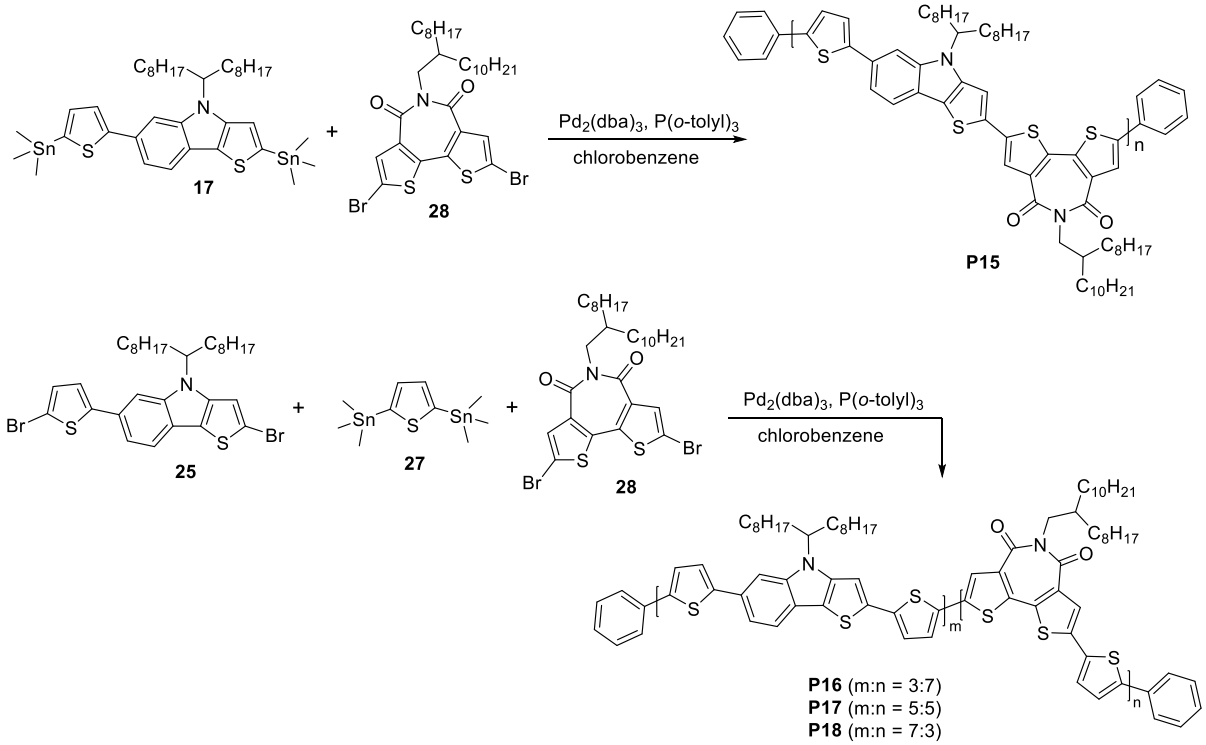

Scheme 9. Synthetic towards the synthesis of **P15, P16, P17, P18**

The UV-Vis absorption spectra of the copolymers in o-DCB solution gave absorption maxima in the range between 512 and 553 nm. The thin film absorption maxima of **P15**, **P16** and **P17** showed red –shifted absorption maxima compared to the maxima in solution. On the other hand, the thin film absorption maximum of **P18** was blue-shifted by 6 nm compared to the maximum in solution. The optical band gaps were estimated from the absorption onsets of **P15**, **P16**, **P17** and **P18** to be 1.8, 1,8, 1.9, and 1.9 eV, respectively. **P18** with lowest amount of BTI units showed the highest molar absorption coefficient of 5.32 $x10^5$ M^{-1} cm^{-1} at around 520 nm in *o*-DCB solution and turned out to afford the efficient PSC with improved J_{SC} value compared to the devices fabricated from the other three polymers. The frontier molecular orbital energy levels of the polymers were determined by cyclic voltammetry. Thus, the HOMO energy levels of **P15**, **P16**, **P17**, and **P18** were estimated from the onset potentials of oxidation to be -5.7, -5.8, -5.8 and -5.7 eV, respectively. Likewise, the LUMO energy levels of **P15**, **P16**, **P17**, and **P18** were estimated from the onset potentials of reduction to be, -3.94, -4.02, -3.87 and -3.78, respectively. Fullerene-based OSCs with the conventional device structure of ITO/PEDOT:PSS/polymers:$PC_{71}BM$/Al were used to study the photovoltaic performances of the polymers. Thus, BHJ devices were fabricated by spin-coating *o*-DCB solutions of polymer:$PC_{71}BM$ blends with different blend ratios. The device fabricated from **P15**:$PC_{71}BM$ (1:3) with diiodooctane (DIO) additive exhibited a PCE of 1.39% with a V_{OC} of 0.77 V, a J_{SC} of 2.66 mA/cm^2, and a *FF* of 67%. On the other hand, the **P18**:$PC_{71}BM$ (1:2)-based device, with DIO additive, afforded the highest PCE of 2.64% with V_{OC} of 0.72 V, a J_{SC} of 6.78 mA/cm^2, and a *FF* of 54%. The **P18**-based devices gave relatively higher PCEs compared to the other devices presumably because of the highest molar absorption coefficient and better hole mobility of **P18**, and optimal morphology of the **P18**:$PC_{71}BM$ blend films resulting in higher J_{SC} values.

4. Objective of the Work

The overall objective of this work is to synthesize and characterize conjugated polymers for possible application in solar cell devices. Monomers comprising of the 4*H*-thieno[3,2-*b*]indole moiety will be prepared starting from small chemical entities. Homopolymers and copolymers will be prepared from bis(stannylated) compounds by reaction with dibromides using the Stille polycondensation polymerization reaction. NMR spectroscopy will be used to characterize intermediate compounds and monomers. The optical and electrochemical properties of the polymers will be determined by using UV-Vis spectroscopy and cyclic voltammetry, respectively. The highest occupied molecular orbital (HOMO) and lowest unoccupied molecular orbital (LUMO) energy levels will be calculated from the onsets of oxidation and reduction potentials obtained from cyclic voltammograms. The electrochemical band gaps will be determined from the energy differences between the HOMO and LUMO while the optical band gaps will be calculated from the onsets of absorption in the UV-Vis spectra.

5. Results and Discussion

In the course of this work, four 4*H*-thieno[3,2-*b*]indole-based monomers were synthesized and characterized by their ^{1}H- and ^{13}C-NMR spectra. The monomers were subsequently polymerized by using the Stille polycondensation polymerization reaction. The synthesis of monomers and polymers are described below.

5.1 2-Bromo-6-(5-bromothiophene-2-yl)-4-(2-ethylhexyl)-7-fluoro-4*H*-thieno[3,2-*b*]indole (34)

2-Bromo-6-(5-bromothiophene-2-yl)-4-(2-ethylhexyl)-7-fluoro-4*H*-thieno[3,2-*b*]indole (**34**) was synthesized starting from 1,4-dibromo-2-fluorobenzene (**29**) as shown in **Scheme 10**. Thus, nitration of 1,4-dibromo-2-fluorobenzene (**29**) with ammonium nitrate at room temperature gave 1,4-dibromo-2-fluoro-5-nitrobenzene (**30**), which was converted to 2',2''-(2-fluoro-5-nitro-1,4-phenylene)dithiophene (**31**) by the Stille coupling reaction with 2-tributhylstannylthiophene in toluene using dichlorobis(triphenylphosphine)palladium(II) as catalyst. The structures of compounds **30** and **31** were confirmed by their ^{1}H-NMR and ^{13}C-NMR spectra.

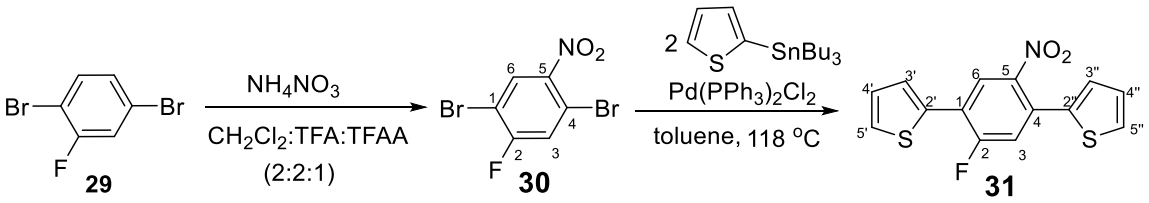

Scheme 10. Syntheses of compounds **30** and **31.**

The ^{1}H-NMR spectrum of compound **30** (**Table 1, Appendix 1**) showed two doublets at δ8.23 (*J* = 6.4 Hz) and 7.60 (*J* = 7.6 Hz) due to H-F couplings, suggesting that C-5 was the site of nitration. The doublet at δ8.23 corresponds to H-6 because of the lower coupling constant value of 6.4 Hz while the second doublet at δ7.60 is attributed to H-3 because it exhibited a higher coupling constant due to its proximity to the fluorine atom at C-2. Besides, H-6 is more deshielded than H-3 due to the presence of the strongly electron withdrawing (-I, -M) nitro group at C-5, *ortho* to H-6, while H-3 is *meta* to the nitro group where the nitro group is electron withdrawing only by the inductive effect (-I). The ^{13}C-NMR spectrum of compound **30** (**Table 2, Appendix 2**) showed six carbon signals.

Assignment of the signals to each carbon atom is made by taking the electronic effects of both the nitro group and the fluorine atom into account in addition to the C-F coupling constant values. The most downfield signal at δ 160.62, with a very strong one-bond C-F coupling (J = 257 Hz), is attributed to C-2. The signal at δ146.06 can be assigned to C-5 to which the electron withdrawing nitro group is attached. The methine carbon signals (DEPT-135 spectrum) at δ130.92 (J = 2 Hz) and 122.87 (J = 27 Hz) are assigned to C-6 and C-3, respectively.

Table 1: The ^{1}H-NMR (400 MHz, $CDCl_3$) data (δ_{ppm}) of compounds **30** and **31**.

30	**31**
8.23	8.10
(1H, *d*, *J* = 6.4 Hz, H-6)	(1H, *d*, *J* = 6.8 Hz, H-6)
7.60	7.60
(1H, *d*, *J* = 7.6 Hz, H-3)	(1H, *dt*, *J* = 1.2, 3.6 Hz, H-3')
	7.50*
	(1H, *dd*, *J* = 1.2, 5.2, Hz, H-5')
	7.48*
	(1H, *dd*, *J* = 1.2, 5.2, Hz, H-5")
	7.34
	(1H, *d*, *J* = 11.2 Hz, H-3)
	7.19
	(1H, *ddd*, 0.8, 3.6, 5.2 Hz,, H-4')
	7.16
	(1H, *dd*, *J* = 1.2, 3.6 Hz, H-3")
	7.13
	(1H, *dd*, *J* = 3.6, 5.2 Hz, H-4")

*Assignments may be interchangeable.

The ^{1}H-NMR spectrum of compound **31** (**Table 1** and **Appendix 4)** showed seven signals in the aromatic region. The most downfield signal at δ8.10 appeared as a doublet (J = 6.8 Hz) due to H-F coupling and is assigned to H-6. The doublet of triplets at δ7.60 (J = 1.2, 3.6 Hz) is due to H-3'. This signal pattern was observed due to the long range coupling of H-3' with

the fluorine at C-2 besides coupling to the protons on the thiophene ring. The doublet of doublets at δ7.50 and 7.48 are due to H-5' and H-5", respectively. The signal at δ7.34 appears as doublet (J = 11.2 Hz) due to a three-bond H-F coupling and is attributed to H-3. The doublet of doublet of doublets at δ7.19 (J = 0.8, 3.6, 5.2 Hz) is attributed to H-4' which shows coupling to the fluorine at C-2 over six bonds in addition to couplings with the thiophene ring protons. The doublet of doublets at δ7.16 (J = 1.2, 3.6 Hz) and 7.13 (J = 3.6, 5.2 Hz) are assigned to H-3" and H-4", respectively. The ^{13}C-NMR and DEPT-135 spectra of compound **31** (**Table 2** and **Appendix 5**) revealed a total of fourteen carbon signals in the aromatic region of which six are due to quaternary carbon atoms and the remaining eight due to methine carbon atoms. The most downfield quaternary carbon signal at δ159.19 appeared as a doublet (J = 256 Hz) and can be assigned to C-2 attached to the electron withdrawing fluorine atom. The quaternary carbon signal at δ145.42 is attributed to C-5 containing the nitro group. The remaining quaternary carbon signals appeared at δ135.87, 134.12 (J = 4 Hz), 128.87 (J = 10 Hz), and 122.78 (J = 1.5 Hz) and are assigned to C-2", C-4, C-1, and C-2', respectively. The methine carbon signals appeared at δ128.9, 128.18, 127.98, 127.82, 127.75, 124.52 (J = 6 Hz), and 119.79 (J = 26 Hz) and are due to C-4", C-5' & 5", C-4', C-3', C-3", C-6, C-3, respectively.

Table 2: The ^{13}C-NMR (100 MHz, $CDCl_3$) data (δ_{ppm}) of compounds **30** and **31.**

Carbon	**30** $\delta_{(ppm)}$ (J_{Hz})	**31** $\delta_{(ppm)}$ (J_{Hz})
1	108.82 (*d, J* = 23 Hz)	128.87 (*d, J* = 10 Hz)
2	160.62 (*d, J* = 257 Hz)	159.19 (*d, J* = 256 Hz)
3	122.87 (*d, J* = 27 Hz)	119.79 (*d, J* = 26 Hz)
4	114.88 (*d, J* = 9 Hz)	134.12 (*d, J* = 4 Hz)
5	146.06	145.42
6	130.92 (*d, J* = 2 Hz)	124.49 (*d, J* = 6 Hz)
2'	-	122.78 (*d, J* = 1.5 Hz)
3'	-	127.82
4'	-	127.98
5'	-	128.18
2"	-	135.87
3"	-	127.75

4"	-	127.89
5"	-	128.18

5.2 Synthesis of 2-bromo-6-(5-bromothiophen-2-yl)-4-(2-ethylhexyl)-7-fluoro-4*H*-thieno[3,2-*b*]indole (34)

The synthesis of compound **34** started first by reductive Cadogan cyclization of compound **31** with triphenylphosphine and *o*-dichlorobenzene as a solvent at high temperature to give compound **32.** Compound **32** was *N*-alkylated with 2-ethylhexylbromide using potassium hydroxide as a base in *N*,*N*-dimethylformamide solvent system to afford compound **33.** Subsequent bromination of compound **33** with *N*-bromosuccinimide yielded compound **34** as shown in **Scheme 11**.

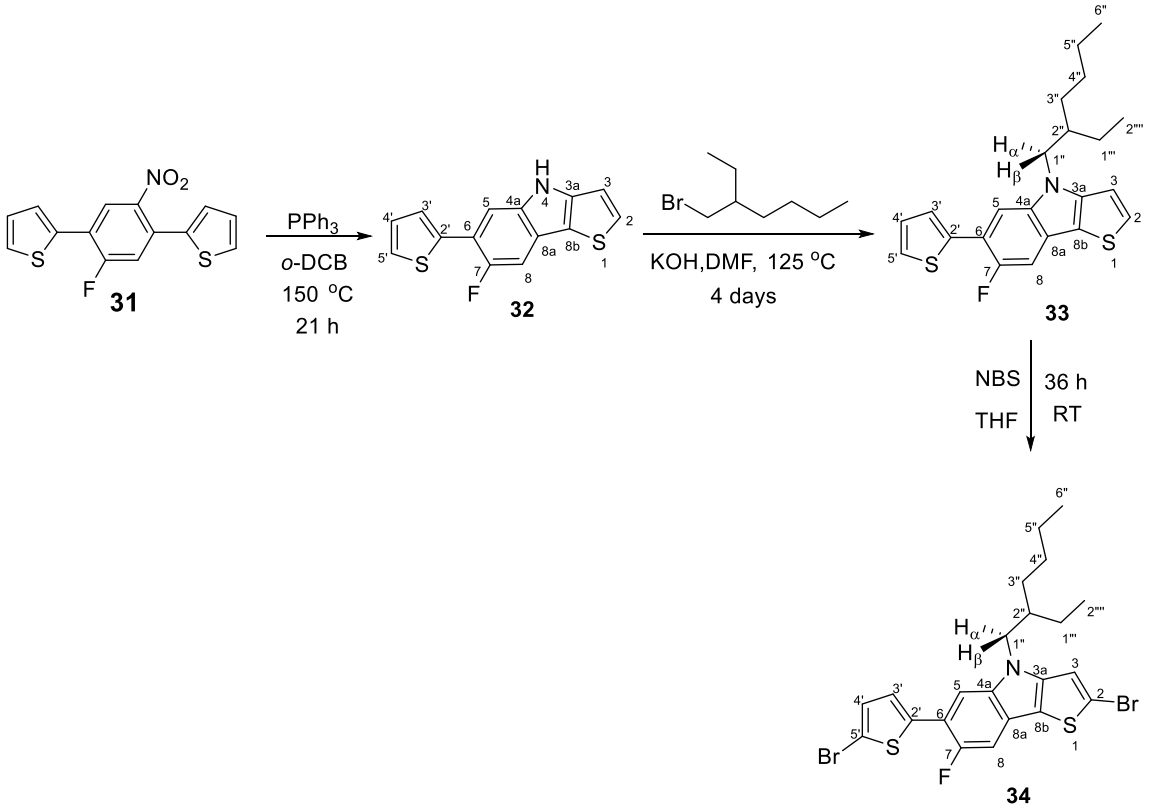

Scheme 11. Synthesis of compound **34.**

The ^{1}H-NMR spectrum of compound **32** (**Table 3** and **Appendix 7**) revealed seven resonances in the aromatic region. The most downfield signal at δ8.10 appeared as a broad singlet and is attributed to the *N*-H (H-4). The doublet at δ7.45 (*J* = 5.6 Hz) is assigned to H-5 and the other doublet at δ7.50 (*J* = 11.6 Hz) is assigned to H-8, both showing long-range

couplings with the fluorine at C-7. The unresolved multiplet at δ7.50 is due to H-3'. The doublet of doublets at δ7.37 (*J* = 1.2, 5.2 Hz), 7.60 (*J* = 1.2, 5.2 Hz), and 7.04 (*J* = 1.2, 5.2 Hz) correspond to H-5', H-2 and H-3, respectively. The doublet of doublet of doublets at δ 7.16 (*J* = 0.8, 3.6, 5.2 Hz) is due to H-4'. The ^{13}C-NMR spectrum of compound **32** (**Table 4** and **Appendix 8**) showed fourteen signals in aromatic region of which seven signals are due to quaternary carbon atoms and the remaining seven are due to methine carbon atoms (DEPT-135). The most downfield signal at δ154.36 appeared as a doublet (*J* = 238.9 Hz) and can be assigned to C-7 attached to electron withdrawing fluorine atom. The quaternary carbon signal at δ145.15 is assigned to C-4a attached to electronegative nitrogen atom. The methine carbon signals at δ128.41, 127.79, 125.83 (*J* = 6.7 Hz), 125.06, 111.62, 110.98 (*J* = 6 Hz), and 105.11 (*J* = 26 Hz) are due to C-5', C-2, C-5, C-3, C-4', C-3', C-8, respectively. The remaining quaternary carbon signals at δ138.57 (*J* = 3 Hz), 137.85, 121.51 (*J* = 1.1 Hz), 117.86, and 117.70 (*J* = 3.6 Hz) can be assigned to C-8a, C-2', C-8b, C-3a, and C-6, respectively.

Table 3: The ^{1}H-NMR (400 MHz, $CDCl_3$) data (δ_{ppm}) of compounds **32, 33** and **34.**

32 $\delta_{(ppm)}$ (J_{Hz})	**33** $\delta_{(ppm)}$ (J_{Hz})	**34** $\delta_{(ppm)}$ (J_{Hz})
8.10	7.57	7.41
(1H, *s*, N-H (H-4))	(1H, *d*, *J* = 6.0 Hz, H-5)	(1H, *d*, *J* = 6.4 Hz, H-5)
7.60	7.54	7.38
(1H, *dd*, *J* = 1.2, 5.2 Hz, H-2)	(1H, *dt*, *J* = 1.2, 5.2 Hz, H-5')	(1H, *d*, *J* = 11.6 Hz, H-8)
7.50	7.50	7.22
(1H, *m*, H-3')	(1H, *d*, *J* = 11.6 Hz, H-8)	(1H, *dd*, *J* = 1.2. 4.0 Hz, H-3'),
7.49	7.43	7.10
(1H, *d*, *J* = 11.6 Hz, H-8)	(1H, *d*, *J* = 5.2 Hz, H-2)	(1H, *dd*, *J* = 0.8. 4.0 Hz,, H-4')
7.42	7.40	7.08
(1H, *d*, *J* = 5.6 Hz, H-5)	(1H, *dd*, *J* = 0.8, 5.2 Hz, H-4')	(1H, *s*, H-3)
7.37	7.20	4.02*
(1H, *dd*, *J* = 1.2, 5.2 Hz, H-5')	(1H, *ddd*, *J* = 0.4, 3.6, 5.1 Hz, H-3')	(1H, *dd*, *J* = 8.0, 14.6 Hz, H-1"α)
7.16	7.05	4.08*
(1H, *ddd*, *J* = 0.8, 3.6, 5.2 Hz, H-4')	(1H, *d*, *J* = 5.6 Hz, H-3)	(1H, *dd*, *J* = 7.2, 14.6 Hz, H-1"β')

7.04	4.09*	1.96
(1H, *dd*, *J* = 1.2, 5.2 Hz, H-3)	(1H, *dd*, *J* = 7.6, 14.6 Hz, H-1"α)	(1H, *septet*, *J* = 6.4 Hz, H-2")
	4.15*	1.32
	(1H, *dd*, *J* = 7.2, 14.6 Hz, H-1"β')	(8H, *m*, H-3", 1"', 4", 5")
	2.01	0.94
	(2H, *septet*, *J* = 6.4 Hz, H-2")	(3H, *t*, *J* = 7.2 Hz, H-6")
	1.42	0.91
	(8H, b*m*, H-3", H-4", H-5", H-1"')	(3H, *t*, *J* = 7.2 Hz, H-2"')
	0.97	
	(3H, *t*, *J* = 6.8 Hz,, H-6")	
	0.93	
	(3H, *t*, *J* = 7.2 Hz,, H-2"')	

*Assignments of H-1"α and H-1"β may be interchangeable.

Table 4: The ^{13}C-NMR (100 MHz, $CDCl_3$) data (δ_{ppm}) of compounds **32, 33** and **34.**

Carbon	**32** $\delta_{(ppm)}$ (J_{Hz})	**33** $\delta_{(ppm)}$ (J_{Hz})	**34** $\delta_{(ppm)}$ (J_{Hz})
2	127.80	110.67	114.09
3	125.06 (*d*, *J* = 3.6 Hz)	110.67	111.83
3a	117.86	115.33 (*d*, *J* = 4 Hz)	120.79 (*d*, *J* = 11 Hz)
4a	145.16	147.72	145.42
8a	138.57 (*d*, *J* = 3 Hz)	139.04 (*d*, *J* = 3 Hz)	137.12
8b	121.51 (*d*, *J* = 1.1 Hz)	120.91 (*d*, *J* = 11 Hz)	115.26 (*d*, *J* = 4 Hz)
5	114.88 (*d*, *J* = 9 Hz)	127.95 (*d*, *J* = 25 Hz)	125.85 (*d*, *J* = 6 Hz)
6	117.70 (*d*, *J* = 3.6Hz)	117.23 (*d*, *J* = 16 Hz)	116.71(*d*, *J* = 17 Hz)
7	154.36 (*d*, *J* = 238.9 Hz)	153.99 (*d*, *J* = 238 Hz)	153.97 (*d*, *J* = 239 Hz)
8	105.11 (*d*, *J* = 26 Hz)	105.09	104.93(*d*, *J* = 26 Hz)
2'	137.85	138.39	140.24 (*d*, *J* = 3.0 Hz)

3'	110.98 (*d*, *J* = 4.2 Hz)	125.76 (*d*, *J* = 7.0 Hz)	130.54
4'	111.62	109.22	108.75 (*d*, *J* = 4.0 Hz)
5'	128.42	124.92 (*d*, *J* = 3.0 Hz)	114.09
1"	--	49.44	49.56
2"	--	40	39.98
3"	--	30.87	30.77
4"	--	24.31	24.24
5"	--	23.06	23.01
6"	--	10.86	10.82
1'"	--	28.77	28.70
2'"	--	14.10	14.04

The ^{1}H-NMR spectrum of compound **33** (**Table 3** and **Appendix 10**) revealed seven proton resonances in the aromatic and four signals in the aliphatic region. The most downfield signal at δ7.57 appeared as a doublet (*J* = 6.0 Hz) and is attributed to H-5. The doublet at δ7.50 (*J* = 11.6 Hz) corresponds to H-8 and the other two doublets at δ7.43 (*J* = 5.2 Hz), and 7.05 (*J* =5.6 Hz) can be assigned to H-2 and H-3, respectively. The doublet of triplets at δ7.54 (*J* = 1.2, 5.2 Hz) is attributed due to H-5' and the doublet of doublets at δ7.40 (*J* = 0.8, 5.2 Hz) can be accounted to H-4' The signal at δ7.20 appeared as a doublet of doublet of doublets (*J* = 0.4, 3.6, 5.1 Hz) due to long range H-F coupling and is attributed to H-3' The signals due to the diastereotopic protons at C-1" appeared as doublets of doublets at δ4.09 and 4.15. This signal pattern indicates a second-order splitting pattern where $\Delta\nu/J \leq 10$.[17] The septet at δ2.01 is attributed to H-2" which has three methylene groups as its coupling partners. The broad multiplet centered at δ1.42 is due to four methylene groups while the triplets at δ0.93 and 0.97 are due to the terminal methyl groups. The ^{13}C-NMR spectrum of compound **33** (**Table 4** and **Appendix 11**) showed fourteen signals in the aromatic region and eight signals in the aliphatic region. The DEPT-135 spectrum revealed seven methine carbon signals in the aromatic region and one methine, five methylene and two methyl carbon signals in the aliphatic region in agreement with structure **33**. The most downfield signal at δ153.99 appeared as a doublet (*J* = 238 Hz) and is assigned to C-7 attached to electron withdrawing fluorine atom. The quaternary carbon signal at δ147.72 is attributed to C-4a attached to

electronegative nitrogen atom. Assignment of the remaining carbon resonances is given in **Table 4**. Both the ^{1}H- and ^{13}C-NMR data discussed above agree very well with the structure of compound **33.** The ^{1}H-NMR spectrum of compound **34** (**Table 3** and **Appendix 13**) revealed five proton resonances in the aromatic and four signals in the aliphatic region. The most downfield doublet at δ7.40 (J = 6.4 Hz) appeared as a doublet and is accounted for H-5. The doublet at δ7.38 (J = 11.6 Hz) corresponds to H-8 and the doublet of doublets at δ7.22 (J = 1.2, 4.0 Hz) is due to H-3'.The doublet of doublets at δ7.10 (J = 0.8, 4.0 Hz) is assigned to H-4' and the singlet at δ7.08 is attributable to H-3. The doublet of doublets at δ4.02 and 4.08, integrating for one proton each, are due to the diastereotopic methylene protons C-1". The one-proton septet at δ1.96 is due to H-2" while the eight-proton multiplet centered at δ1.32 is due the methylene protons H-3", H-1'", H-4" and H-5". The three-proton triplets at δ0.94 and 0.91 are attributed to the terminal methyl protons H-6" and H-2'", respectively. The ^{13}C-NMR spectrum of compound **34** (**Table 4**) displayed a total of twenty-two carbon resonances of which fourteen appeared in the aromatic region and eight in the aliphatic region. The DEPT-135 spectrum revealed nine of the fourteen carbon atoms are quaternary while the remaining five are methine carbon atoms. Out of the eight signals in the aliphatic region, five are due to methylene carbons, one is due to a methine carbon and two are due to terminal methyl groups in agreement with structure **34**. The assignments of the signals to each carbon atom are given in **Table 4.**

5.3 Synthesis of 2-bromo-6-(5-bromothiophen-2-yl)-7-fluoro-4-octyl)-4*H*-thieno[3,2-*b*]indole (36)

Compound **36** contains a straight chain octyl group on the nitrogen atom of the 6-(thiophen-2-yl)-4*H*-thieno[3,2-*b*]indole moiety. **Scheme 12** shows the synthesis of compound **36** starting from compound **32**. Thus, *N*-alkylation of **32** with 1-bromooctane using NaH as a base afforded **35**, which was subsequently brominated with NBS in THF to give **36**. Compounds **35** and **36** were characterized based on their ^{1}H- and ^{13}C-NMR spectra as discussed below.

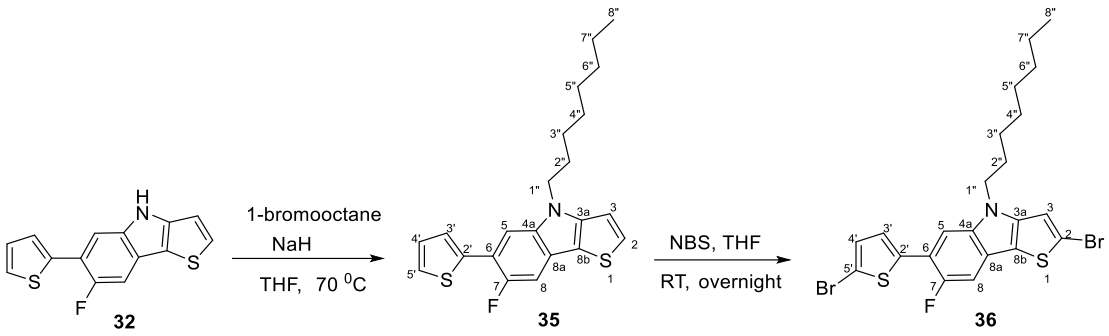

Scheme 12. Synthesis of compound **35** and **36**

The ^{1}H-NMR spectrum of compound **35** (**Table 5** and **Appendix 16**) revealed seven resonances in the aromatic and four signals in the aliphatic region. The most downfield doublet signal at δ7.56 (*J* = 6.4 Hz) appeared as a doublet and is due to H-5 which shows long-range coupling with the fluorine at C-7. The doublet at δ7.51 (*J* = 11.2 Hz) corresponds to H-8 which exhibits a J^{3} coupling with the fluorine at C-7. The doublets at δ7.45 (*J* = 5.2 Hz), and 7.10 (*J* = 5.2 Hz) are assignable to H-2 and H-3, respectively. The doublet of triplets resonance at δ7.53 (*J* = 1.2, 4.0 Hz) is attributable to H-3' and the doublet of doublets at δ7.40 (*J* = 1.2, 5.2 Hz) is accounted to H-5'. The doublet of doublet of doublets (*ddd*) at δ7.20 (*J* = 0.4, 4.0, 5.2 Hz) is assigned to H-4'. Surprisingly, H-4' showed a long-range coupling over six bonds to the fluorine at C-7. The most downfield aliphatic protons signal appeared at δ4.3 as a triplet (*J* = 7.2 Hz) and is due to H-1". The two-proton pentet at δ1.89 is attributed to H-2". The ten-proton broad signal centered at δ1.31 corresponds to ten protons and is due to the methylene groups H-3" to H-7". The triplet at δ0.9 (*J* = 6.8 Hz) is assigned to the terminal methyl protons H-8". The ^{13}C-NMR of compound **35** (**Table 6** and **appendix 17**) displayed a total of twenty-two carbon resonances of which fourteen appeared in the aromatic region and seven in the aliphatic region. The DEPT-135 spectrum revealed seven quaternary and seven methine carbon signals in the aromatic region. Out of the eight signals in the aliphatic region, seven are due to methylene carbons and one is due to a methyl carbon. Assignments of the carbon resonances to the carbon atoms in **35** is given in **Table 6.** Both the ^{1}H- and ^{13}C-NMR data agree very well with the structure of compound **35.**

Table 5: The ^{1}H-NMR (400 MHz, $CDCl_3$) data (δ_{ppm}) of compounds **35** and **36.**

35 $\delta_{(ppm)}$ (J_{Hz})	**36** $\delta_{(ppm)}$ (J_{Hz})
7.56	7.41
(1H, *d*, *J* = 6.4 Hz, H-5)	(1H, *d*, *J* = 6.4 Hz, H-5)

7.53

(1H, *dt*, *J* = 1.2, 4.0 Hz, H-3')

7.51

(1H, *d*, *J* = 11.2 Hz, H-8)

7.45

(1H, *d*, *J* = 5.2 Hz, H-2)

7.40

(1H, *dd*, *J* = 1.2, 5.2 Hz, H-5')

7.20

(1H, *ddd*, *J* = 0.4, 4.0, 5.2 Hz, H-4')

7.10

(1H, *d*, *J* = 5.2 Hz, H-3)

4.30

(2H, *t*, *J* = 7.2 Hz, H-1'')

1.89

(2H, *pentet*, *J* = 7.2 Hz, H-2'')

1.31

(10H, *m*, H-3''-H-7'')

0.90

(3H, *t*, *J* = 6.8 Hz, H-8'')

7.38

(1H, *d*, *J* = 11.2 Hz, H-8)

7.23

(1H, *dd*, *J* = 1.2, 4.0 Hz, H-3')

7.10

(1H, *s*,,H-3)

7.09

(1H, *d*, *J* = 4. 0Hz, H-4')

4.18

(2H, *t*, *J* = 7.2 Hz, H-1'')

1.85

(2H, *m*, H-2'')

1.30

(10H, *m*, H-3''-H-7'')

0.90

(3H, *t*, *J* = 6.8Hz, H-8'')

The ^{1}H-NMR spectrum of compound **36** (**Table 5** and **Appendix 19**) revealed five resonances in the aromatic and four signals in the aliphatic region. The most downfield doublet at δ7.41 (*J* = 6.4 Hz) appeared as a doublet and is due to H-5, which is long-range coupled to the fluorine at C-7. The doublet at δ7.38 (*J* = 11.2 Hz) corresponds to H-8, which shows a three-bond coupling to the fluorine at C-7. The doublet of doublets signal at δ7.23 (*J* = 1.2, 4.0 Hz) is accounted for H-3', which exhibits a five-bond coupling to the fluorine at C-7. The singlet at δ7.10 is assigned to H-3 while the broad doublet at δ7.09, one end of which overlaps with the singlet at δ7.10, is attributed to H-4'. The aliphatic region of the ^{1}H-NMR spectrum shows a downfield triplet at δ4.18 (*J* = 7.2 Hz) due to H-1'' and a pentet at δ1.84 assigned to H-2''. The unresolved broad signal centered at δ1.29 is due to the methylene

protons H-3" - H-7". The terminal methyl protons signal appeared at δ0.90 as a triplet (J = 6.8 Hz).

The ^{13}C-NMR spectrum of compound **36** (**Table 6** and **Appendix 20**) displayed a total of twenty-two carbon resonances, of which fourteen appeared in the aromatic region and eight in the aliphatic region. The DEPT-135 spectrum revealed five methine carbon signals in the aromatic region in agreement with introduction of two bromine atoms in the structure of **35**. . Out of the eight signals in the aliphatic region, seven are due to methylene carbons and one is due to a methyl carbon. The most downfield signal at δ153.96 (J = 238 Hz) appeared as a doublet and can be assigned to C-7 attached to electron withdrawing fluorine atom. **Table 6** shows assignments of the carbon signals to the carbon atoms in **36.** Both the ^{1}H- and ^{13}C-NMR data agreed very well with the structure of compound **36.**

5.4 Synthesis of 2-bromo-(5-bromothiephen-2-yl)-4-decyl-7-flouro-4*H*-thieno(3,2-*b*) indole (38)

The synthesis of compound **38** followed a similar approach to the preparation of compounds **34** and **36** described above. Thus, alkylation of compound **32** with 1-bromodecane using sodium hydride as a base in tetrahydrofuran solvent system gave compound **37,** which was subsequently brominated at room temperature with *N*-bromosuccinimide to afford compound **38.** Compounds **37** and **38** were characterized based on their ^{1}H- and ^{13}C-NMR spectra as described below.

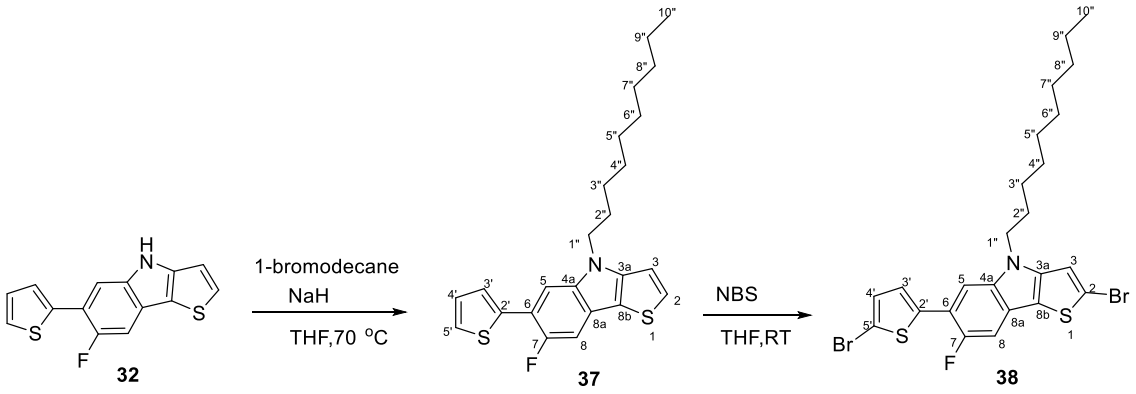

Scheme 13. Synthesis of compounds **37** and **38.**

The ^{1}H-NMR spectrum of compound **37** (**Table 7** and **Appendix 22**) displayed seven proton resonances in the aromatic region and four signals in the aliphatic region. The most

downfield signal at δ7.57 appeared as a doublet (J = 6.4 Hz) due to J^4 coupling with the fluorine at C-7 and is assigned to H-5. The signal with a doublet of triplets splitting pattern at δ7.55 (J = 1.2, 1.2, 3.6 Hz) is attributable to H-3' which is long-range coupled with the fluorine at C-7 in addition to the couplings with 4' and H-5'. The doublet at δ7.51 (J = 11.2 Hz) corresponds to H-8, which shows a three-bond coupling to the fluorine at C-7. The two doublets at δ7.44 (J = 5.2 Hz), and 7.01 (J = 5.2 Hz) are assigned to H-2 and H-3, respectively. The doublet of doublets at δ7.40 (J = 1.2, 5.2 Hz) is accounted for H-5' while the doublet of doublet of doublets (ddd) at δ7.20 (J = 0.8, 3.6, 5.2 Hz) is assigned to H-4'. The signal due to H-4', besides coupling to H-3' and H-5', shows a 0.8 Hz coupling with the fluorine at C-7 over six bonds. The triplet at δ4.26 (J = 7.2 Hz) is due to the H-1'' on the decyl side chain. The pentet at δ1.90 (J = 7.2 Hz) is due to H-2''. The signals due to H-3'' – H-9'' appeared as unresolved broad multiplet centered at δ1.32. The triplet at δ0.95 is assigned to the terminal methyl protons (H-10'').

Table 6: The ^{1}H-NMR (400 MHz, $CDCl_3$) data (δ_{ppm}) of compounds **37** and **38.**

37 $\delta_{(ppm)}$ (J_{Hz})	**38** $\delta_{(ppm)}$ (J_{Hz})
7.57 (1H, *d*, *J* = 6.4 Hz, H-5)	7.43 (1H, *d*, *J* = 5.6 Hz, H-5)
7.55 (1H, *dt*, *J* = 1.2, 1.2, 3.6 Hz, H-3')	7.40 (1H, *d*, *J* = 11.2 Hz, H-8)
7.51 (1H, *d*, *J* = 11.2 Hz, H-8)	7.24 (1H, *dd*, *J* = 1.2, 4 Hz, H-3')
7.44 (1H, *d*, *J* = 5.2 Hz, H-2)	7.12 (1H, *s*, H-3)
7.40 (1H, *dd*, *J* = 1.2, 5.2 Hz, H-5')	7.0 (1H, *m*, H-4')
7.20 (1H, *ddd*, *J* = 0.8, 3.6, 5.2 Hz, H-4')	4.2 (2H, *t*, *J* = 7.2 Hz, H-1'')
7.01 (1H, *d*, *J* = 5.2 Hz, H-3)	1.3 (16H, *bm*, H-2''-9'')
4.26 (2H, *t*, *J* = 7.2 Hz, H-1'')	0.9 (3H, *t*, *J* = 6.8 Hz, H-10'')

	1.90 (2H, *pentet*, *J* = 7.2 Hz, H-2") 1.32 (14H, *bm*, H-3"-H-9") 0.93 (3H, *t*, H-10")

The ^{13}C-NMR spectrum of compound **37** (**Table 8** and **Appendix 23**) displayed a total of twenty-four carbon resonances, of which fourteen appeared in the aromatic region and ten in the aliphatic region. The DEPT-135 spectrum revealed seven quaternary and seven methine carbon signals in the aromatic region. Out of the ten signals in the aliphatic region, nine are due to methylene carbons and one is due to a methyl carbon in agreement with the structure of compound **37**. **Table 8** shows assignment of the carbon resonances to each carbon atom.

Table 7: The ^{13}C-NMR (100 MHz, $CDCl_3$) data (δ_{ppm}) of compounds **37** and **38.**

Carbon	**37** $\delta_{(ppm)}$ (J_{Hz})	**38** $\delta_{(ppm)}$ (J_{Hz})
2	128.13	106.37
3	110.54	113.96
3a	147.38	140.16
4a	138.10	136.76
5	125.85 (*d*, *J* = 6.5 Hz)	125.91 (*d*, *J* = 6.2 Hz)
6	117.32 (*d*, *J* = 16.7 Hz)	111.85 (*d*, *J* = 4.5 Hz)
7	154.07 (*d*, *J* = 238 Hz)	154.01 (*d*, *J* = 261 Hz)
8	105.14 (*d*, *J* = 26 Hz)	104.97 (*d*, *J* = 26.1 Hz)
8a	121.04 (*d*, *J* = 10.7 Hz)	116.84
8b	115.48 (*d*, *J* = 4.2 Hz)	115.30
2'	139.06 (*d*, *J* = 3.5 Hz)	145.07
3'	109.06 (*d*, *J* = 4.2 Hz)	108.64 (*d*, *J* = 4.2 Hz)
4'	124.98 (*d*, *J* = 3.5 Hz)	130.50
5'	127.83	107.65

1"	45.36	45.52
2"	29.44	29.27
3"	27.22	27.06
4"	29.42	29.25
5"	29.63	29.46
6"	29.82	29.89
7"	29.69	29.52
8"	32.02	31.86
9"	22.84	22.68
10"	14.30	14.14

The ^{1}H-NMR spectrum of compound **38** (**Table 7** and **Appendix 25**) revealed five resonances in the aromatic region and four signals in the aliphatic region in agreement with the fact that compound **37** was bis(brominated) at positions 2 and 5'. The most downfield doublet signal at δ 7.43 (J = 5.6 Hz) appeared as a doublet due to H-F coupling and is due to H-5. The doublet at δ 7.4 (J = 11.2 Hz) corresponds to H-8, which also exhibits an H-F coupling over three bonds. The doublet of doublets at δ 7.24 (J = 1.2 Hz, 4.0 Hz) is assignable to H-3' which couples with H-4' and with fluorine at C-7. The singlet at δ 7.12 is assigned to H-3 and the doublet of doublets at δ 7.09 (J = 0.8, 4.0 Hz) is accounted to H-4', where the 0.8 Hz coupling is due to coupling with fluorine at C-7 over six bonds. The most downfield signal in the aliphatic region appears as a triplet δ4.2 (J = 7.2 Hz) and is attributed to H-1". The unresolved two-proton multiplet at δ1.85 is due to H-2". The broad signal centered at δ1.30 integrates for fourteen protons and is due to methylene protons H-3" – H-9". The three-proton triplet at δ0.89 (J = 6.8 Hz) is due to the terminal methyl protons (H-10"). The ^{13}C-NMR spectrum of compound **38** (**Table 8** and **Appendix 26**) displayed a total of twenty-four carbon resonances, of which fourteen appeared in the aromatic region and ten in the aliphatic region. The DEPT-135 spectrum revealed nine quaternary and five methine carbon signals in the aromatic region. Out of the ten signals in the aliphatic region, nine are due to methylene carbons and one is due to a methyl carbon. **Table 8** gives assignments of the carbon signals. Both the ^{1}H- and ^{13}C-NMR data agree very well with the structure of compound **38**.

5.5 Synthesis of 2-bromo-6-(5-bromothiophen-2-yl)-7-fluoro-4-(2-(2-methoxyethoxy) ethyl)-4*H*-thieno[3,2-*b*]indole (43)

The synthesis of compound **43** commenced by first preparing 2-(2-methoxyethoxy)ethyl 4-methylbenzenesulfonate (**41**) as an alkylating agent. **Scheme 14** shows the preparation of **41** starting from 2-(2-methoxyethoxy) ethan-1-ol (**39**). Thus, the reaction of **39** with *p*-toluenesulfonyl chloride (**40**) in tetrahydrofuran (THF) using sodium hydroxide as a base afforded 2-(2-methoxyethoxy)ethyl 4-methylbenzenesulfonate (**41**) in high yield. Compound **41** was characterized based on its ^{1}H- and ^{13}C-NMR spectra as discussed below.

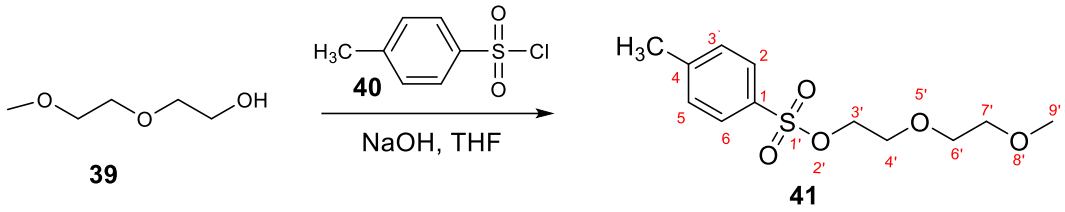

Scheme 14. Synthesis of compound **41.**

The ^{1}H-NMR spectrum of compound **41** (**Appendix 28**) revealed two resonances in the aromatic and four signals in the aliphatic region. The most downfield doublet at δ7.71 (*J* = 8.4 Hz) is due to H-2 and H-6 on the benzene ring. The other doublet at δ7.27 (*J* = 8.4 Hz) corresponds to two protons and is assigned to H-3 and H-5. The triplet at δ4.10 (*J* = 4.8 Hz) is assigned to H-3'. The triplet at δ3.60 (*J* = 4.8 Hz) is due to H-4'. The multiplets centered at δ3.49 and 3.39 are accounted to H-6' and H-7', respectively. The three-proton singlets at δ3.26 and 2.4 are due to the methyl group on the aromatic ring and the terminal methyl group at C-9'.

The ^{13}C-NMR spectrum of compound **41** (**Table 9, Appendix 29**) displayed a total of ten carbon resonances, of which four appeared in the aromatic region and six in the aliphatic region. The DEPT-135 spectrum revealed two quaternary and two methine carbon signals in the aromatic region. Out of the six signals in the aliphatic region, four are due to methylene carbons and two is due to methyl carbons. **Table 9** gives the assignments of the carbon resonances to the carbon atoms of **41**. Both the ^{1}H- and ^{13}C-NMR spectra confirmed the structure of compound **41.**

Table 8: The ^{13}C-NMR (100 MHz, $CDCl_3$) data (δ_{ppm}) of compound **41.**

Carbon	**41** $\delta_{(ppm)}$
1	132.79
2 &6	127.87
3 & 5	129.82
4	144.85
3'	69.29
4'	68.56
6'	70.50
7'	71.68
9'	58.9
CH_3	21.54

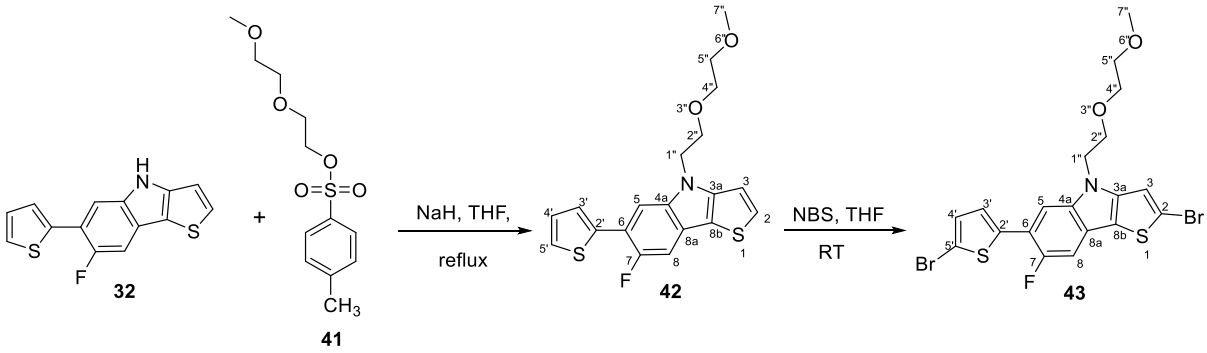

Scheme 15. Synthesis of compound **43**

Scheme 15 depicts the synthesis of compound **43** starting from compound **32**. Thus, alkylation of **32** with 2-(2-methoxyethoxy)ethyl 4-methylbenzenesulfonate (**41**) using sodium hydride as a base in tetrahydrofuran as a solvent yielded compound **42** which was subsequently converted to compound **43** without further purification by bromination with *N*-bromosuccinimide at room temperature. The structure of compound **43** was confirmed by its ^{1}H- and ^{13}C-NMR spectra as discussed below.

The ^{1}H-NMR spectrum of compound **43** (**Table 10, Appendix 31**) showed five resonances in the aromatic region and five signals in the aliphatic region. Similar to the ^{1}H-NMR spectra of fluorine-containing compounds discussed above, the spectrum of **43** is also characterized by

long-range H-F couplings. The most downfield doublet at δ7.51 (J = 6.0 Hz) is due to H-5. The one-proton doublet at δ7.36 (J = 11.6 Hz) is assigned to H-8 and the doublet of doublets at δ7.23 (J = 1.2, 4.0 Hz) is assignable to H-3'. The singlet at δ 7.18 is attributed to H-3 while the doublet of doublets at δ 7.08 (J = 0.8, 4.0 Hz) is accounted for H-4'. The two triplets at δ4.4 (J = 5.2 Hz) and 3.85 (J = 5.2 Hz) are due to H-1" and H-2", respectively. The two multiplets at δ3.53 and 3.45 are due to H-5" and H-4", respectively, and the singlet at δ3.3 is assigned to the terminal methyl protons (H-7").

Table 9: The ^{1}H-NMR (400 MHz, $CDCl_3$) data (δ_{ppm}) of compound **43.**

43 $\delta_{(ppm)}$ (J_{Hz})
7.51
(1H, *d*, *J* = 6.0 Hz, H-5)
7.36
(1H, *d*, *J* = 11.6 Hz, H-8)
7.23
(1H, *dd*, *J* = 1.2, 4.0 Hz, H-3')
7.18
(1H, *s*, H-3)
7.08
(1H, *dd*, *J* = 0.8, 4.0 Hz, H-4')
4.40
(2H, *t*, *J* = 5.2 Hz, H-1")
3.85
(2H, *t*, *J* = 5.2 Hz, H-2")
3.53
(2H, *m*, H-5"),
3.45
(2H, *m*, H-4")
3.3
(3H, *s*, H-7")

The ^{13}C-NMR spectrum of compound **43 (Table 11, Appendix 32**) revealed a total of nineteen carbon resonances, of which fourteen appeared in the aromatic region and five in the

aliphatic region. The DEPT-135 spectrum revealed nine quaternary and five methine carbon resonances in aromatic region and five methylene and one methyl carbon signals in the aliphatic region. Out of the five signals in the aliphatic region, four are due to methylene carbons and one is due to methyl carbon. **Table 11** gives assignments of the carbon resonances to each carbon atom in compound **43**. Both the ^{1}H- and ^{13}C-NMR data confirmed the identity of compound **43**.

Table 10: The ^{13}C-NMR (100 MHz, $CDCl_3$) data (δ_{ppm}) of compound **43.**

Carbon	**43** $\delta_{(ppm)}$ (J_{Hz})
2	115.03
3	114.66
3a	137.01
4a	145.39
5	125.8 (*d, J* = 6 Hz)
6	116.7 (*d, J* = 16 Hz)
7	154.1 (*d, J* = 239 Hz)
8	104.83 (*d, J* = 26 Hz)
8a	120.9 (*d, J* = 11 Hz)
8b	111.87 (*d, J* = 6 Hz)
2'	140.09
3'	108.93 (*d, J* = 4 Hz)
4'	130.45
5'	115.6
1"	45.66
2"	70.16
4"	70.87
5"	71.97
7"	59.11

5.6 Synthesis and characterization of polymers **P19**, **P20**, **P21**, **P22** and **P23**

In the course of this work, four donor copolymers and one donor-acceptor (D-A) terpolymer were synthesized and partially characterized. The syntheses and characterization of these polymers are described below.

5.6.1. Synthesis of polymers **P19**, **P20**, **P21**, **P22** and **P23**

Scheme 16 shows the syntheses of polymers **P19**, **P20**, **P21, P22**, and terpolymer **P23. P19** was prepared by the palladium-catalyzed Stille- polycondensation polymerization reaction of 2-bromo-6-(5-bromothiophen-2-yl)-4-(2-ethylhexyl)-7-fluoro-4*H*-thieno[3,2-*b*]indole (**34**) and commercially available donor monomer 4,8-bis(4,5-dioctylthiophen-2-yl)benzo[1,2-*b*:5,4-*b*]dithiophene-2,6-diyl)bis(trimethylstannane) (**44**). Similarly, **P20, P21** and **P22** were synthesized by the reactions of 2-bromo-6-(5-bromothiophen-2-yl)-7-fluoro-4-(2-(2-methoxyethoxy)ethyl)-4*H*-thieno[3,2-*b*]indole (**43**), 2-bromo-6-(5-bromothiophen-2-yl)-7-fluoro-4-octyl-4*H*-thieno[3,2-*b*]indole (**36**) and 2-bromo-6-(5-bromothiophen-2-yl)-4-decyl-7-fluoro-4*H*-thieno[3,2-*b*]indole (**38**) with compound **44**, respectively. The terpolymer **P23** was synthesized by the copolymerization of compounds **36**, **44** and 4,7-dibromo-5,6-difluorobenzo[*c*][1,2,5]thiadiazole (**45**). All polymers were end capped with 2-bromothiophene and 2-(tributylstannyl)thiophene. After the reactions were completed, the resulting polymers were precipitated from acetone or methanol and purified by Soxhlet extraction with acetone and diethyl ether to remove low molecular weight oligomers and some residual catalysts. Finally, the chloroform extract was collected and further purified by silica gel column chromatography. The chloroform solutions of all polymers were concentrated and precipitated from acetone or methanol followed by membrane filtration gave the pure polymers. All polymers were obtained in high yield and showed good solubility in chloroform and *o*-dichlorobenzene. The chloroform solutions of **P19**, **P20**, **P21** and **P22** were observed to be red while the solution of the terpolymer **P23** was blue.

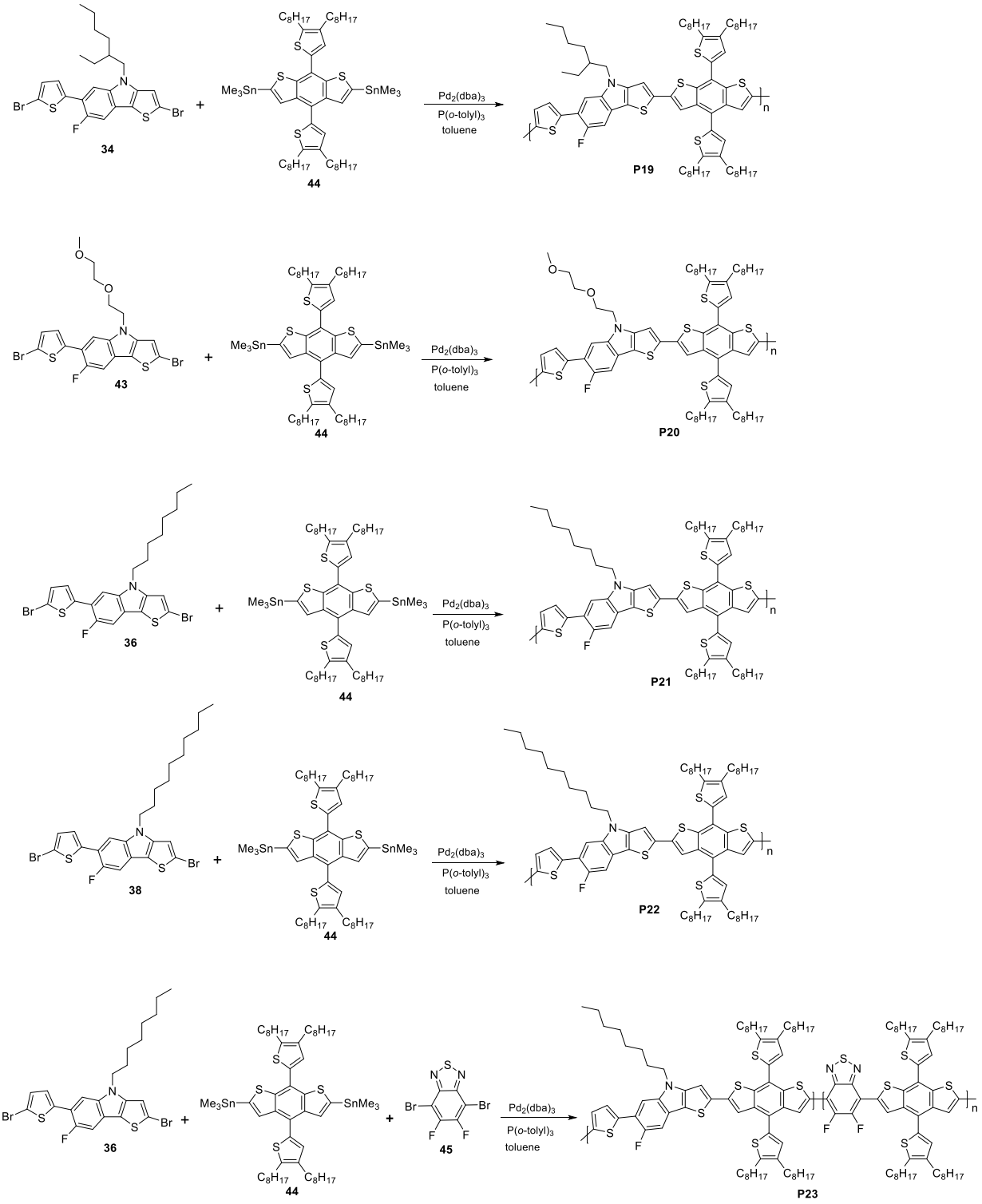

Scheme 16. Syntheses of **P19**, **P20**, **P21**, **P22**, and **P23.**

5.6.2. Optical properties of polymers P19, P20, P21, P22 and P23

The UV-Vis absorption spectra of all copolymers were recorded both in chloroform solutions and as thin films. The thin films were prepared by spin coating the chloroform solutions of the polymers on glass slides. **Figure 5** shows the UV-Vis absorption spectra of **P19**, **P20**, **P21**, **P22** and **P23** in solution and as thin films. The spectrum of **P19** in chloroform solution showed two absorption maxima at 369.99 and 547.8 nm. On the other hand, the thin film spectrum of **P19** displayed maxima at 376.27 and 554.5 nm. Likewise, the absorption maxima in chloroform solution of **P20** appeared at 366.92 and 547.5 nm and the corresponding maxima in the thin film spectrum were at 380.94 and 553.5 nm. The spectrum of **P21** in chloroform solution revealed two absorption maxima at 354.22 and 539.87 nm whereas the spectrum of the thin film displayed maxima at 380.65 and 555.10 nm. Similarly, the absorption maxima of **P22** in chloroform solution appeared at 355.68 and 540.01nm and the corresponding maxima in the thin film spectrum appeared at 365.03 and 544.92 nm. The absorption maxima at shorter wavelengths are due to the π-π transitions while the longer wavelength absorption maxima are due to intramolecular charge transfer (ICT) from the donor to the acceptor.[9] The slight difference observed in the absorptions of all polymers is due to differences in the alkyl side chains. The absorption maxima of the polymers exhibited slight red shifts in going from solutions to solid films, which is due to interchain interaction of the polymers in the solid state.[34] The normalized UV-Vis absorption spectrum of **P23** in chloroform solution showed two absorption maxima at 337.28 and 536.22 nm whereas the spectrum of the thin film displayed maxima at 340.63 and 542.84 nm. Unlike polymers **P19** – **P22**, **P23** showed wider absorption at longer wavelength, which is presumably due to the strongly electron deficient 4,7-dibromo-5,6-difluorobenzo[*c*][1,2,5]thiadiazole moiety.

The onsets of absorption (λ_{onset}) in the thin film spectra of the polymers were used to calculate the optical band gaps (E_g^{opt}) according to **Equation 1.**[35]

$$E_g^{opt} = hc/\lambda_{onset} = 1240/\lambda_{onset} \quad (1)$$

Where E_g^{opt} is optical band gap of the polymers, h is the plank constant (6.626×10^{-34} m^2kg/s), c is the speed of light (3×10^8 m/s), and λ_{onset} is the onset of optical absorption. The onsets of absorption in the spectra of thin films of **P19**, **P20, P21, P22 and P23** were estimated to be 597.5, 594.8, 564.4, 594 nm and 719, respectively, and their corresponding optical band gaps were calculated to be 2.07, 2.08, 2.20, 2.09 and 1.72 eV, respectively. **Table 12** summarizes the optical properties of the polymers.

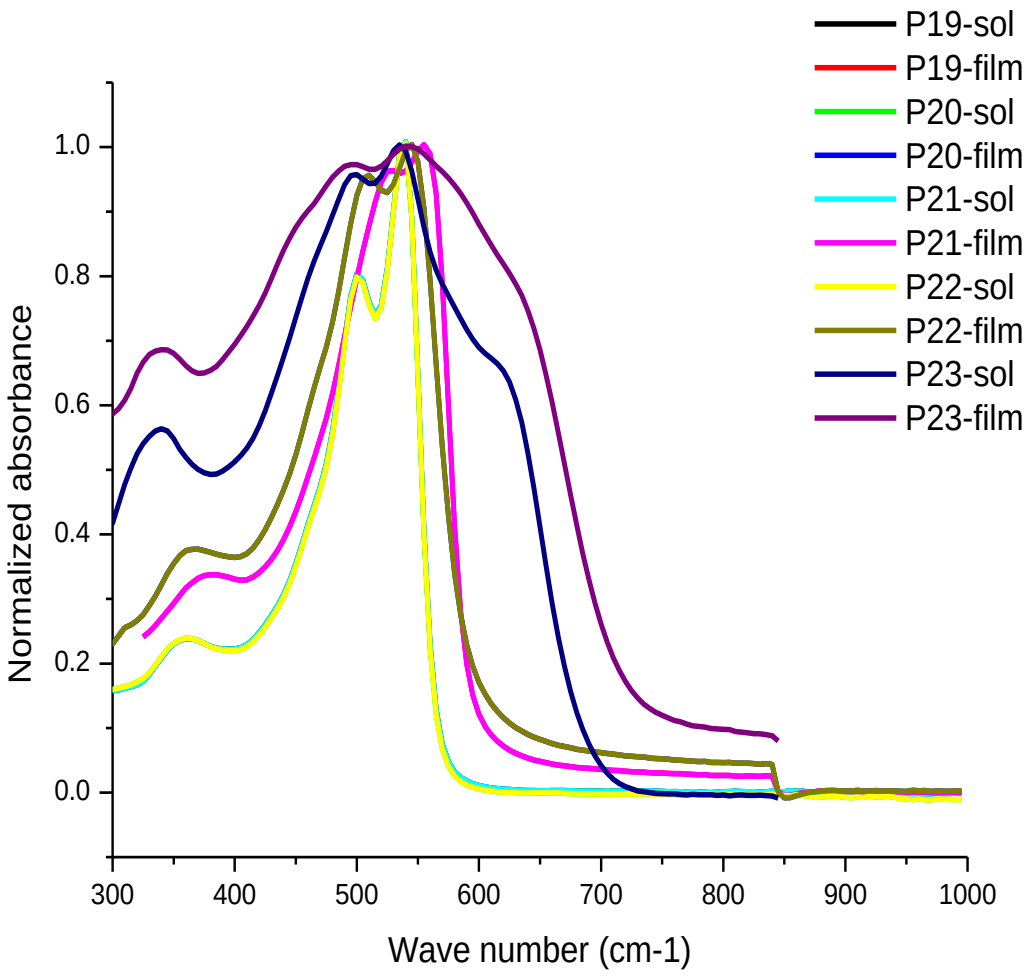

Figure 5. UV–vis absorption spectra of **P19, P20, P21, P22** and **P23** in dilute chloroform solutions and as thin films.

Table 11: Optical properties of **P19**, **P20, P21, P22** and **P23** in solution and as thin films.

Copolymers	λ_{max} (nm)		$\lambda_{max(onset)}$ (nm)	E_g^{opt} (eV)
	Solution	Thin film		
P19	369.99, 547.80	376.27, 554.50	597.5	2.07
P20	366.92, 547.50	380.94, 553.50	594.8	2.08
P21	354.22, 539.87	380.65, 555.10	564.4	2.20
P22	355.68, 540.01	365.03, 544.92	594.0	2.09
P23	337.28, 536.22	340.63, 542.84	719.0	1.72

The effect of the concentration of **P19** on absorption was studied by varying the concentration of the polymer in chloroform from 0.1- 0.003125 g/L. As shown in **Figure 6**, the absorption maxima increased with concentration. **Figure 7** depicts a plot of the concentration of **P19** against absorbance. The extinction coefficient was calculated from the slope of the graph to be 16.33 $gLcm^{-1}$. As can be seen from **Figure 7**, absorption is directly proportional to the concentration, thus as concentration increases, absorbance increases.

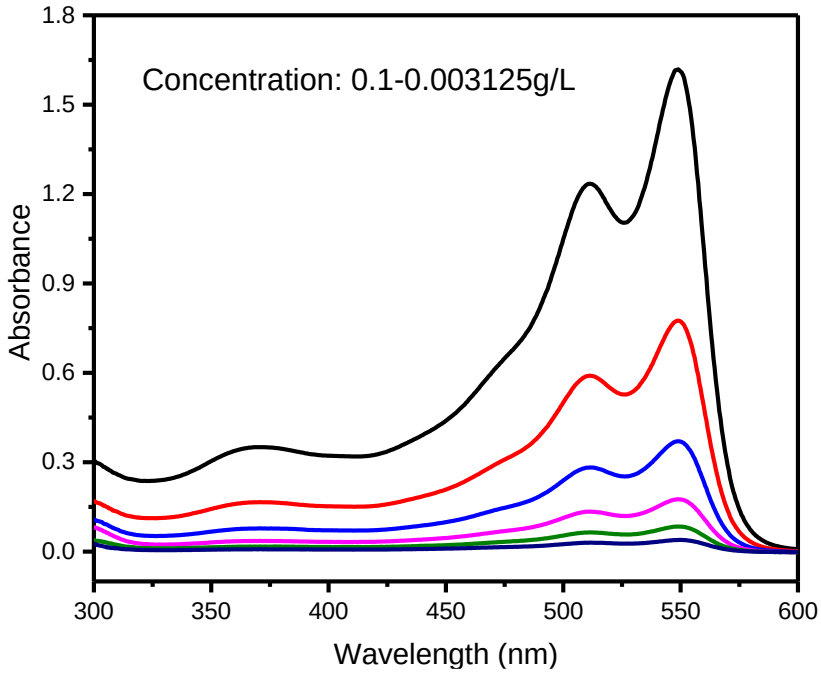

Figure 6. The effect concentration on optical absorption for chloroform solutions of **P19**.

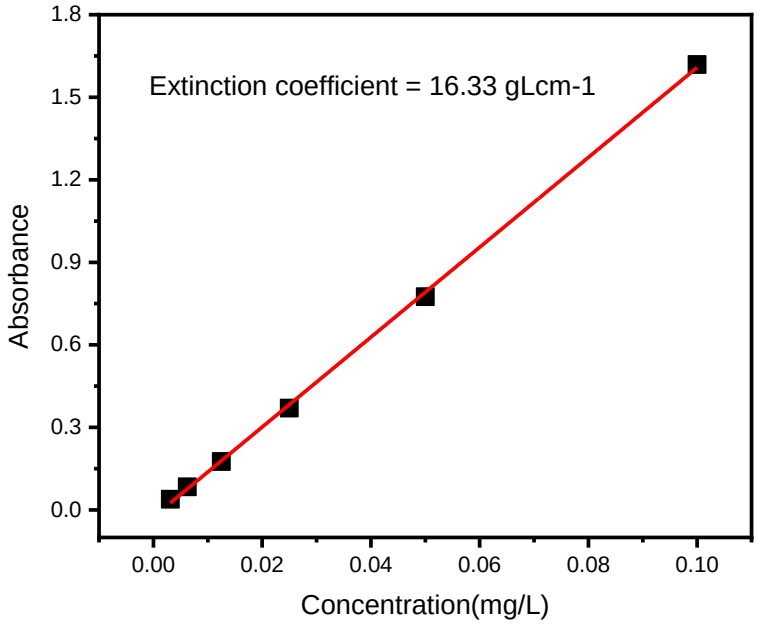

Figure 7. A plot of concentration *versus* absorbance for **P19**

5.6.3. Electrochemical properties of polymers **P19**, **P20**, **P21**, **P22** and **P23**

The electrochemical properties of all polymers were measured by cyclic voltammetry (CV) in anhydrous acetonitrile (CH_3CN) in the presence of 0.1 M tetrabutylammonium perchlorate (Bu_4NClO_4) using a three-electrode system with glassy carbon as the working electrode, platinum wire as the counter or auxiliary electrode and silver wire as the reference under nitrogen atmosphere at room temperature at a scan rate of 50 mV/s. The CV technique was used to determine the onsets of oxidation and reduction potentials of the polymers. **Figure 8** shows the cyclic voltammograms of **P19, P20, P21, P22** and **P23**. The onset potentials were determined from the intersection of the two tangents drawn at the rising current and baseline charging current of the CV traces.[36] These values could be used to determine the energy levels of the HOMO and LUMO of the polymers.[23] Thus, the HOMO energy levels of all polymers were calculated from the onsets of oxidation potentials (E^{ox}_{onset}) using **Equation 2**[24] and the LUMO energy levels were calculated from the HOMO energy levels and the optical band gaps of the polymers using **Equation 3.**

$$E_{HOMO} = - (E_{ox} + 4.4)\ (eV) \qquad (2)$$

$$E_{LUMO} = (E_{HOMO} + E^{opt}_{g}) \qquad (3)$$

Thus, the E^{ox}onset of **P19, P20, P21, P22** and **P23** were estimated to be 1.03, 0.91, 0.9, 0.95 and 1.07 eV and corresponding to HOMO energy levels of -5.43, -5.31, -5.30, -5.35 and -5.47 eV, respectively. The LUMO energy levels of **P19, P20, P21, P22** and **P23** were calculated to be -3.33, -3.23, -3.10, -3.26 and -3.75eV, respectively, from their HOMO energy levels and optical band gaps using **Equation 3**. The HOMO energy level of **P19** is lower than **P20** by -0.12 eV and the HOMO energy level of **P22** is deeper than **P21** by -0.05 eV. This difference in the HOMO energy levels is presumably due to differences in the side chains on the polymer backbones. **P23** showed a deeper HOMO energy level than the other four polymers probably because of the additional electron withdrawing fluorine atoms attached to the polymer backbone.[32, 33] **Table 13** summarizes the electrochemical data of **P19** - **P23**.

Table 12: Electrochemical properties of **P19, P20, P21, P22,** and **P23.**

Copolymers	E_{ox} (V)	HOMO (eV)	LUMO (eV)
P19	1.03	-5.43	-3.33
P20	0.91	-5.31	-3.23
P21	0.90	-5.30	-3.10
P22	0.95	-5.35	-3.26
P23	1.07	-5.47	-3.75

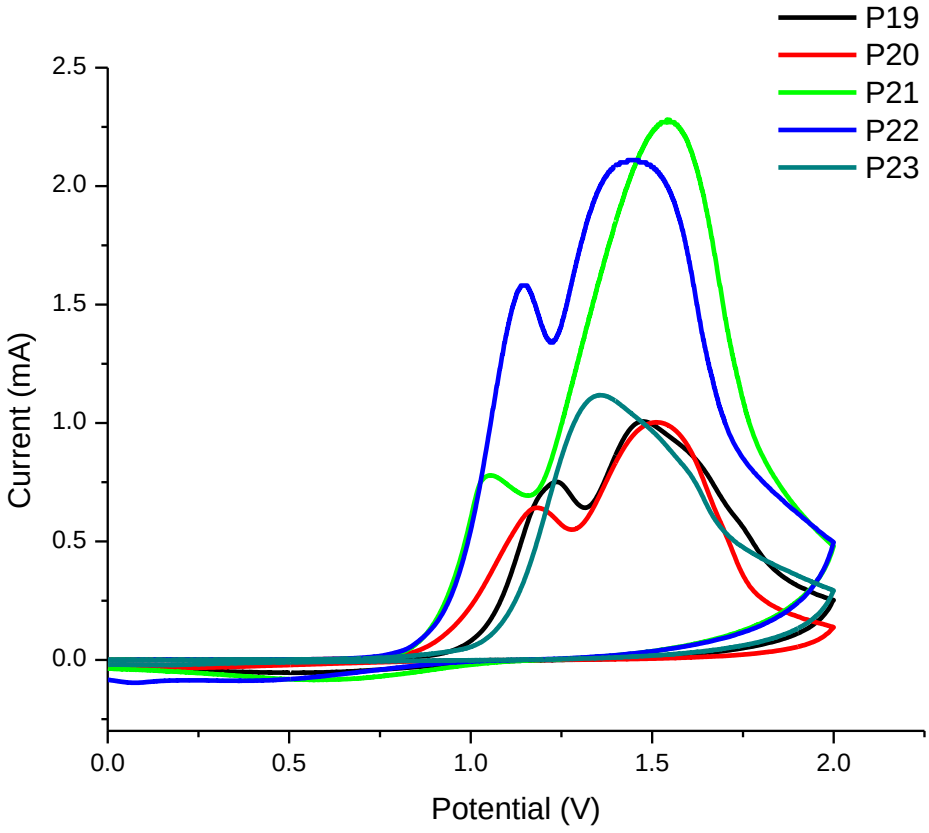

Figure 8. Cyclic voltammograms of **P19**, **P20, P21, P22** and **P23**

6. Conclusion

In the course of this work, four donor monomers (**34**, **36**, **38**, **43**), with 6-(thiophen-2-yl)-4*H*-thieno[3,2-*b*]indole basic skeleton and different side chains on the nitrogen atom, were synthesized starting from 1,4-dibromo-2-fluorobenzene (**29**) and ammonium nitrate. The monomers were characterized based on their ^{1}H- and ^{13}C-NMR spectra. All monomers and intermediate compounds containing fluorine in their structures gave interesting ^{1}H- and ^{13}C-NMR spectra with H-F and C-F couplings. Four polymers (**P19** – **P22**) were prepared by the reaction of these monomers with 4,8-bis(4,5-dioctylthiophen-2-yl)benzo[1,2-*b*:5,4-*b*]dithiophene-2,6-diyl)bis(trimethylstannane) (**44**). One terpolymer (**P23**) was prepared by the co-polymerization of monomer **36**¸with the bis(stannylated)_ monomer **44** and 4,7-dibromo-5,6-difluorobenzo[*c*][1,2,5]thiadiazole (**45**). All polymerization reactions were conducted using the palladium-catalyzed Stille polymerization reaction. The polymers had good solubilities in chloroform and *o*-dichlorobenzene. **P19** – **P22** are high band gap polymers exhibited narrower absorption (350-550) while the terpolymer (**P23**) a medium band gap polymer showed a broader absorption (300-700) in UV-Vis range. The optical band gaps of **P19, P20, P21, P22** and **P23** were estimated from the onsets of absorption in their UV-Vis absorption spectra to be 2.07, 2.08, 2.20, 2.09, and 1.72 eV, respectively. The HOMO energy levels of **P19**, **P20**, **P21**, **P22** and **P23** were determined to be -5.43, -5.31, -5.30, -5.35, and -5.47, and the LUMO energy levels were -3.33, -3.23, -3.10, -3.26, and -3.75, respectively.

7. Experimental

7.1 General

All starting materials were purchased from commercial sources (Sigma-Aldrich, SOLARMER) and were used without further purification. Analytical thin layer chromatographic experiments were done on Merck 0.25 mm silica gel 60 F_{254} pre-coated plates on aluminum. Visualization was performed by an ultraviolent lamp at 254 and 365 nm. Column chromatography was conducted using silica gel as a stationary phase and different kinds of solvents as eluents. The polymers were purified by Soxhlet extraction using acetone and diethyl ether. The high molecular weight polymers were extracted using chloroform. The chloroform solutions of the polymers were further purified by passing them through short columns of silica gel. Purified polymers were collected by membrane filtration (PTFE 0.45 μm).

7.2 Reagents

The following chemicals were used: dichloromethane, chloroform, *o*-dichlorobenzene, trifluoroacetic acid, trifluoroacetic anhydride, 2-bromothiophene, 2-(tributylstannyl)thiophene, tri(*o*-tolyl)phosphine, tris(dibenzylideneacetone)palladium(0), toluene, triphenylphosphine, 1,4-dibromo-2-flourobenzene, methanol, pentane, hexane, potassium hydroxide, *N*,*N*-dimethylformamide (DMF), sodium hydride, tetrahydrofuran (THF), *N*-bromosuccinimide (NBS), 1-bromo-2-ethylhexane, 1-bromooctane, 1-bromodecane, 2-(2-methoxyethoxy)ethan-1-ol, *p*-toluenesulfonyl chloride, magnesium sulfate ($MgSO_4$), sodium sulfate (Na_2SO_4), petroleum ether, acetone, diethyl ether, dichlorobis(triphenylphosphine)palladium(II), (4,8-bis(4,5-dioctylthiophen-2-yl)benzo[1,2-*b*:5,4-*b'*]dithiophene-2,6-diyl)bis(trimethylstannane), 4,7-dibromo-5,6-difluorobenzo[*c*][1,2,5]thiadiazole.

7.3 Instruments

The ^{1}H- and ^{13}C-NMR spectra were recorded on a Bruker Avance 400 spectrometer at 400.13 and 100.6 MHz, respectively, with $CDCl_3$ and CD_2Cl_2 as solvents. ^{1}H and ^{13}C chemical shifts (δ) were reported in ppm using the residual protonated solvent resonance as an internal standard. The coupling constants are reported in hertz (Hz). Splitting patterns are designed as singlet (*s*), doublet (*d*), triplet (*t*), multiplet (*m*), doublet of doublets (*dd*), doublet of triplets (*dt*), doublet of doublet of doublet (*ddd*), *pentet* and *septet*. Cyclic voltammetry (CV)

measurements were carried out on a CH-instruments 650A electrochemical workstation in anhydrous acetonitrile (CH_3CN) in the presence of 0.1M tetrabutylammonium perchlorate (Bu_4NClO_4) using a three-electrode system glassy carbon as working electrode, platinum wire as counter electrode, and silver wire as reference electrode under nitrogen atmosphere at room temperature at a scan rate of 50 mV/s. UV-Vis absorption spectra were recorded on a Perkin-Elmer Lambda 950 and cary60-UV-Vis spectrometer. FT-IR spectra of the monomers were recorded on a Perkin-Elmer spectrum 65 IR spectrometer in the range of 4000- 400 cm^{-1} as KBr pellets.

7.4. Cyclic voltammetric measurements

In the CV experiments, a three electrode setup was used, with glassy carbon as working electrode, platinum wire as counter electrode, and silver wire as reference electrode. Tetrabutylammonium perchlorate (0.1 M) in acetonitrile was used as a supporting electrolyte. Thin polymer films were cast from chloroform solution on to the working electrode. The platinum disk was polished with Al_2O_3 slurry followed by thoroughly rinsing with deionized water, and acetonitrile for each experiment. The electrolyte was purged with nitrogen gas before and in between the measurements. During each scan a flow of nitrogen was kept over the liquid surface in the cell. The potential of the quasi reference electrode was corrected to the Ag/AgCl reference electrode by measuring the ferric/ferrous (Fe^{III}/Fe^{II}) redox couple in the supporting electrolyte-solvent system, which was found to be 0.1 V *versus* Ag/AgCl.

7.5. UV-Vis characterization of the polymers

The UV-Vis absorption spectra of all polymers were recorded using the chloroform solutions of each polymer and as thin films. The thin films were prepared by spin-coating the chloroform solutions of the polymers on glass plates.

7.6. Synthetic procedures

1,4-Dibromo-2-fluoro-5-nitrobenzene (30)[20]

1,4-Dibromo-2-flourobenzene (**29**) (10.08 g, 39.7 mmol) was dissolved in a mixture of dichloromethane (20 mL), trifluoroacetic acid (20 mL), and trifluoroacetic anhydride (10 mL) and cooled in ice/water bath. To the stirred solution, ammonium nitrate (3.88 g, 8.6 mmol) was added and a color change from white to light red was observed and the mixture was allowed to warm to room temperature and stirred overnight. Then, the content was poured in to water and the aqueous layer was separated and exhaustively extracted with DCM. The

combined organic phase was dried over anh. Na_2SO_4 and the solvent was removed by rotary evaporation to afford compound **30** (11.04 g, 93.6%) as a reddish orange solid. ^{1}H-NMR (CD_2Cl_2, 400 MHz): δ8.23 (1H, *d*, *J* = 6.4 Hz, H-6), 7.60 (1H, *d*, *J* = 7.6 Hz, H-3) ; ^{13}C-NMR (CD_2Cl_2): δ160.62 (*d*, *J* = 257 Hz, C-2), 146.06 (C-5), 130.92 *(d*, *J* = 2 Hz, C-6), 122.87 *(d*, *J* = 27 Hz, C-3), 114.88 *(d*, *J* = 9 Hz, C-4), 108.82 *(d*, *J* = 23 Hz C-1).

2,2'-(2-Fluoro-5-nitro-phenylene)dithiophene (**31**)[21]

1,4-Dibromo-2-fluoro-5-nitrobenzene (**30**) (11.04 g, 37.17 mmol) and dichlorobis(triphenylphosphine)palladium(II) (0.52 g, 0.74 mmol) were dissolved in toluene (144.5 mL) and refluxed at 118 ^{o}C under nitrogen atmosphere while stirring. After refluxing for 1 h, 2-(tributylstannyl)thiophene (34.68 g, 29.7 mL, 92.93 mmol,) was added with syringe through a septum and continued stirring overnight. During the reaction, a deep black color was observed. The progress of the reaction was monitored by TLC using *n*-pentane:toluene (1:1) as eluent. When the starting material was completely consumed, the reaction mixture was allowed to cool to room temperature and the solvent was removed by rotary evaporation. The residue was taken up in *n*-pentane and the solid material was separated by suction filtration over a sintered glass funnel and washed with *n*-pentane several times to remove the impurities. The fine grey powder was dried and collected. More of the product was obtained from the mother liquor after removal of the solvent and column filtration of the residue over silica gel. Elution was first made with *n*-pentane to remove the impurities and the desired compound was obtained by elution with *n*-pentane:toluene (1:1). The residue obtained after removal of the solvent was washed with hexane several times to remove traces of impurities. This was combined with the grey powder to afford compound **31** (10.47 g, 92.3%). ^{1}H-NMR ($CDCl_3$, 400 MHz): δ8.10 (1H, *d*, *J* = 6.8 Hz, H-6), 7.60(1H, *dt*, *J* = 1.2, 1.2, 3.6 Hz, , H-3'), 7.50 (1H, *dd*, *J* = 1.2, 5.2, Hz, H-5'), 7.48 (1H, *dd*, *J* = 1.2, 5.2, Hz, H-5"), 7.34 (1H, *d*, *J* = 11.2 Hz, H-3), 7.19 (1H, *ddd*, 0.8, 3.6, 5.2 Hz,, H-4'), 7.16 (1H, *dd*, *J* = 1.2, 3.6 Hz, H-3"), (1H, *dd*, *J* = 3.6, 5.2 Hz, H-4"); ^{13}C-NMR ($CDCl_3$): δ159.19 (*d*, *J* = 256 Hz, C-2), 145.42 (C-5), 135.87 (C-2"), 134.12 *(d*, *J* = 4 Hz, C-4), 128.87 (d, *J* = 10 Hz, C-1), 128.18 (C-5'& C-5"), 127.98 (C-4'), 127.89 (C-4"). 127.82 (C-3'), 127.75 (C-3"), 122.78 (*d*, *J* = 1.5 Hz, C-2'), 124.49 *(d*, *J* = 6, C-6), 119.79 *(d*, *J* = 26 Hz, C-3).

7-Fluoro-6-(thiophen-2-yl)-4*H*-thieno[3,2-*b*]indole (32)[22]

2,2'-(2-Flouro-5-nitro-1,4-phenylene)dithiophene (**31**) (10.47 g, 34.3 mmol) and triphenylphosphine (22.34 g, 85.18 mmol) were dissolved in *o*-dichlorobenzene (69 mL) and heated at 150 ^{o}C with vigorous stirring under nitrogen atmosphere for 21 h during which time a color change from grey to deep brown was observed. After the reaction completed, hexane was added to the reaction mixture to precipitate out the triphenylphosphine oxide byproduct and the resulting precipitate was separated by suction filtration over a sintered glass. Then the filtrate was concentrated under reduced pressure on a rotary evaporator to yield a crude product, which was chromatographed over silica gel using chloroform:hexane (1:1) as eluent. The product was further purified by recrystallization from chloroform:hexane (1:1) to yield compound **32** (7.96 g, 84.90%). as a light yellow solid. ^{1}H-NMR (400 MHz, $CDCl_3$): δ8.10 (1H, *s*, N-H (H-4)), 7.60 (1H, *dd*, *J* = 1.2, 5.2 Hz, H-2), 7.50 (1H, *m*, H-3'), 7.45 (1H, *d*, *J* = 11.6 Hz, H-8), 7.42 (1H, *d*, *J* = 5.6 Hz, H-5), 7.37 (1H, *dd*, *J* = 1.2, 5.2 Hz, H-5'), 7.16 (1H, *ddd*, *J* = 0.8, 3.6, 5.2 Hz, H-4'), 7.04 (1H, *dd*, *J* = 1.2, 5.2 Hz, H-3); ^{13}C-NMR ($CDCl_3$): δ 154.36 *(d, J* = 238.9 Hz, C-7), 145.16 (C-4a), 138.57 *(d, J*= 3.0 Hz, C-8a), 137.85 (C-2'), 128,42 (C-5'), 127.80 (C-2), 125.83 *(d, J* = 6.7 Hz, C-5), 125.06 *(d, J* = 3.6 Hz, C-3), 121.51 (*d, J* = 1.1 Hz, C-8b), 117.86 (C-3a), 117.7 *(d, J* = 3.6 Hz, C-6), 111.62 (C-4'), 110.98 *(d, J* = 4.2 Hz, C-3'), 105.11 *(d, J* = 26 Hz, C-8). IR ν_{max} cm^{-1} (KBr): 1729, 1627, 1567, 1466.

4-(2-Ethylhexyl)-7-fluoro-6-(thiophen-2-yl)-4*H*-thieno[3,2-*b*]indole (33)[25]

In a two-necked round bottom flask, KOH (7.4 g, 131.72 mmol) was dissolved in *N*,*N*-dimethylformamide (29.5 mL) and the resulting solution was stirred at 125 ^{o}C until all potassium hydroxide pellets were dissolved. Then 7-fluoro-6-(thiophen-2-yl)-4*H*-thieno[3,2-*b*]indole (**32**) (1.25 g, 4.57 mmol) was added carefully with solid addition boat and the content was stirred for another 45 min. 2-Ethylhexylbromide (1.44 g, 1.3 mL, 7.47 mmol) was then added dropwise and the mixture was heated following the progress of the reaction by TLC using chloroform:hexane (1:1) as eluent. After four days, the reaction was stopped and the mixture was allowed to cool to room temperature. It was then acidified with 2N HCl and the organic layer was extracted several times with dichloromethane, dried over anh. Na_2SO_4 and concentrated by rotary evaporation to yield a reddish yellow solid product which was a mixture of the desired product and unreacted starting material. Partial purification was first achieved by precipitation of the starting material from toluene and then from hexane.

Finally, the mixture was purified by column chromatography over silica gel using chloroform:hexane (1:1) as eluent to yield compound **33** as a reddish yellow oil (0.25 g, 14.4%). ^{1}H-NMR ($CDCl_3$, 400 MHz): δ7.57 (1H, *d*, *J* = 6.0 Hz, H-5), 7.54 (1H, *dt*, *J* = 1.2, 5.2 Hz, H-5'), 7.50 (1H, *d*, *J* = 11.6 Hz, H-8), 7.43 (1H, *d*, *J* = 5.2 Hz, H-2), 7.40 (1H, *dd*, *J* = 0.8, 5.2 Hz, H-4'), 7.20 (1H, *ddd*, *J* = 0.4, 3.6, 5.1 Hz, H-3'), 7.05 (1H, *d*, *J* = 5.6 Hz, H-3), 4.09 (1H, *dd*, *J* = 7.6, 14.6 Hz, H-1"α), 4.15 (1H, *dd*, *J* = 7.2, 14.6 Hz, H-1"β), 2.01 (2H, *septet*, *J* = 6.4 Hz, H-2"), 1.42 (8H, *m*, H-3", H-4", H-5", H-1'"), 0.97 (3H, *t*, *J* = 6.8 Hz,, H-6"), 0.93 (3H, *t*, *J* = 7.2 Hz,, H-2'"); ^{13}C-NMR($CDCl_3$): δ153.99 (*d*, *J* = 238 Hz, C-7), 147.72 (C-4a), 139.04 (*d*, *J* = 3 Hz, C-8a), 138.39 (C-2'), 127.95 (*d*, *J* = 25 Hz, C-5), 125.76 (*d*, *J* = 7.0 Hz, C-3'), 124.92 (*d*, *J* = 3.0 Hz, C-5'), 120.91 (*d*, *J* = 11 Hz, C-8b), 117.23 (*d*, *J* = 16 Hz, C-6), 115.33 (*d*, *J* = 4 Hz, C-3a), 110.67 (C-2 & 3), 109.22 (C-4'), 105.09 (C-8), 49.44 (C-1"), 40.0 (C-2"), 30.87 (C-3"), 24.31 (C-4"), 23.06 (C-5"), 10.86 (C-6"), 28.77 (C-1'"), 14.10 (C-2'"); IR ν_{max} cm^{-1} (KBr): 2928, 1468, 1324, 1165, 705, 656.

2-Bromo-6-(5-bromothiophen-2-yl)-4-(2-ethylhexyl)-7-fluoro-4*H*-thieno[3,2-*b*]indole (34)[26]

4-(2-Ethylhexyl)-7-fluoro-6-(thiophen-2-yl)-4*H*-thieno[3,2-*b*]indole (**33**) (0.84 g, 2.18 mmol) and *N*-bromosuccinimide (0.78 g, 4.36 mmol) were dissolved in THF (106 mL) and stirred overnight at room temperature under nitrogen atmosphere. The progress of the reaction was monitored by TLC in chloroform:hexane (1:2) as eluent. After every 4 h, *N*-bromosuccinimide (0.1 equiv) was added and after 36 h the reaction was stopped and the solvent was removed under reduced pressure. The residue was then washed with methanol and the methanol extract was concentrated and dichloromethane was added to precipitate out succinimide. The succinimide was separated by decantation and the supernatant was concentrated under reduced pressure. Hexane was added to the residue and the insoluble material was separated by decantation. The solvent was then removed from the supernatant by rotary evaporation to afford a mixture of mono and dibrominated compounds as a yellowish oil, which was further purified by column chromatography over silica gel using hexane:chloroform (100:1) as eluent to afford compound **34** (0.49 g, 49.3%). ^{1}H-NMR ($CDCl_3$ 400 MHz): δ7.41 (1H, *d*, *J* = 6.4 Hz, H-5), 7.38 (1H, *d*, *J* = 11.6 Hz, H-8), 7.22 (1H, *dd*, *J* = 1.2. 4.0 Hz, H-3'), 7.10 (1H, *dd*, *J* = 0.8. 4.0 Hz, H-4'), 7.08 (1H, *s*, H-3), 4.02 (1H, *dd*, *J* = 8.0, 14.6 Hz, H-1"α), 4.08 (1H, *dd*, *J* = 7.2, 14.6 Hz, H-1"β), 1.96 (1H, *septet*, *J* = 6.4

Hz, H-2''), 1.32 (8H, *m*, H-3'', 1''', 4'', 5''), 0.94 (3H, *t*, *J* = 7.2 Hz, H-6''), 0.91 (3H, *t*, *J* = 7.2 Hz, H-2'''); ^{13}C-NMR ($CDCl_3$ 100 MHz): δ153.97 (*d*, *J* = 239 Hz, C-7), 145.42 (C-4a), 140.24 (*d*, *J* = 3.0 Hz, C-2'), 137.12 (C-8a), 130.54 (C-3'), 125.85 (*d*, *J* = 6 Hz, C-5), 120.79 *(d*, *J* = 11 Hz, C-3a), 116.71 (*d*, *J* = 17 Hz, C-6), 115.26 *(d*, *J* = 4 Hz, C-8b), 114.09 (C-5' & C-2), 111.83 (C-3), 49.56 (C-1''), 39.98 (C-2''), 30.77 (C-3''), 24.24 (C-4''), 23.01 (C-5''), 10.82 (C-6''), 28.70 (C-1'''), 14.04 (C-2'''); IR ν_{max} cm^{-1} (KBr) : 2928, 1466, 1167, 794, 638.

7-Fluoro-4-octyl-6-(thiophen-2-yl)-4*H*-thieno[3,2-*b*]indole (**35**)

In a 250 mL two-necked round bottom flask, NaH (8.85 g, 368.86 mmol) and tetrahydrofuran (83 mL) were added and the resulting mixture was stirred under nitrogen atmosphere at 70 ^{o}C. After 2 h, 7-fluoro-6-(thiophen-2-yl)-4*H*-thieno[3,2-*b*]indole (**32**) (3.5 g, 12.09 mmol) was added with a solid addition boat and the mixture was allowed to stir for another 2 h. Then 1-bromooctane (2.8 g, 2.53 mL, 14.50 mmol) was added dropwise and heated to reflux. The progress of the reaction was monitored by TLC using chloroform:hexane (1:1) as eluent. When the starting material was completely consumed after 20 h, the reaction mixture was cooled to room temperature and acidified with 2N HCl and extracted exhaustively with dichloromethane. The organic layer was dried over anh. $MgSO_4$ and concentrated by rotary evaporation to yield a crude product which was a mixture of the alkylating reagent and desired product. The crude product was dissolved in chloroform and adsorbed on silica gel and applied on a column of silica gel and eluted with chloroform: hexane (1:8) to yield compound **35** (2.17 g, 43.95%) as a colorless oil. ^{1}H-NMR($CDCl_3$, 400MHz): δ7.56 (1H, *d*, *J* = 6.4 Hz, H-5), 7.53 (1H, *dt*, *J* = 1.2, 4.0 Hz, H-3'), 7.51 (1H, *d*, *J* = 11.2 Hz, H-8), 7.45 (1H, *d*, *J* = 5.2 Hz, H-2), 7.40 (1H, *dd*, *J* = 1.2, 5.2 Hz, H-5'), 7.20 (1H, *ddd*, *J* = 0.4, 4.0, 5.2 Hz, H-4'), 7.10 (1H, *d*, *J* = 5.2 Hz, H-3), 4.30 (2H, *t*, *J* = 7.2 Hz, H-1''), 1.89 (2H, *pentet*, *J* = 7.2 Hz, H-2''), 1.31 (10H, *m*, H-3''-H-7''), 0.90 (3H, *t*, *J* = 6.8 Hz, H-8''); ^{13}C- NMR($CDCl_3$): δ 153.98 (*d*, *J* = 238 Hz, C-7), 147.30 (C-4a), 138.94 (*d*, *J* = 3 Hz, C-2'), 138.03 (C-3a), 129.55 (*d*, *J* = 11 Hz, C-8a), 128.14 (C-5'), 127.76 (C-4'), 125.81 (*d*, *J* = 6 Hz, C-5), 124.98 (*d*, *J* = 3 Hz, C-3'), 117.27 (*d*, *J* = 17 Hz, C-6), 115.4 (*d*, *J* = 4 Hz, C-8b), 110.50 (C-2), 109.09 (*d*, *J* = 4 Hz, C-3), 105.13 (*d*, *J* = 26 Hz, C-8), 45.43 (C-1''), 31.82 (C-6''), 29.77 (C-5''), 29.29 (C-4''), 29.19 (C-2''), 27.1(C- 3''), 22.65 (C-7''), 14.13 (C-8''); IR ν_{max} cm^{-1} (KBr): 2926, 1469, 1325, 1081, 704, 656.

2-Bromo-6-(5-bromothiophen-2-yl)-7-fluoro-4-octyl)-4*H*-thieno[3,2-*b*]indole (**36**)

In a 250 mL round bottom flask, 7-fluoro-4-octyl-6-(thiophen-2-yl)-4*H*-thieno[3,2-*b*] indole (**35**) (1.91 g, 4.95 mmol) and *N*-bromosuccinimide (1.76 g, 9.91 mmol) were dissolved in tetrahydrofuran (242 mL) and stirred for 17 h at room temperature under nitrogen atmosphere. The progress of the reaction was monitored by TLC using hexane:chloroform (100:1) as eluent. When the reaction was completed after 17 h**,** the solvent was removed by rotary evaporation and the crude product was washed exhaustively with methanol to remove succinimide from the product. The supernatant was concentrated and was washed further with hexane. The insoluble succinimide was removed by decantation and removal of the solvent from the supernatant afforded compound **36** (2.62 g, 97.48%) as a yellowish oil. ^{1}H-NMR(400 MHz, $CDCl_3$): δ7.41 (1H, *d*, *J* = 6.4 Hz, H-5), 7.38 (1H, *d*, *J* = 11.2 Hz, H-8), 7.23 (1H, *dd*, *J* = 1.2, 4.0 Hz, H-3'), 7.10 (1H, *s*, H-3), 7.09 (1H, *d*, *J* = 4.0 Hz, H-4'), 4.18 (2H, *t*, *J* = 7.2 Hz, H-1"), 1.85 (2H, *m*, H-2"), 1.30 (10H, *m*, H-3"-H-7"), 0.90 (3H, *t*, *J* = 6.8Hz, H-8"); ^{13}C- NMR ($CDCl_3$): δ153.96 (*d*, *J* = 238 Hz, C-7), 145.05 (C-4a), 140.17 (*d*, *J* = 3 Hz, C-2'), 136.73 (C-3a), 130.49 (C-4'), 125.87 (*d*, *J* = 6 Hz, C-5), 120.84 (*d*, *J* = 11 Hz, C-8a), 116.715 (*d*, *J* = 17 Hz, C-6), 115.29 (C-8b), 113.95 (C-3), 111.85 (C- 2 &5'), 108.57 (*d*, *J* = 4 Hz, C-3'), 104.93 (*d*, *J* = 26 Hz, C-8), 45.48 (C-1"), 31.81 (C-6"), 29.16 (C-2"), 29.24 (C-4"), 27.08 (C-3"), 22.65 (C-7"), 14.13 (C-8").

4-Decyl-7-fluoro-6-(thiophen-2-yl)-4*H*-thieno[3,2-*b*]indole (**37**)

In a 250 mL two-necked round bottom flask, tetrahydrofuran (52 mL) and NaH (5.50 g, 229.35 mmol) were placed and the mixture was stirred under nitrogen atmosphere for 1 h at 70 ^{o}C. Then 7-fluoro-6-(thiophen-2-yl)-4*H*-thieno[3,2-*b*]indole (**32**) (2.17 g, 7.96 mmol) was added carefully with a solid addition boat and the mixture was allowed to stir for another 2 h. Then 1-Bromodecane (1.67 g, 7.55 mmol) was then added dropwise and the mixture was heated to reflux following the progress of the reaction by TLC using chloroform:petroleum ether (1:1) as eluent. When the starting material was completely consumed after 20 h, the reaction mixture was cooled to room temperature and was acidified with 2N HCl and extracted exhaustively with dichloromethane. The organic layer was dried over anh. $MgSO_4$ and the solvent was removed by rotary evaporation. The crude product was adsorbed on silica gel and chromatographed over silica gel using petroleum ether:chloroform (8:1) as eluent to afford compound **37** (0.82 g, 25%) as light yellow oil. ^{1}H-NMR (400MHz, $CDCl_3$): δ7.57

(1H, *d*, *J* = 6.4 Hz, H-5), 7.55 (1H, *dt*, *J* = 1.2, 1.2, 3.6 Hz, H-3'), 7.51 (1H, *d*, *J* = 11.2 Hz, H-8), 7.44 (1H, *d*, *J* = 5.2 Hz, H-2), 7.40 (1H, *dd*, *J* = 1.2, 5.2 Hz, H-5'), 7.20 (1H, *ddd*, *J* = 0.8, 3.6, 5.2 Hz, H-4'), 7.01 (1H, *d*, *J* = 5.2 Hz, H-3), 4.26 (2H, *t*, *J* = 7.2 Hz, H-1"), 1.90 (2H, *pentet*, *J* = 7.2 Hz, H-2"), 1.32 (14H, *bm*, H-3"-H-9"), 0.93 (3H, *t*, H-10"); ^{13}C-NMR($CDCl_3$): δ154.07 (*d*, *J* = 238 Hz, C-7), 147.38 (C-3a), 139.05 (*d*, *J* = 3.5 Hz C-2'), 138.10 (C-4a), 128.13 (C-2), 127.83 (C-5'), 125.85 (*d*, *J* = 6.5 Hz, C-5), 124.98 (*d*, *J* = 3.5 Hz, C-4'), 121.04 (*d*, *J* = 10.7 Hz, C-8a), 117.32 (d, J = 17Hz, C-6), 115.48 (*d*, *J* = 4.2 Hz), 110.54(C-3), 109.06 (*d*, *J* = 4.2 Hz, C-3'), 105.14(*d*, *J* = 26Hz, C-8), 45.36 (C-1"), 32.02 (C-8"), 29.82 (C-6"), 29.69 (C-7"), 29.44 (C-2"), 29.63 (C-5"), 29.42 (C-4"), 27.22 (C- 3"), 22.84(C-9"), 14.30 (C-10".

2-Bromo-(5-bromothiephen-2-yl)-4-decyl-7-flouro-4*H*-thieno[3,2-*b*]indole (**38**)

In a 100 mL round bottom flask, 7-fluoro-4-decyl-6-(thiophen-2-yl)-4*H*-thieno[3,2-*b*]indole (**37**) (0.77 g, 1.87 mmol) and *N*-bromosuccinimide (0.66 g, 3.71 mmol) were dissolved in tetrahydrofuran (90.9 mL) and the mixture was stirred for 20 h at room temperature under nitrogen atmosphere. The progress of the reaction was monitored by TLC using hexane:chloroform (100:1) as eluent. When the reaction was completed after 20 h, the solvent was removed by rotary evaporation to yield a crude product which was then washed exhaustively with methanol to remove succinimide from the product. The supernatant was concentrated and hexane was added to precipitate out more succinimide. It was then decanted and the solvent was removed to give compound **38** (0.601 g, 77.93%) as a yellow oil. ^{1}H-NMR (400MHz, $CDCl_3$): δ7.43 (1H, *d*, *J* = 5.6 Hz, H-5), 7.40 (1H, *d*, *J* = 11.2 Hz, H-8), 7.24 (1H, *dd*, *J* = 1.2, 4 Hz, H-3'), 7.12 (1H, *s*, H-3), 7.0 (1H, *m*, H-4'), 4.20 (2H, *t*, *J* = 7.2 Hz, H-1"), 1.30 (16H, *bm*, H-2"-9"), 0.90 (3H, *t*, *J* = 6.8 Hz, H-10"); ^{13}C-NMR ($CDCl_3$): δ154.01 (*d*, *J* = 261 Hz, C-7), 140.16 (C-3a), 145.07 (C-2'), 136.76 (C-4a), 130.50 (C-4'), 125.91 (*d*, *J* = 6.2 Hz, C-5), 116.84 (C-8a), 115.30 (C-8b), 113.96 (C-3), 111.85 (*d*, *J* = 4.5 Hz, C-6), 108.64 (*d*, *J* = 4.2 Hz, C-3'), 107.65 (C-5'), 106.37 (C-2), 104.97 (*d*, *J* = 26.1 Hz), C-8), 45.52 (C-1"), 29.27 (C-2"), 27.06 (C-3"), 29.25 (C-4"), 29.46 (C-5"), 29.89 (C-6"), 29.52 (C-7"), 31.86 (C-8"), 22.68 (C-9"), 14.14 (C-10").

2-(2-Methoxyethoxy) ethyl 4-methylbenzenesulfonate (**41**)

In a 100 mL round bottom flask containing 2-(2-methoxyethoxy) ethan-1-ol (**39**) (4.95 mL**)** in THF (7.8 mL), NaOH (2.21 g, 55 mmol) dissolved in water (3 mL) was added and the mixture was cooled to 0 ^{o}C. *p*-Toluenesulfonyl chloride (8.58 g,45 mmol) in THF (10.5 mL) was added dropwise through a pressure equalizing dropping funnel to the reaction mixture over 35 min and the mixture was stirred for 24 h at room temperature under nitrogen atmosphere. It was then washed with distilled water and acidified with 2N HCl and extracted with dichloromethane and concentrated under reduced pressure to give compound **41** (9.5 g, 82.6%) as a pale yellow oil. ^{1}H-NMR (400 MHz, $CDCl_3$): δ7.71 (2H, *d*, *J* = 8.4 Hz, H-2 & H-6), 7.27 (2H, *d*, *J* = 8.4 Hz, H-3 & H-5), 4.10 (2H, *t*, *J* = 4.8 Hz, H-3'), 3.60 (2H, *t*, *J* = 4.8 Hz, H-4'), 3.49 (2H, *m*, H-6'), 3.39 (2H, *m*, H-7'); ^{13}C-NMR ($CDCl_3$): δ144.85 (C-4), 132.79 (C-1), 129.82 (C-3 & C-5), 127.87 (C-2 &C-6), 71.68 (C-7'), 70.50 (C-6'), 68.56 (C-4'), 69.29 (C-3'), 58.9 (C-9'), 21.54 (CH_3).

7-Fluoro-4-(2-(2-methoxyethoxy)ethyl)-6-(thiophen-2-yl)-4*H*-thieno[3,2-*b*]indole (**42**)

In a two-necked round bottom flask containing THF (52 mL), NaH (5.5 g, 229.35 mmol) was added and the mixture was stirred under nitrogen atmosphere for 1 h at 70 ^{o}C. Then 7-fluoro-6-(thiophen-2-yl)-4*H*-thieno[3,2-*b*]indole (**32**) (2.1 g, 7.9 mmol) was added carefully with a solid addition funnel and the mixture was stirred for another 2 h. 2-(2-Methoxyethoxy)ethyl 4-methylbenzenesulfonate (**41**) (1.5 mL) was added to the solution dropwise and heated under reflux for 12 h following the progress of the reaction by TLC using chloroform:hexane (1:1) as eluent. After the reaction was completed, the mixture was cooled to room temperature and was acidified with 2N HCl and exhaustively extracted with dichloromethane. The organic layer was dried over anh. $MgSO_4$, filtered and the solvent was removed. Attempted purification of the crude product by column chromatography over silica gel using chloroform:hexane (4:1) as eluent did not yield compound **42** as a pure product. Thus, the mixture was carried over to the next step without further purification.

2-Bromo-6-(5-bromothiophen-2-yl)-7-fluoro-4-(2-(2-methoxyethoxy)ethyl)-4*H*-thieno-[3,2-*b*]indole (**43**)

In a two-necked round bottom flask, 7-fluoro-4-(2-(2-methoxyethoxy)ethyl)-6-(thiophen-2-yl)-4*H*-thieno[3,2-*b*]indole (**42**) (1.89 g, 2.4 mmol) and *N*-bromosuccinimide (0.85 g, 4.78 mmol) were dissolved in tetrahydrofuran (116.5 mL) and stirred for 17 h at room temperature under nitrogen atmosphere. The progress of the reaction was monitored by TLC using chloroform:hexane (1:1) as eluent. When the reaction was to complete after 17 h, the mixture was cooled and concentrated by rotary evaporation to yield a crude product was taken up in methanol and the insoluble material was separated by decantation. This was repeated several times to afford compound **43** (1.512 g, 80%) as a white solid. ^{1}H-NMR (400 MHz, $CDCl_3$): δ7.51 (1H, *d*, *J* = 6.0 Hz, H-5), 7.36 (1H, *d*, *J* = 11.6 Hz, H-8), 7.23 (1H, *dd*, *J* = 1.2, 4.0 Hz, H-3'), 7.18 (1H, *s*, H-3), 7.08 (1H, *dd*, *J* = 0.8, 4.0 Hz, H-4'), 4.40 (2H, *t*, *J* = 5.2 Hz, H-1''), 3.85 (2H, *t*, *J* = 5.2 Hz, H-2''), 3.53 (2H, *m*, H-5''), 3.45 (2H, *m*, H-4''), 3.30 (3H, *s*, H-7''); ^{13}C-NMR (100 MHz, $CDCl_3$): δ154.10 (*d*, *J* = 239 Hz, C-7), 145.39(C-4a), 140.09(C-2'), 137.01 (C-3a), 130.45 (C-4'), 125.8 *(d*, *J* = 6 Hz, C-5), 120.9 *(d*, *J* = 11 Hz, C-8a), 116.7 (*d*, *J* = 16 Hz, C-6), 115.6 (C-5'), 115.03 (C-2), 114.66 (C-3), 111.87 *(d*, *J* = 6 Hz, C-8b), 108.93 (*d*, *J* = 4 Hz, C-3'), 104.83 (*d*, *J* = 26 Hz C-8), 71.97 (C-5''), 70.87 (C-4''), 70.16 (C-2''), 59.11(C-7''), 45.66 (C-1'').

Synthesis of P19

In a 50 mL two-necked round bottom flask, 2-bromo-6-(5-bromothiophen-2-yl)-4-(2-ethylhexyl)-7-fluoro-4*H*-thieno[3,2-*b*]indole (**34**) (110 mg, 0.2 mmol), $Pd_2(dba)_3$ (3.66 mg, 2 mol%), P(*o*-tolyl)$_3$ (4.87 mg, 8 mol%), and (4,8-bis(4,5-dioctylthiophen-2-yl)benzo[1,2-*b*:5,4-*b'*]dithiophene-2,6-diyl)bis(trimethylstannane) (**44**) (225.8 mg. 0.2 mmol) were placed and the mixture was purged with nitrogen/vacuum cycles. Degassed toluene (8 mL) was then added and the mixture was heated at 100 ^{o}C with vigorous stirring. After 40 min, 2-tributhylstanylthiophene (0.3 mL) was added as an end-capper. After heating for 30 min, 2-bromothiophene (0.3 mL) was added and heating continued for an additional 30 min. The reaction mixture was then cooled to room temperature and the polymer was precipitated by pouring the solution in to acetone and filtered through a thimble. The polymer was then subjected to Soxhlet extraction with acetone, diethyl ether and chloroform. The cooled chloroform extract was concentrated and passed through a short column of silica gel using

chloroform as eluent. The purified polymer was then precipitated from acetone, filtered through 0.45 μm PTFE membrane filter and dried to afford **P19** (209 mg, 88.6%)..

Synthesis of P20

In a 50 mL two-necked round bottom flask, 2-bromo-6-(5-bromothiophen-2-yl)-7-fluoro-4-(2-(2-methoxyethoxy) ethyl)-4*H*-thieno[3,2-*b*]indole (**43**) (106.65 mg, 0.2 mmol), $Pd_2(dba)_3$ (3.66 mg, 2 mol%), P(*o*-tolyl)$_3$ (4.87 mg, 8 mol%), and (4,8-bis(4,5-dioctylthiophen-2-yl)benzo[1,2-*b*:5,4-*b'*]dithiophene-2,6-diyl)bis(trimethylstannane) (**44**) (225.8 mg. 0.2 mmol) were placed and the mixture was purged with nitrogen/vacuum cycles. Then, degassed toluene (8 mL) was added and the mixture was heated at 100 ^oC with vigorous stirring. After 50 min the polymer was end-capped by adding sequentially 2-tributhylstanylthiophene (0.3 mL) and 2-bromothiophene (0.3 mL) at 45 min interval. The mixture was heated for another 50 min, cooled to room temperature and the polymer was precipitated by pouring the mixture in to methanol. The polymer was then collected by filtration through a Soxhlet thimble and was Soxhlet extracted with acetone, diethyl ether and chloroform. The chloroform extract was concentrated and passed through a short column of silica gel using chloroform as eluent and the polymer was precipitated from methanol, filtered by suction over a 0.45 μm PTFE membrane filter and dried to yield **P20** (210.2 mg, 89.5%).

Synthesis of P21

In a 50 mL two necked round bottom flask, 2-bromo-6-(5-bromothiophen-2-yl)-7-fluoro-4-octyl-4*H*-thieno[3,2-*b*]indole (**36**) (110 mg, 0.2 mmol), $Pd_2(dba)_3$ (3.66 mg, 2 mol%), P(*o*-tolyl)$_3$ (4.87 mg, 8 mol%), and (4,8-bis(4,5-dioctylthiophen-2-yl)benzo[1,2-*b*:5,4-*b'*]dithiophene-2,6-diyl)bis(trimethylstannane) (**44**) (225.8 mg. 0.2 mmol) were placed and the mixture was purged with nitrogen/vacuum cycles.. Degassed toluene (8 mL) was then added and the mixture was heated at 100 ^oC with vigorous stirring. After 45 min, the mixture became viscous and the polymer was end-capped by adding sequentially 2-tributhylstanylthiophene (0.3 mL) and 2-bromothiophene (0.3 mL) at 45 min interval. The mixture was heated for another 50 min, cooled to room temperature and the polymer was precipitated by adding the mixture in to methanol. The polymer was then collected by filtration through a Soxhlet thimble and was subjected to Soxhlet extraction with acetone,

diethyl ether and chloroform. The chloroform extract was concentrated, passed through a short column of silica gel using chloroform as eluent, and the polymer was precipitated from methanol. The polymer was finally collected by suction filtration over a 0.45 μm PTFE membrane filter and dried to yield **P21** (208.3 mg, 88.3%).

Synthesis of P22

In a 50 mL two-necked round bottom flask were placed 2-bromo-6-(5-bromothiophen-2-yl)-4-decyl-7-fluoro-4*H*-thieno[3,2-*b*]indole (**38**) (114.3 mg, 0.2 mmol), $Pd_2(dba)_3$ (3.66 mg, 2 mol%), P(*o*-tolyl)$_3$ (4.87 mg, 8 mol%), and (4,8-bis(4,5-dioctylthiophen-2-yl)benzo[1,2-*b*:5,4-*b'*]dithiophene-2,6-diyl)bis(trimethylstannane) (**44**) (225.8 mg, 0.2 mmol) and the mixture was purged with nitrogen/vacuum cycles. Then, degassed toluene (8 mL) was added and the mixture was heated at 100 ^oC with vigorous stirring. After 50 min the mixture became viscous and the polymer was end-capped by adding 2-tributhylstanylthiophene (0.3 mL) and 2-bromothiophene (0.3 mL) at 50 min interval. Heating continued for another 50 min and the reaction mixture was cooled to room temperature and the polymer was precipitated by addition in to an Erlenmeyer flask containing methanol. The polymer was then collected by filtration through a Soxhlet thimble and was Soxhlet extracted with acetone, diethyl ether and chloroform. The chloroform extract was concentrated and was passed through a short column of silica gel using chloroform as eluent. The polymer was then precipitated from acetone and was collected by suction filtration over a 0.45 μm PTFE membrane filter and dried to yield **P22** (202.4 mg, 83.43 %).

Synthesis of P23

In a 50 mL two-necked round bottom flask, 2-bromo-6-(5-bromothiophen-2-yl)-7-fluoro-4-octyl-4*H*-thieno[3,2-*b*]indole (**36**) (54.3 mg, 0.1 mmol), $Pd_2(dba)_3$ (3.66 mg, 2mol%) , P(*o*-tolyl)$_3$ (4.87 mg, 8 mol%), (4,8-bis(4,5-dioctylthiophen-2-yl)benzo[1,2-b:5,4-b']dithiophene-2,6-diyl)bis(trimethylstannane) (**44**) (225.8 mg. 0.2 mmol), and 4.7-dibromo-5,6-diflourobenzo[*c*][1,2,5]thiadiazole (**45**) (32.99 mg, 0.1 mmol) were placed and the mixture was purged with nitrogen/vacuum cycles. Degassed toluene (8 mL) was then added the mixture was heated at 100 ^oC with vigorous stirring. After 75 min, the mixture became viscous and the polymer was end-capped adding 2-tributhylstanylthiophene (0.3 mL) and 2-

bromothiophene (0.3 mL) at 60 min interval. After heating for an additional 60 min the mixture was allowed to cool to room temperature and the polymer was precipitated from methanol, collected by filtration through an extraction thimble and was subjected to Soxhlet extraction with acetone, diethyl ether and chloroform. The chloroform extract was concentrated and passed through column of silica gel using chloroform as eluent. The polymer was then precipitated from methanol and was collected by suction filtration over a 0.45 μm PTFE membrane filter and dried to yield **P23** (229 mg, 84.5%).

8. References

1. X. Zhan, D. Zhu, *Polym. Chem*. **2010**, 1, 1409.
2. G. Sathiyan, G. Siva, E. K. T. Sivakumar, J. Prakash, H. C. Swart, P. Sakthivel, *Colloid Polym. Sci.* **2018**, 296, 1193.
3. Y. J. Cheng, S. H. Yang, C. S. Hsu, *Chem. Rev*. **2009**, 109, 5868.
4. H. Yao, L. Ye, H. Zhang, S. Li, S. Zhang, J. Hou, *Chem. Rev*. **2016**, 116 , 7397.
5. B. A. Abdulahi, X. Xu, P. Murto, O. Inganäs, W. Mammo, E. Wang, *ACS Appl. Energy Mater.* **2018**, 1, 2918.
6. Y. R. Cheon, Y. J. Kim, J. J. Ha, M. J. Kim, C. E. Park, Y. H. Kim, *Macromolecules* **2014**, 47, 8570.
7. J. Yuan, Y. Zhang, L. Zhou, G. Zhang, H.-L. Yip, T.-K. Lau, X. Lu, C. Zhu, H. Peng, P. A. Johnson, M. Leclerc, Y. Cao, J. Ulanski, Y. Li, Y. Zhou, *Joule* **2019**, 3, 1140.
8. Q. Liu, Y. Jiang, K. Jin, J. Qin, J. Xu, W. Li, J. Xiong, J. Liu, Z. Xiao, K. Sun, S. Yang, X. Zhang, L. Ding, *Sci. Bulletin* **2020**, 65, 272.
9. I. Jeong, J. Kim, J. Kim, J. Lee, D. Y. Lee, I. Kim, S. H. Park, H. Suh, *Synth. Met.* **2016**, 213, 25.
10. H. Huang, M. Qiu, Q. Li, S. Liu, X. Zhang, Z. Wang, N. Fu, B. Zhao, R. Yang, W. Huang, *J. Mater. Chem.* C **2016**, 4, 5448.
11. H. Huang, Q. Li, M. Qiu, Z. Wang, X. Zhang, S. Liu, N. Fu, B. Zhao, R. Yang, W. Huang, *RSC Advances* **2016**, 6, 45873.
12. N. Blouin, A. Michaud, M. Leclerc, *Adv. Mater*. **2007**, 19, 2295.
13. R. P. Qin, W. W. Li, C. H. Li, C. Du, C. Veit, H. F. Schleiermacher, M. Andersson, Z. S. Bo, Z. P. Liu, O. Inganäs, U. Wuerfel, F. L. Zhang, *J. Am. Chem. Soc*. **2009**, 13, 114612.
14. H. Yi, S. Al-Faifi, A. Iraqi, D. C. Watters, J. Kingsley, D. G. Lidzey, *J. Mater. Chem.* **2011**, 21, 13649.
15. J. Kim, M. H. Yun, G. Kim, J. Lee, S. M. Lee, S. Ko, Y. Kim, G. K. Dutta, M. Moon, S. Y. Park, D. S. Kim, J. Y. Kim, C. Yang, *ACS Appl. Mater*. *Interfaces* **2014**, 6, 7523.

16. J. R. Tumbleston, A. C. Stuart, E. Gann, W. You, H. Ade, *Adv. Funct. Mater*. **2013**, 23, 3463.

17. P. J. Stevenson, *Org. Biomol. Chem*. **2011**, 9, 2078.

18. M. Wang, X. Hu, L. Liu, C. Duan, P. Liu, L. Ying, F. Huang, Y. Cao, *Macromolecules* **2011**, 44, 894.

19. N. Chakravarthi, K. Kranthiraja, M. Song, K. Gunasekar, P. Jeong, S.-J. Moon, W.S. Shin, I.-N. Kang, J.W. Lee, S.-H. Jin, *Sol. Energy Mater. Sol. Cells*. **2014**, 122, 136.

20. Y. Zhang, S.-C. Chien, K.-S. Chen, H.-L. Yip, Y. Sun, J. A. Davies, F.-C. Chen, A. K.-Y. Jen, *Chem. Commun*. **2011**, 47, 11026.

21. P. Li, O. Fenwick, S. Yilmaz, D. Breusov, D. J. Caruana, S. Allard, U. Scherf, F. Cacialli, *Chem. Commun*. **2011**, 47, 8820.

22. A. W. Freeman, M. Urvoy, M. E. Criswell, *J. Org. Chem.* **2005**, 70, 5014.

23. S. Admassie, O. Inganäs, W. Mammo, E. Perzon, M. R. Andersson, *Synth. Met*. **2006**, 156, 614.

24. A. Misra, P. Kumar, R. Srivastava, S. Dhawan, M. Kamalasanan, S. Chandra, *Indian J. Pure Appl. Phys.* **2005**, 43, 921.

25. Z. Genene, J. Wang, X. Meng, W. Ma, X. Xu, R. Yang, W. Mammo, E. Wang, *Adv. Electron. Mater*. **2016**, 2, 1600084.

26. L. Wang, D. Cai, Q. Zheng, C. Tang, S.-C. Chen, Z. Yin, *ACS Macro Lett.* **2013**, 2, 605.

27. J. Kim, S. Y. Park, G. Han, S. Chae, S. Song, J. Y. Shim, E. Bae, I. Kim , H. J. Kim, J. Y. Kim, H. Suh, *Polymer* **2016**, 95, 36.

28. J. Kim, J. Jeong, J. Lee, S.H. Park, H. Suh, *Macromol. Res.* **2019**, 27, 470.

29. I. Jeong, S. Chae, A. Yi, J. Kim, H. H. Chun, J. H. Cho, H. J. Kim, H. Suh, *Polymer* **2017**, 109, 115.

30. J. Y. Shim, J. Baek, J. Kim, S.Y. Park, J. Kim, I. Kim, H. H. Chun, J. Y. Kim, H. Suh, *Polym*. *Chem*. **2015**, 6, 6011.

31. X-H. Zhang, Y. Cui, R. Katoh, N. Koumura, K. Hara, *J. Phys. Chem. C* **2010,** 114, 18283.

32. N. Leclerc, P. Chávez, O.A. Ibraikulov, T. Heiser, P. Lévêque, *Polymers* **2016**, 8, 11.

33. J. Shin, M. Kim, B. Kang, J. Lee, H.G. Kim, K. Cho *J. Mater. Chem. A,* **2017**, 5, 16702.

34. Z. Li, X. Xu, W. Zhang, X. Meng, W. Ma, A. Yartsev, O. Inganäs, M. R. Andersson, R. A. J. Janssen, E. Wang. *J. Am. Chem. Soc*. **2016**, 138, 10935.

35. J. C. S. Costa, R. J. S. Taveira, C. F. R. A. C. Lima, A. Mendes, L. M. N. B. F. Santos, *Opt. Mat*. **2016**, 58, 51.

36. G. Lu, H. Yang, Y. Zhu, T. Huggins, Z. J. Ren, Z. Liu, W. Zhang, *J. Mater. Chem. A*, **2015**, 3, 4954.

9. Appendices

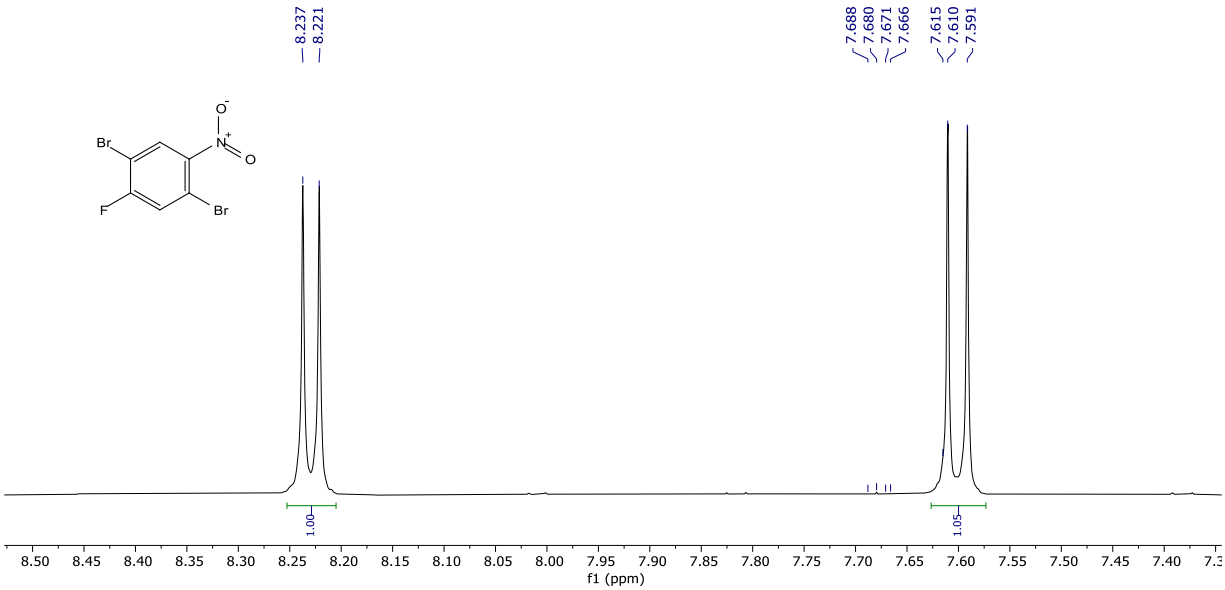

Appendix 1: The ^{1}H-NMR spectrum of 1,4-dibromo-2-fluoro-5-nitrobenzene (**30**).

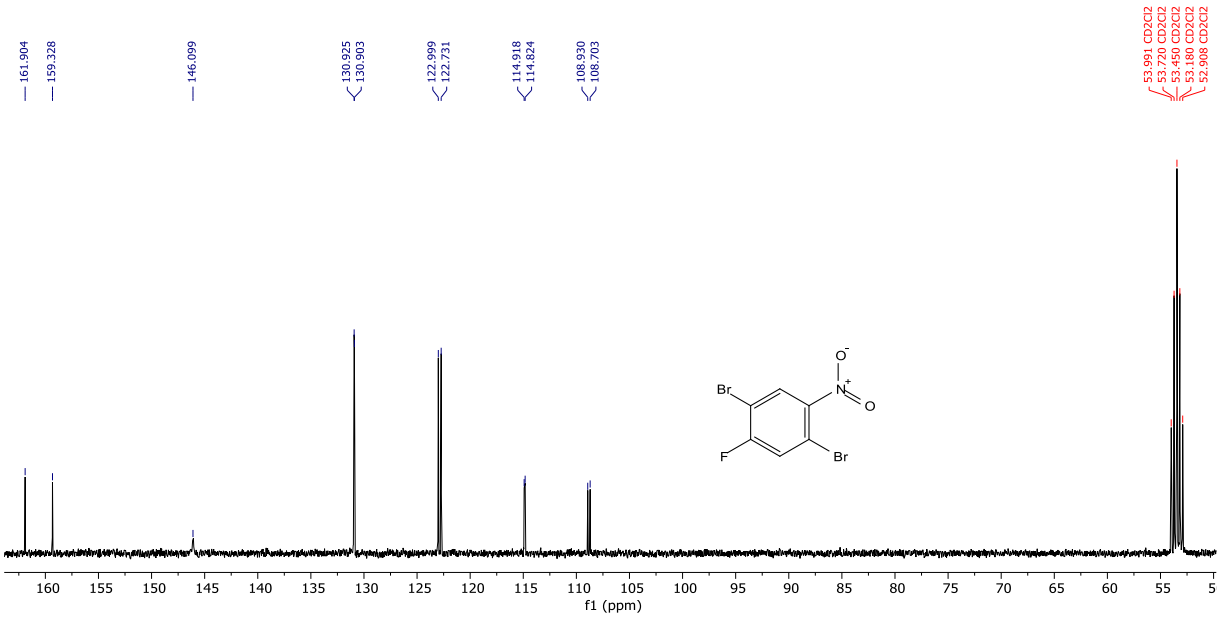

Appendix 2*:* The ^{13}C-NMR spectrum of 1,4-dibromo-2-fluoro-5-nitrobenzene (**30**).

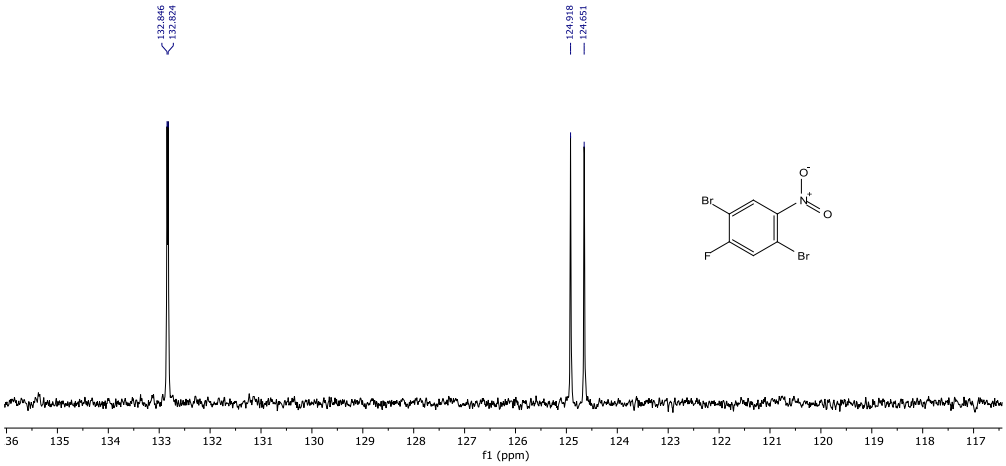

Appendix 3: The DEPT-135 spectrum of 1, 4-dibromo-2-fluoro-5-nitrobenzene (**30**).

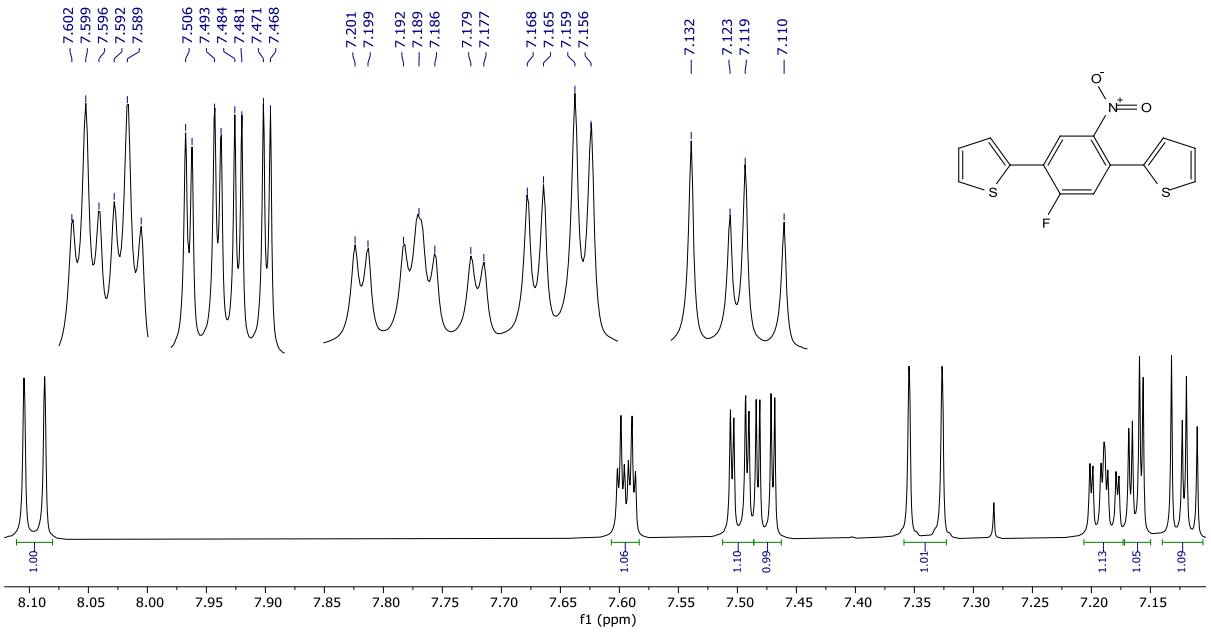

Appendix 4: The ^{1}H-NMR spectrum of 2,2'-(2-fluoro-5-nitro-1,4-phenylene)dithiophene (**31**).

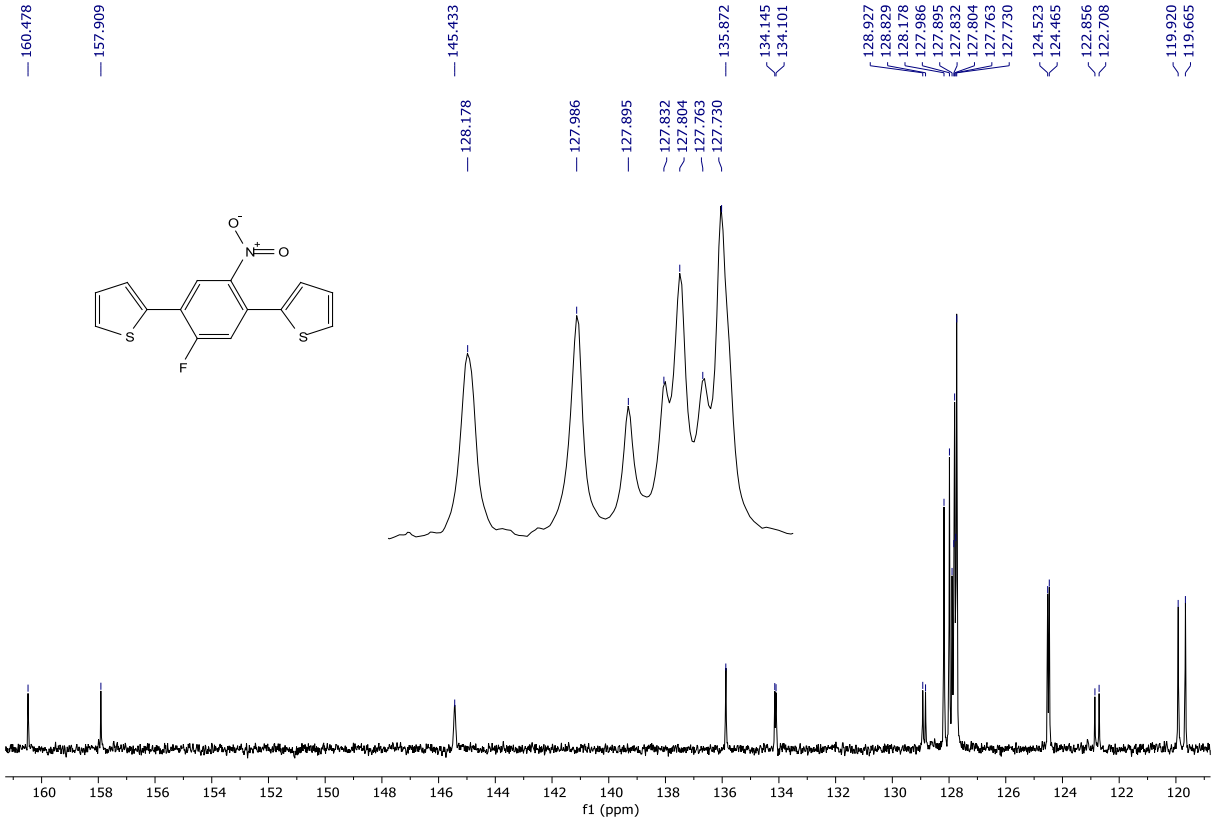

Appendix 5: The ^{13}C-NMR spectrum of 2,2'-(2-fluoro-5-nitro-1,4-phenylene)dithiophene (**31**).

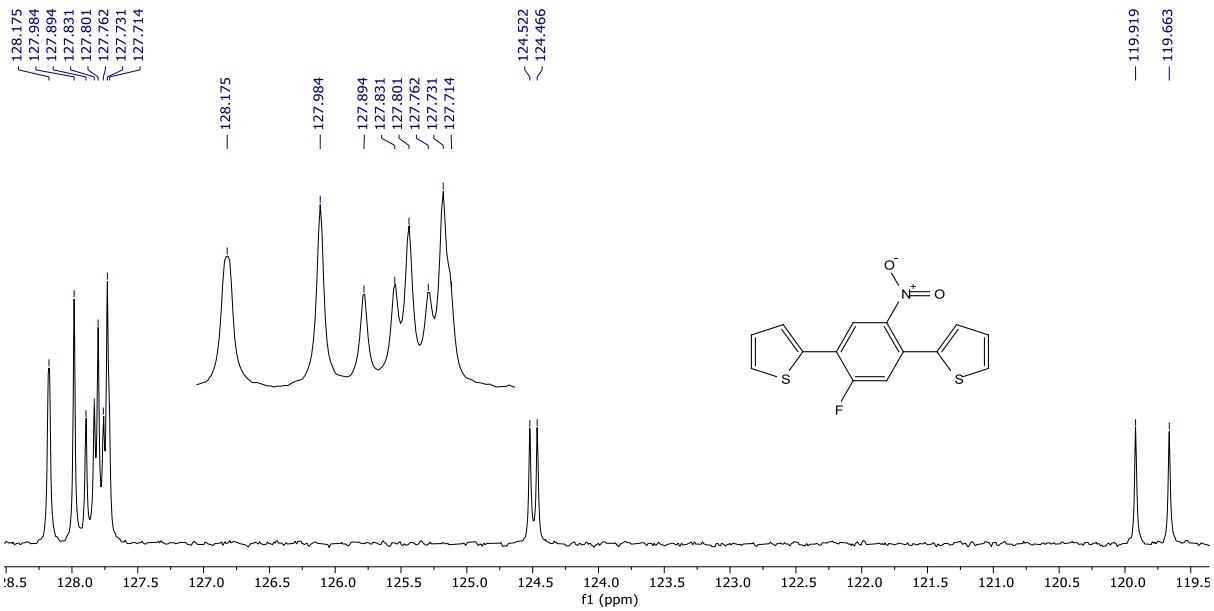

Appendix 6: The DEPT-135 spectrum of 2,2'-(2-fluoro-5-nitro-1,4-phenylene)dithiophene (**31**).

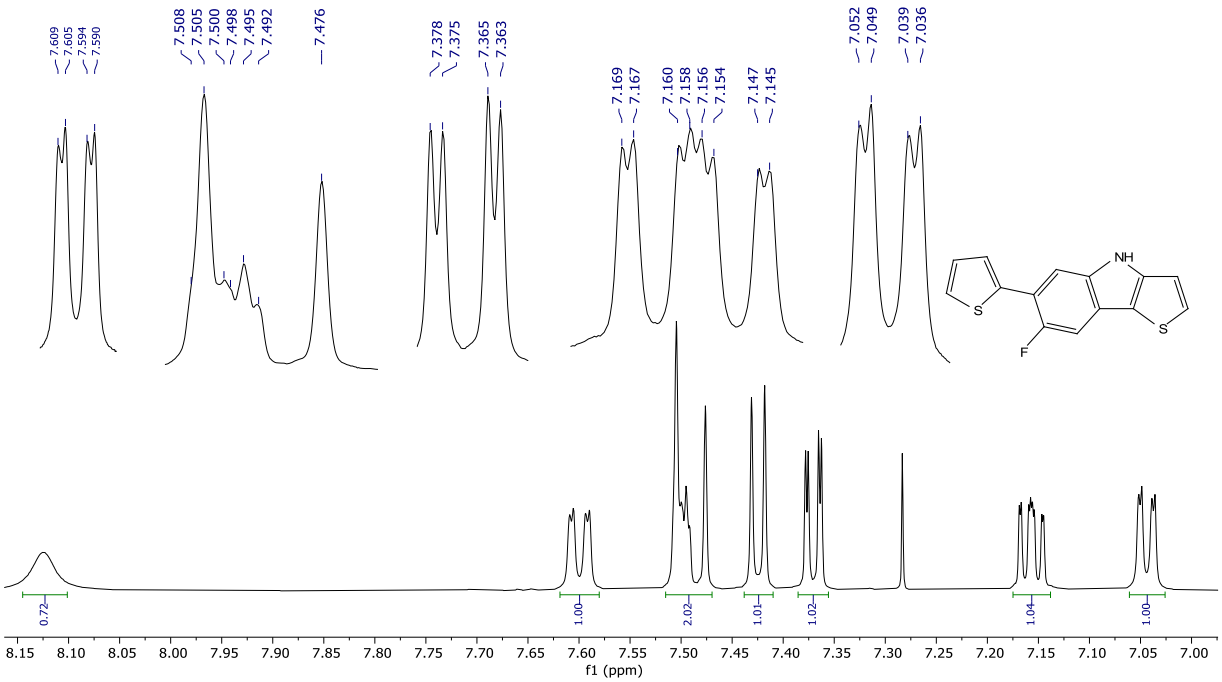

Appendix 7: The ^{1}H-NMR spectrum of 7-fluoro-6-(thiophen-2-yl)-*4H*-thieno[3,2-*b*]indole *(***32***)*.

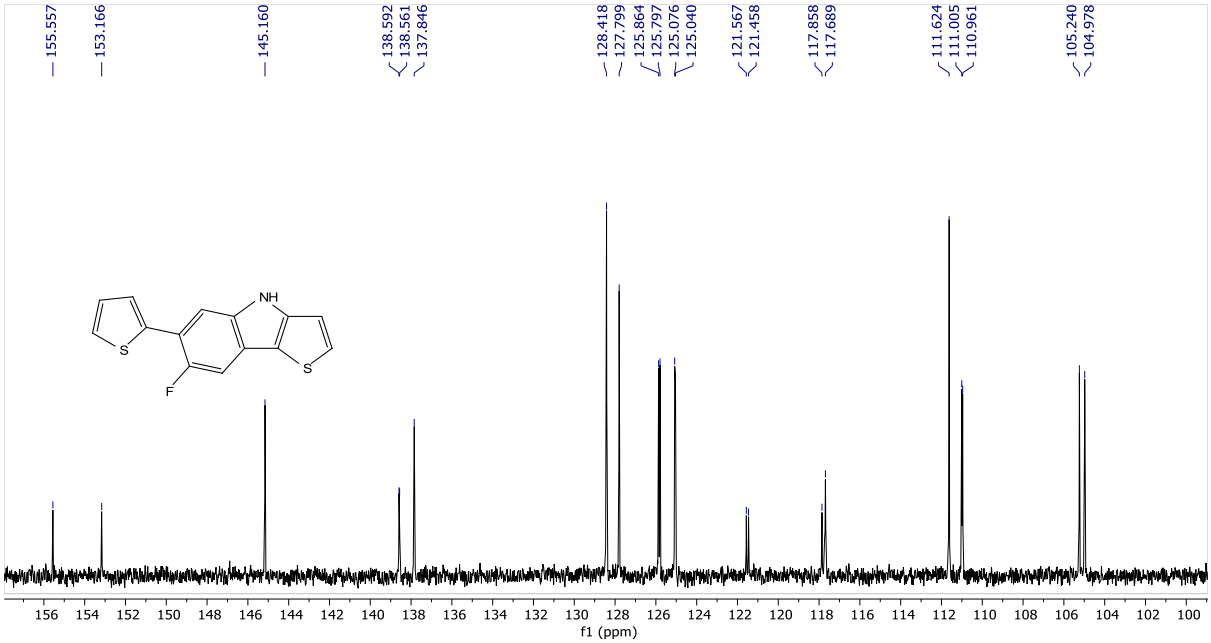

Appendix 8*:* The ^{13}C-NMR spectrum of 7-fluoro-6-(thiophen-2-yl)-4*H*-thieno [3,2-*b*]indole (**32**).

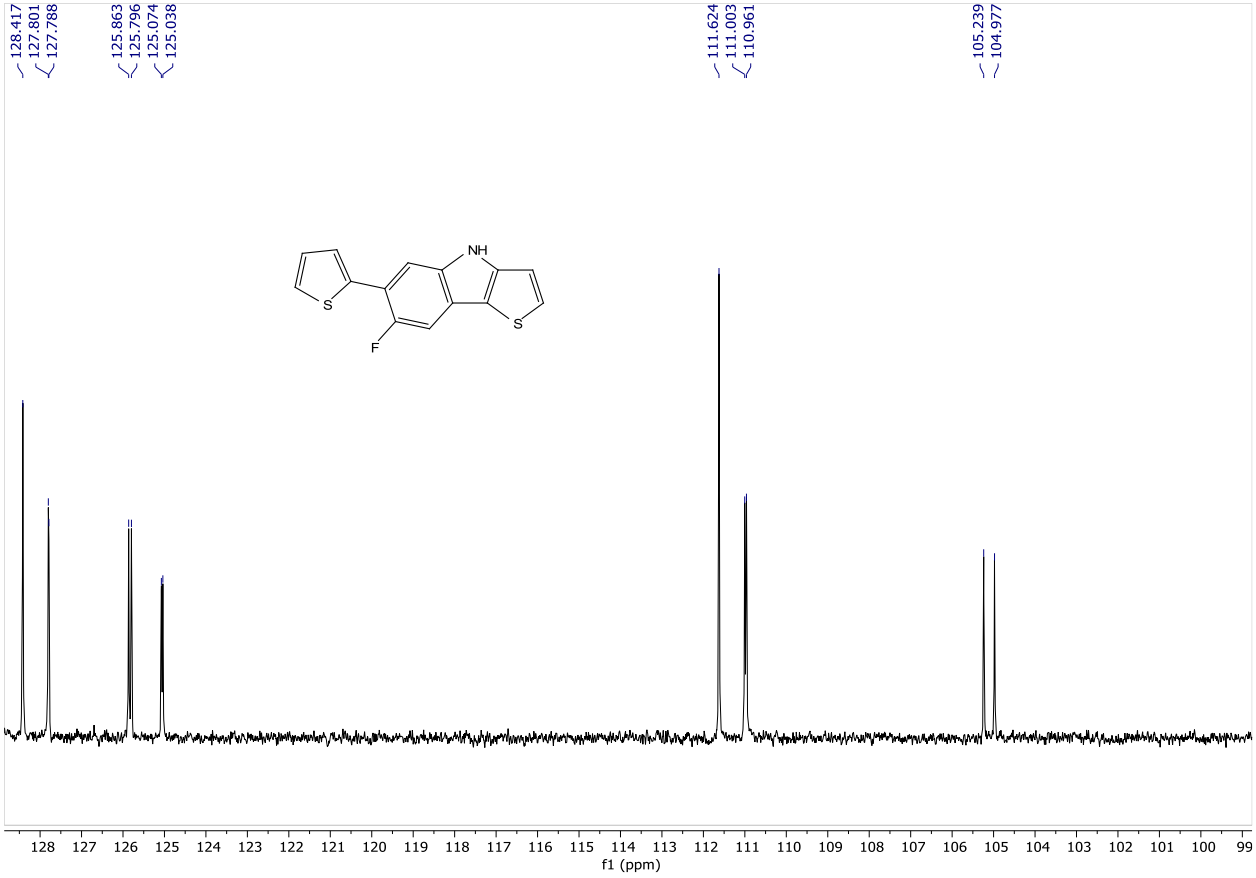

Appendix 9: The DEPT-135 spectrum of 7-fluoro-6-(thiophen-2-yl)-*4H-t*hieno [3,2-*b*]*i*ndole (**32**).

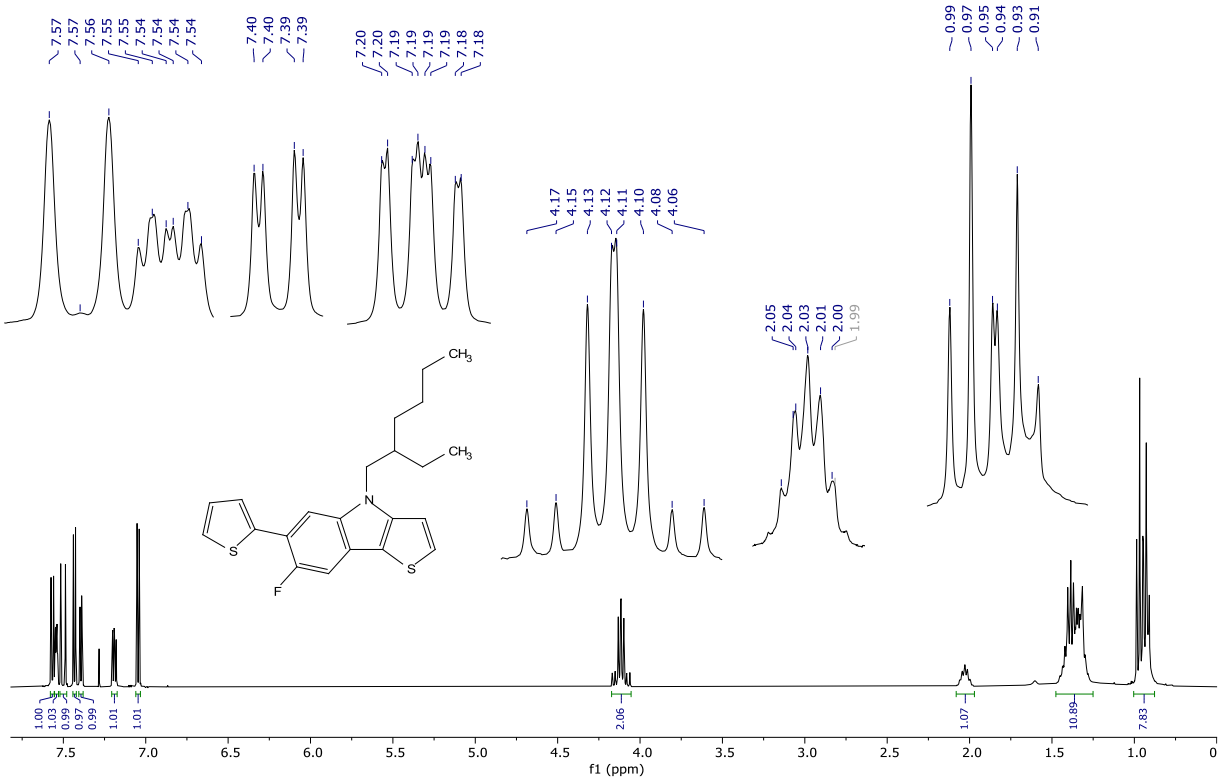

Appendix 10: The ^{1}H-NMR spectrum of 4-(2-ethylhexyl)-7-fluoro-6-(thiophen-2-yl)-*4H*-thieno[3,2-*b*]*i*ndole (**33**).

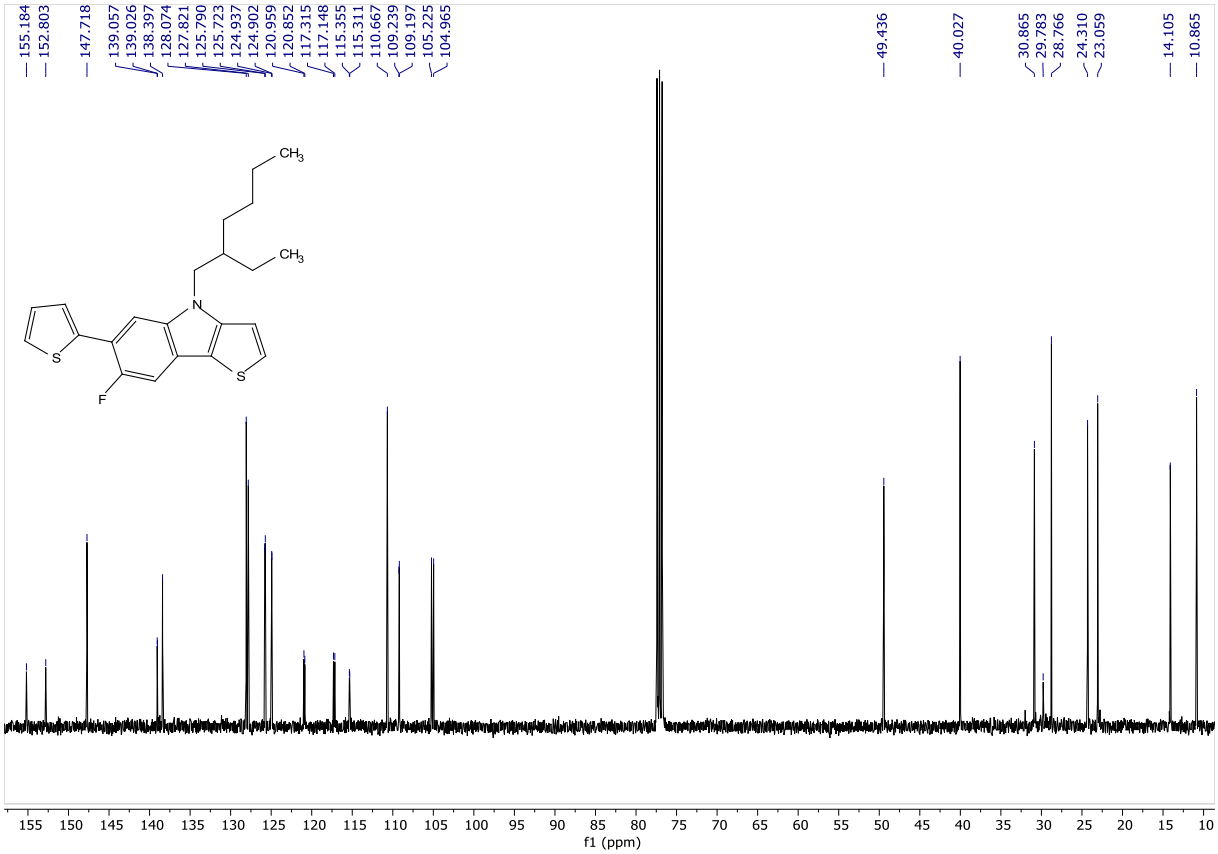

Appendix 11*:* The ^{13}C-NMR spectrum of 4-(2-ethylhexyl)-7-fluoro-6-(thiophen-2-yl*)-4H*-thieno[3,2-*b*]indole (**33**).

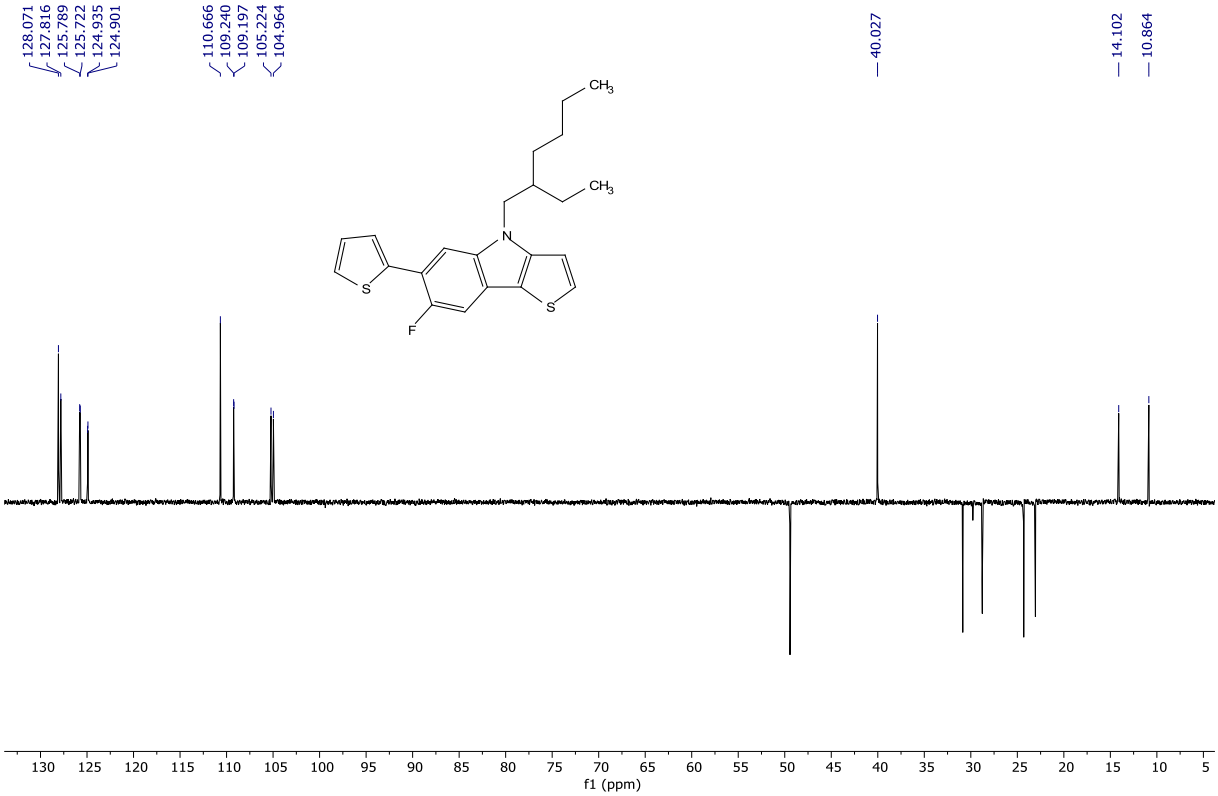

Appendix 12: The DEPT-135 spectrum of 4-(2-ethylhexyl)-7-fluoro-6-(thiophen-2-yl)-*4H*-thieno[3,2-*b*]indole (**33**).

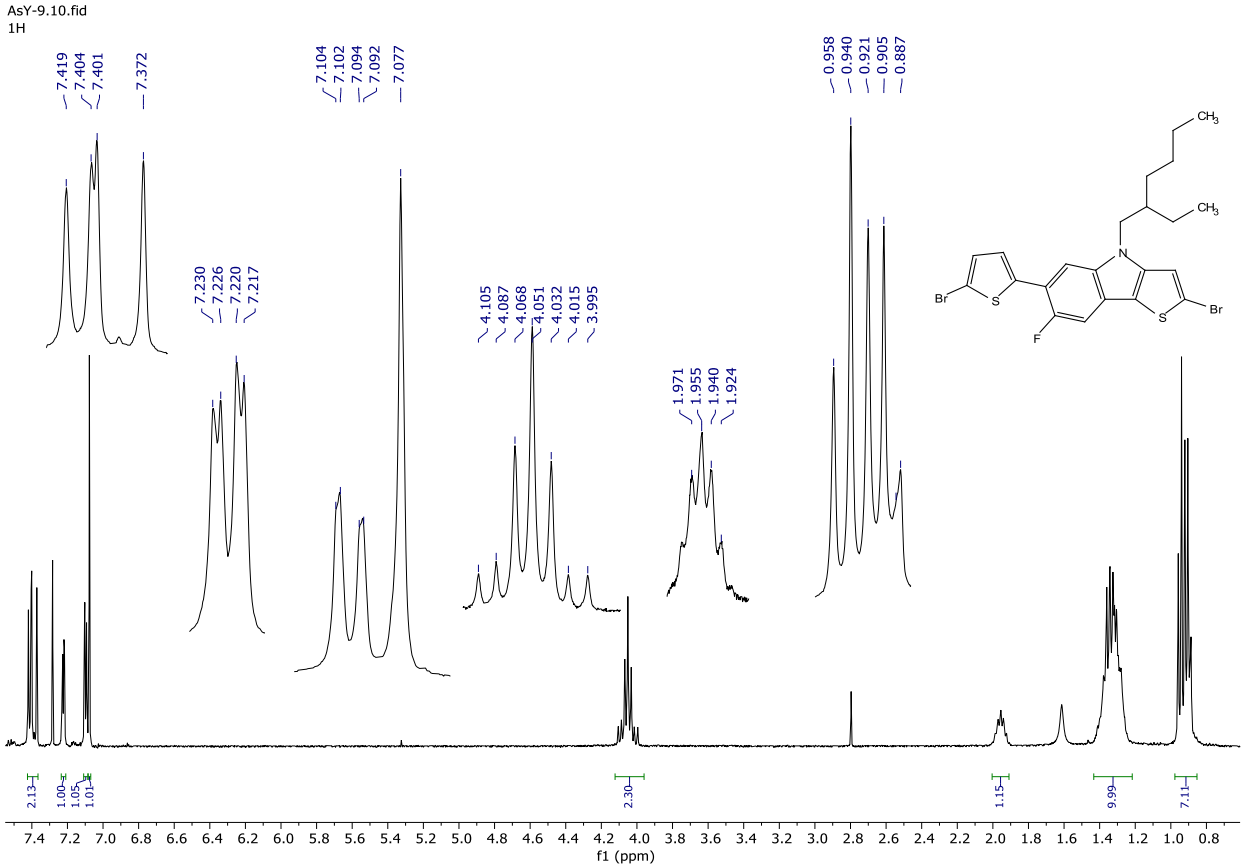

Appendix 13: The ^{1}H-NMR spectrum of 2-bromo-6-(5-bromothiophen-2-yl)-4-(2-ethylhexyl)-7-fluoro-*4H*-thieno[3,2-*b*]indole (**34**).

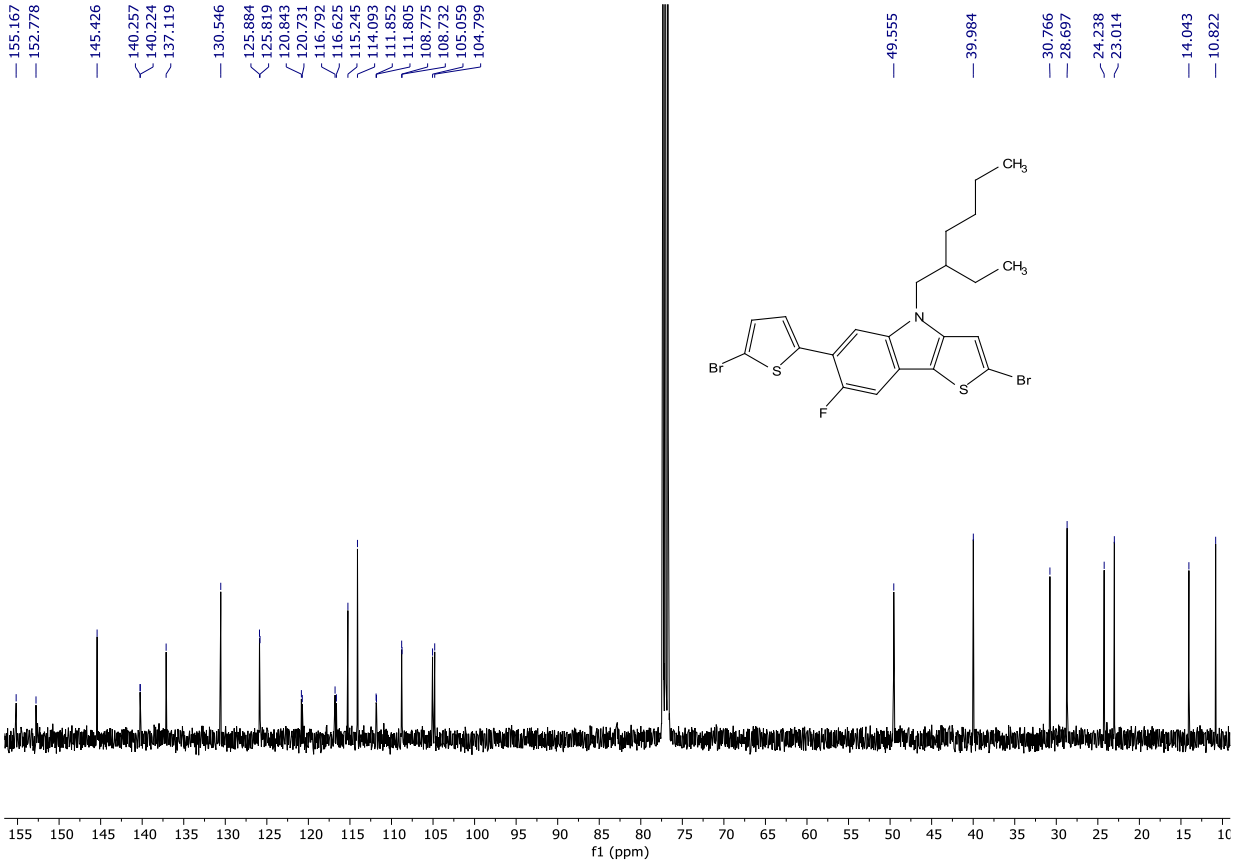

Appendix 14: The ^{13}C-NMR spectrum of 2-bromo-6-(5-bromothiophen-2-yl)-4-(2-ethylhexyl)-7-fluoro-*4H*-thieno[3,2-*b*]indole (**34**).

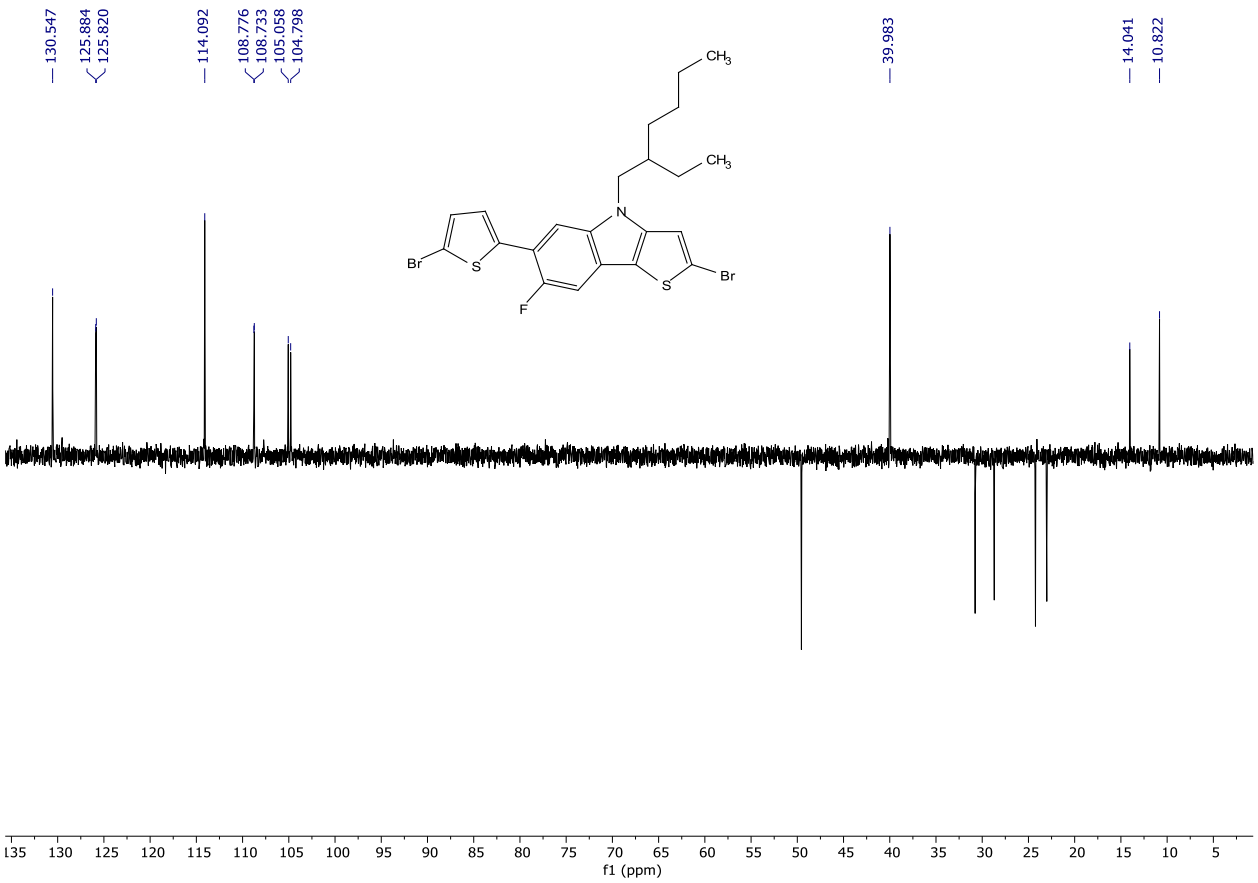

Appendix 15: The DEPT-135 spectrum of 2-bromo-6-(5-bromothiophen-2-yl)-4-(2-ethylhexyl)-7-fluoro-*4H*-thieno[3,2-*b*]indole (**34**).

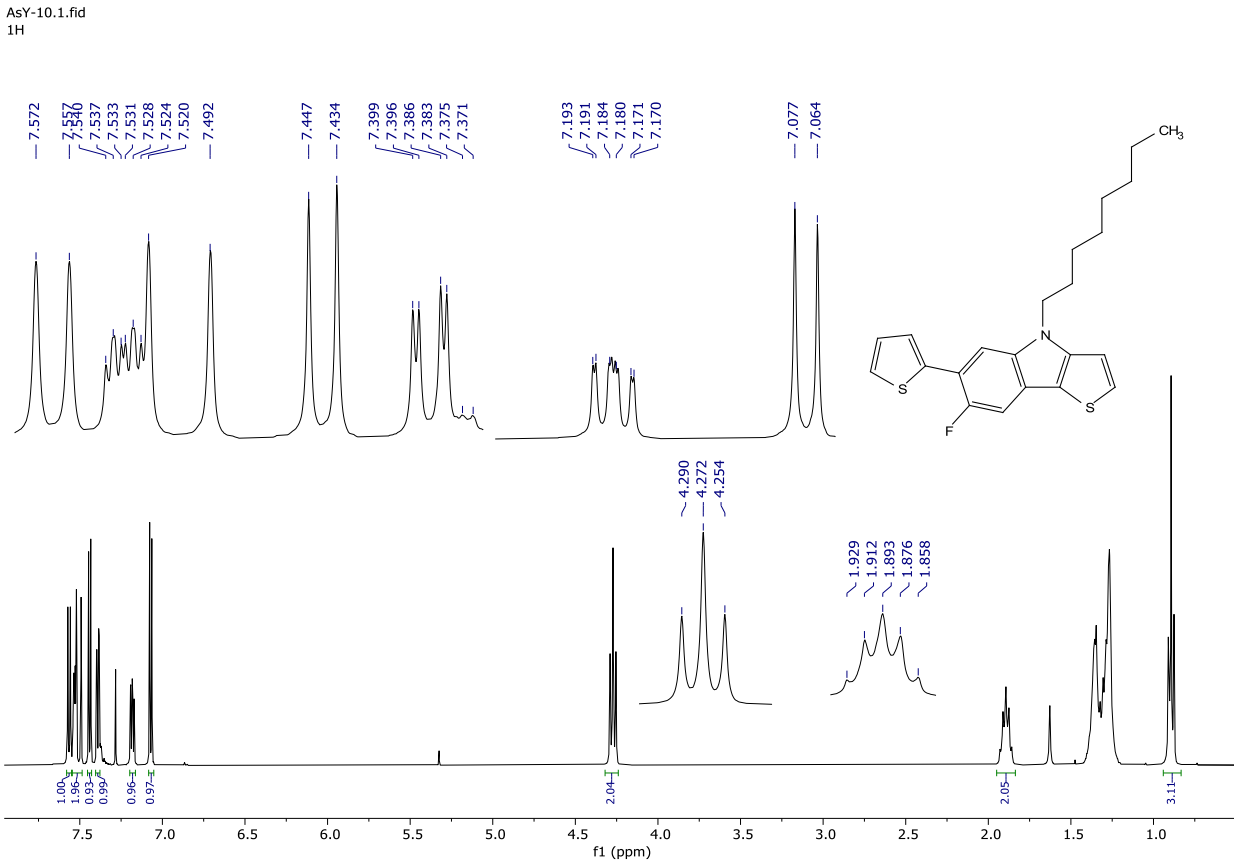

Appendix 16: The ^{1}H-NMR spectrum of 7-fluoro-4-octyl-6-(thiophen-2-yl)-*4H*-thieno[3,2-*b*]indole (**35**).

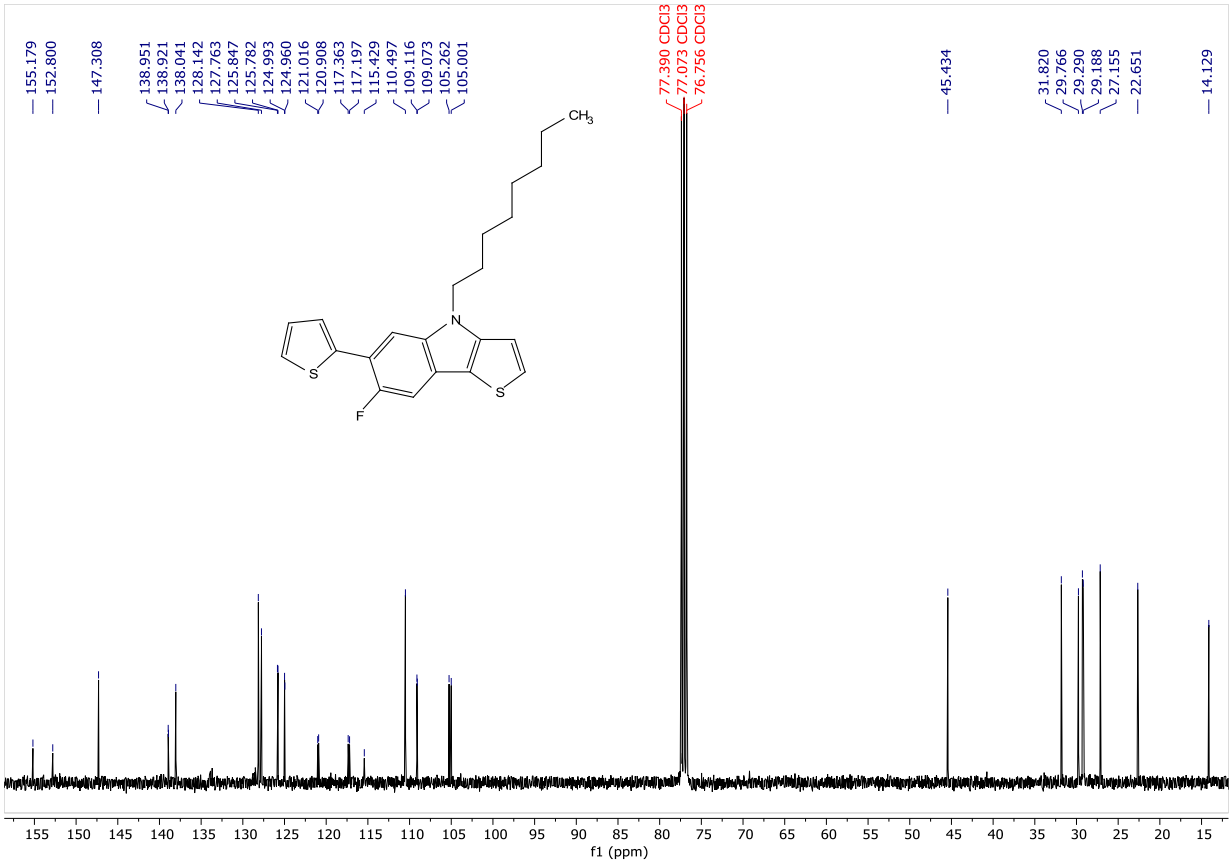

Appendix 17: The ^{13}C-NMR spectrum of 7-fluoro-4-octyl-6-(thiophen-2-yl)-*4H*-thieno[3,2-*b*]indole (**35**).

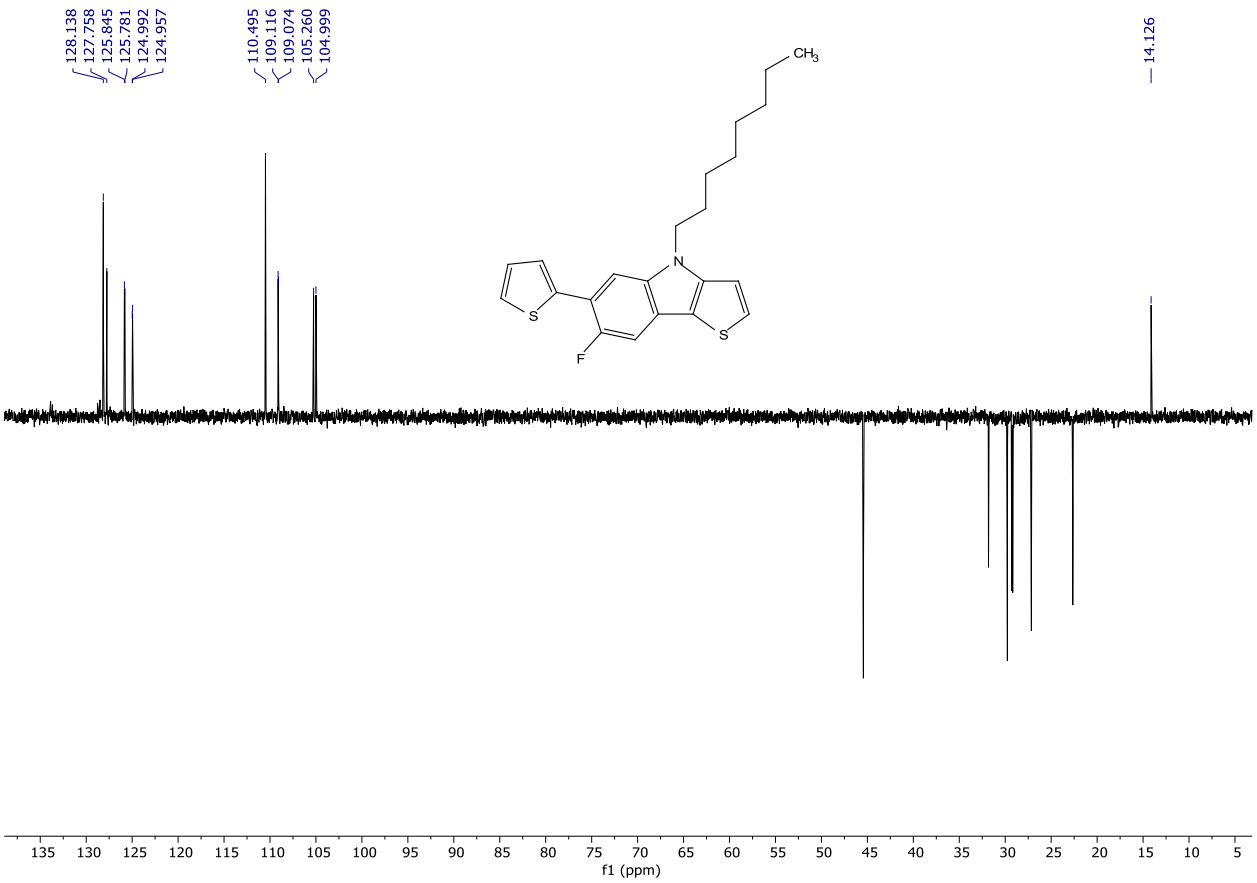

Appendix 18: The DEPT-135 spectrum of 7-fluoro-4-octyl-6-(thiophen-2-yl)-4*H*-thieno[3,2-*b*]indole (**35**).

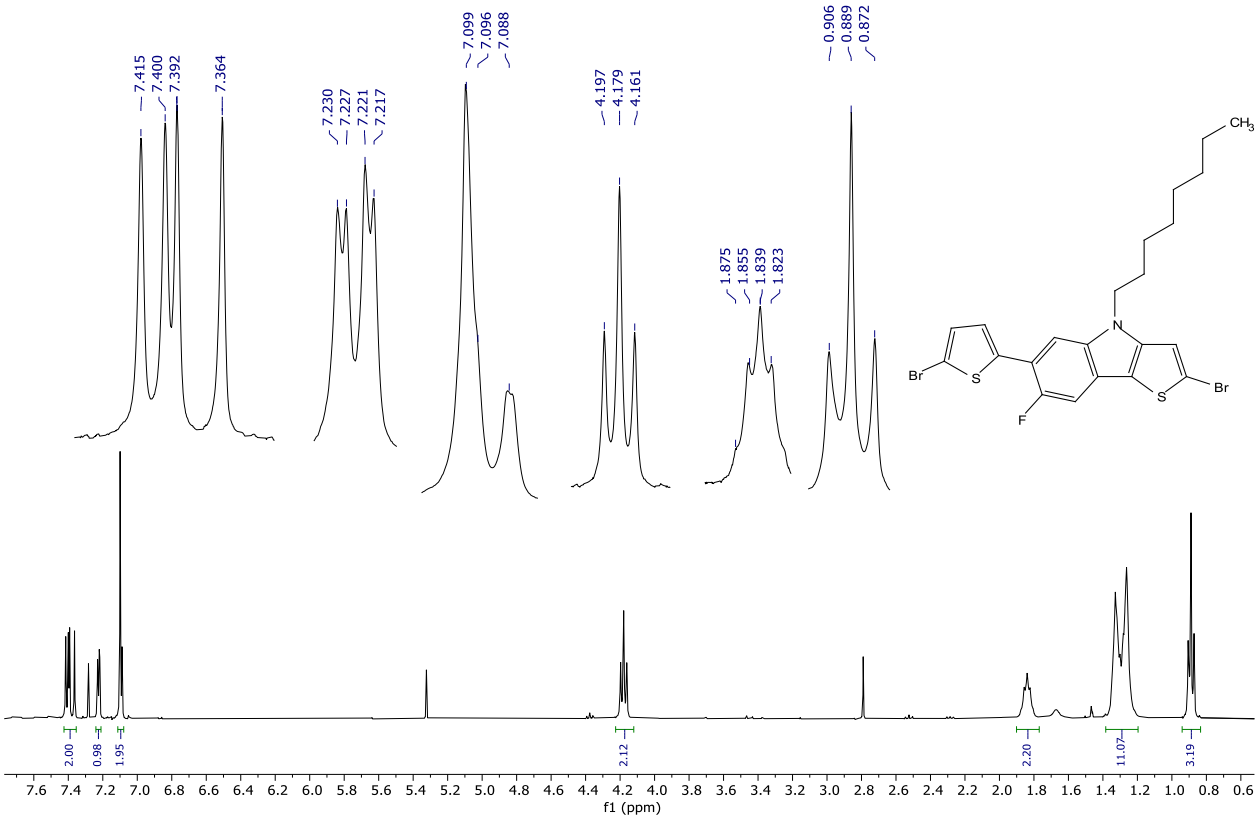

Appendix 19: The ^{1}H-NMR spectrum of 2-bromo-6-(5-bromothiophen-2-yl)-7-fluoro-4-octyl-*4H*-thieno[3,2-*b*]indole (**36**).

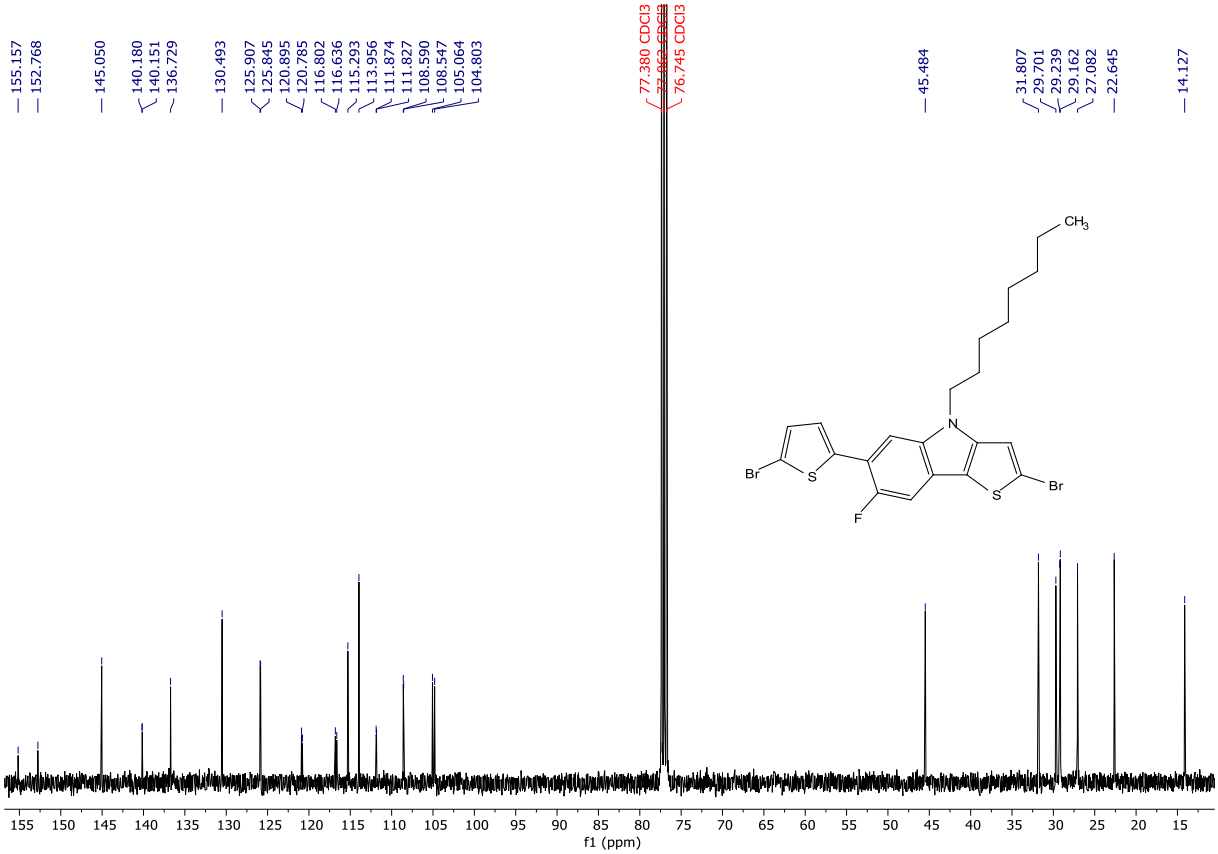

Appendix 20: The ^{13}C-NMR spectrum of 2-bromo-6-(5-bromothiophen-2-yl)-7-fluoro-4-octyl-*4H*-thieno[3,2-*b*]indole (**36**).

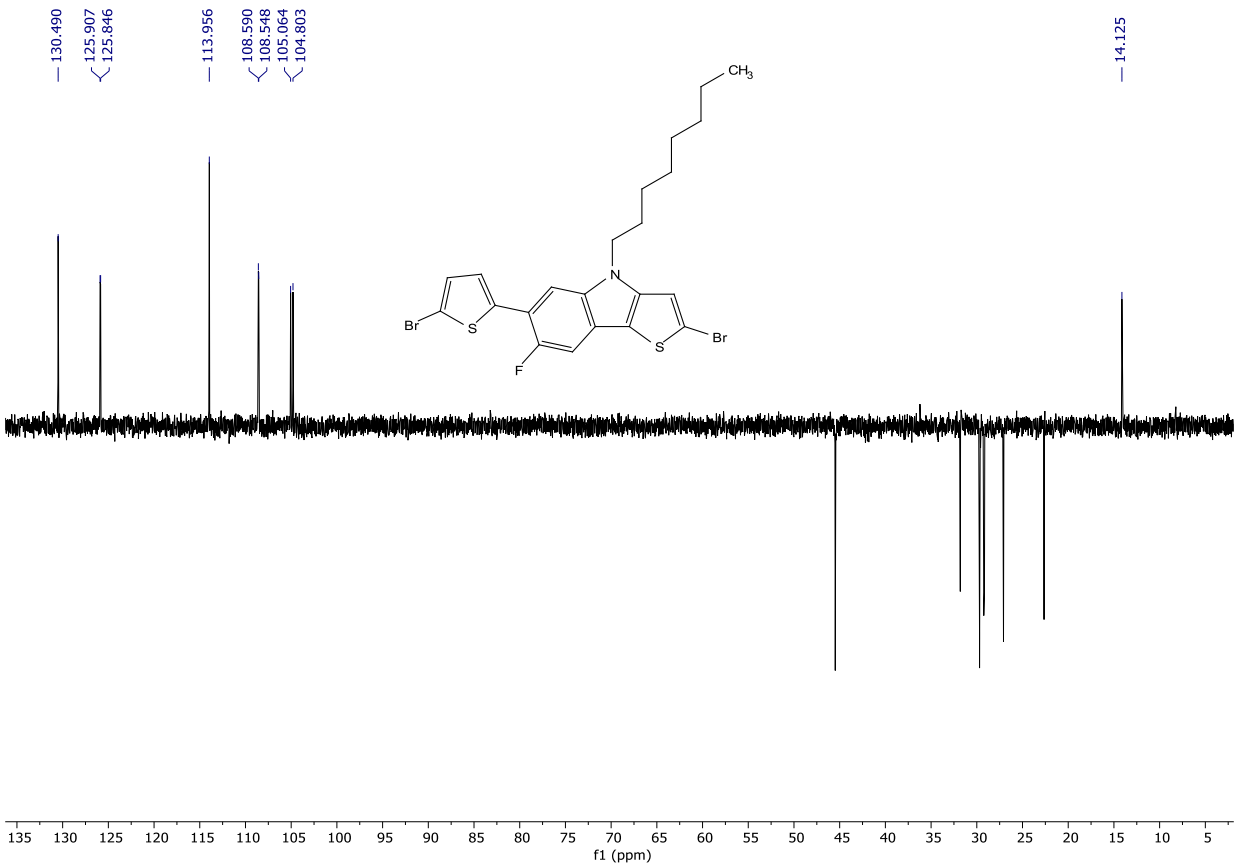

Appendix 21: The DEPT-135 spectrum of 2-bromo-6-(5-bromothiophen-2-yl)-7-fluoro-4-octyl-*4H*-thieno[3,2-*b*]indole (**36**).

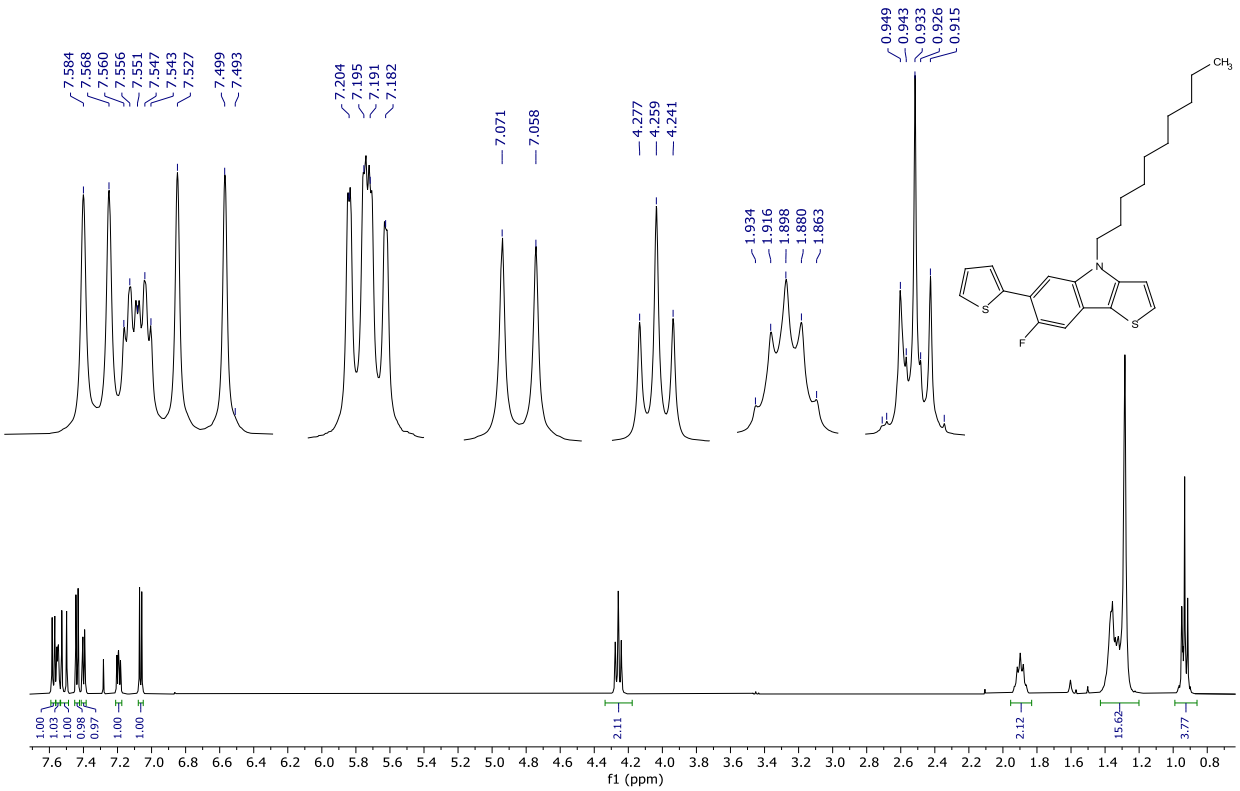

Appendix 22: The ^{1}H-NMR spectrum of 4-decyl-7-fluoro-6-(thiophen-2-yl)-*4H*-thieno[3,2-*b*]indole (**37**).

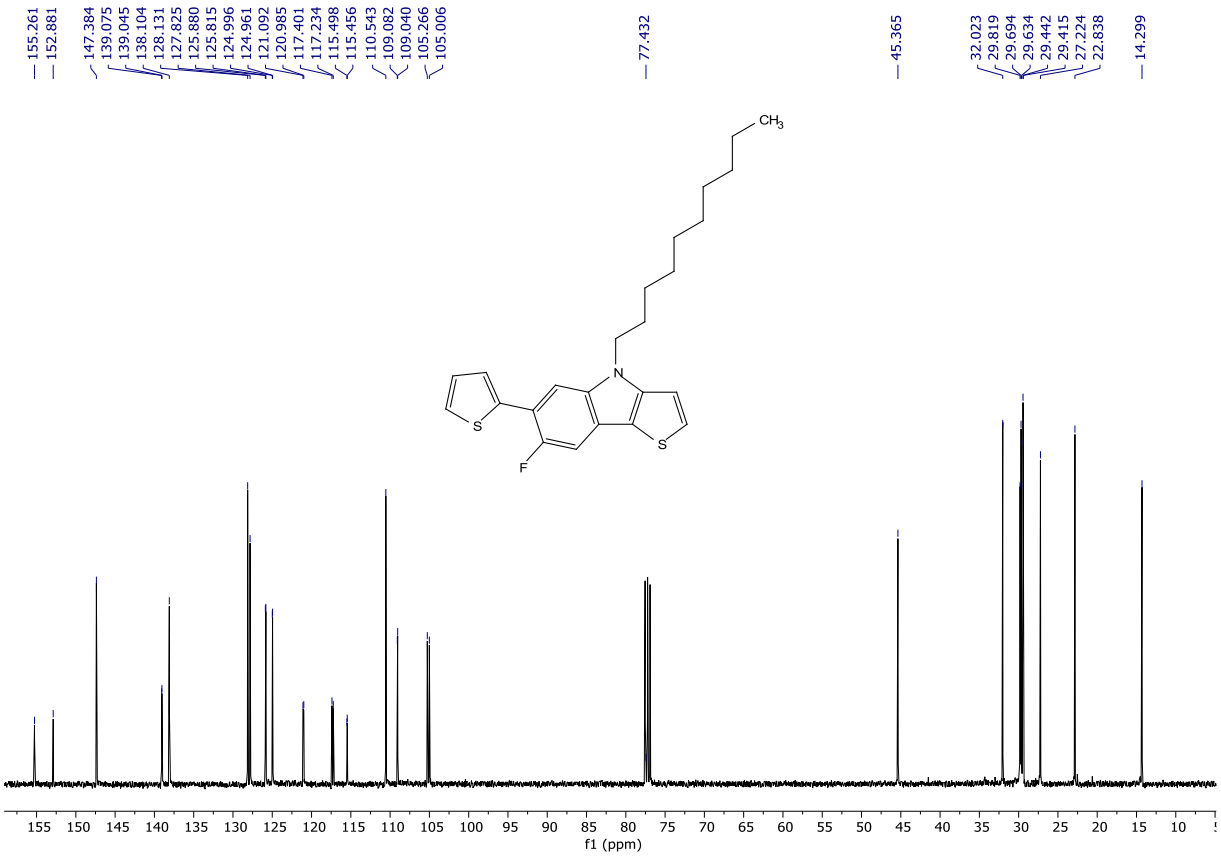

Appendix 23: The ^{13}C-NMR spectrum of 4-decyl-7-fluoro-6-(thiophen-2-yl)-*4H*-thieno[3,2-*b*]indole (**37**).

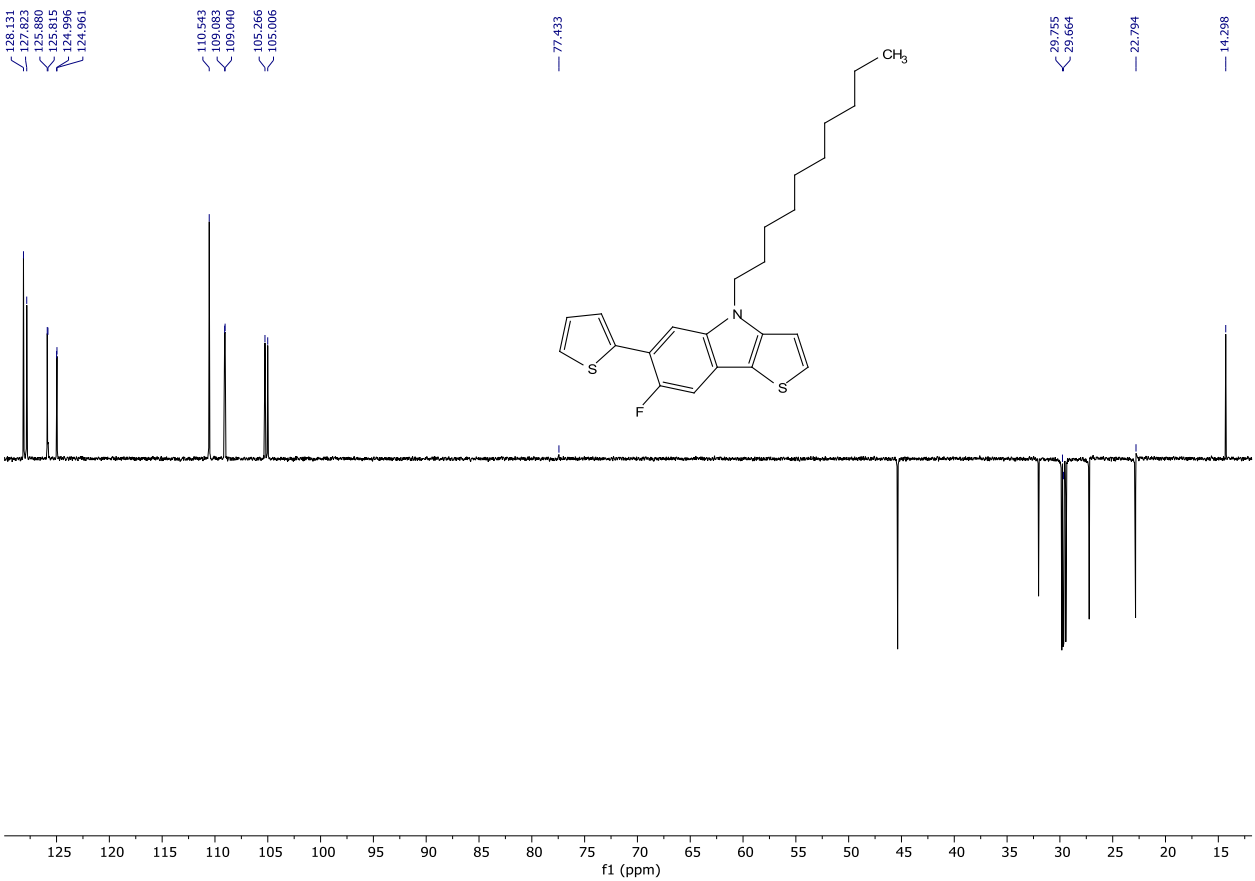

Appendix 24: The DEPT-135 spectrum of 4-decyl-7-fluoro-6-(thiophen-2-yl)-*4H*-thieno[3,2-*b*]indole (**37**).

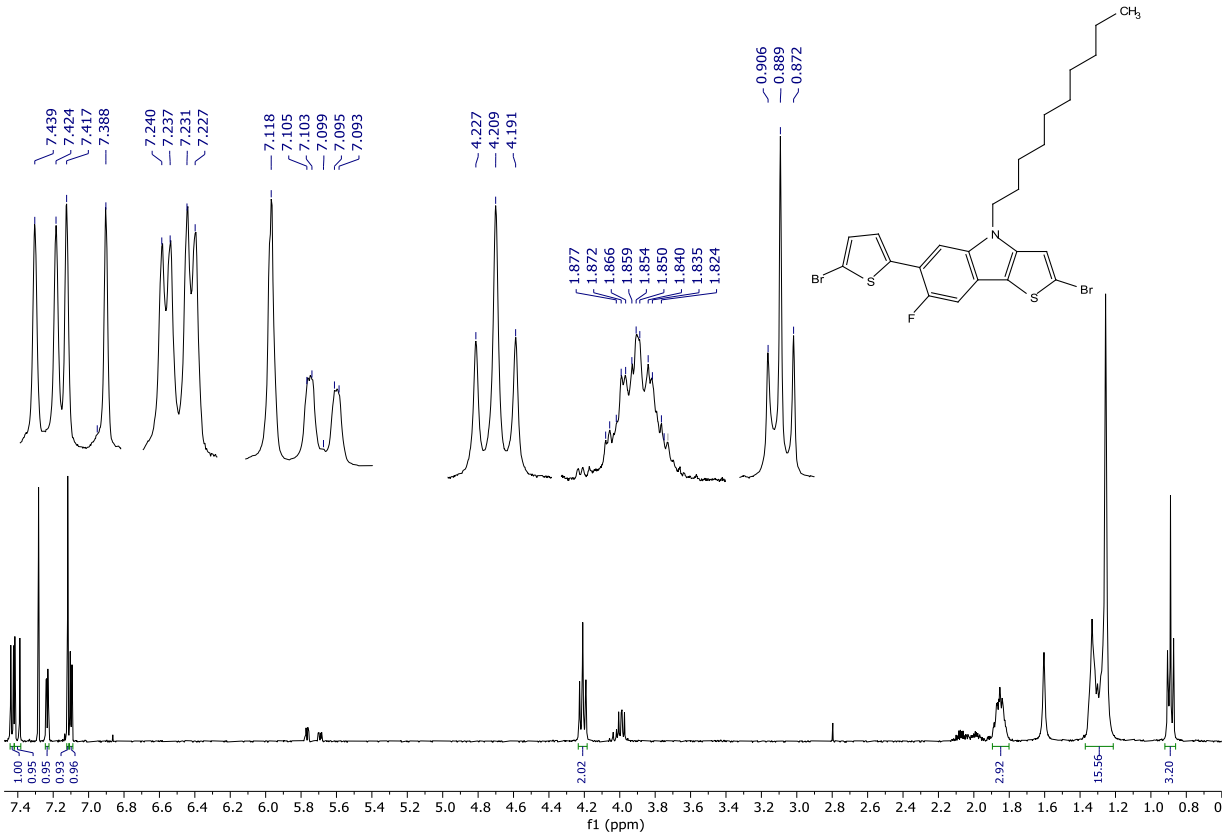

Appendix 25: The ^{1}H-NMR spectrum of 2-bromo-6-(5-bromothiophen-2-yl)-4-decyl-7-fluoro-*4H*-thieno[3,2-*b*]indole (**38**).

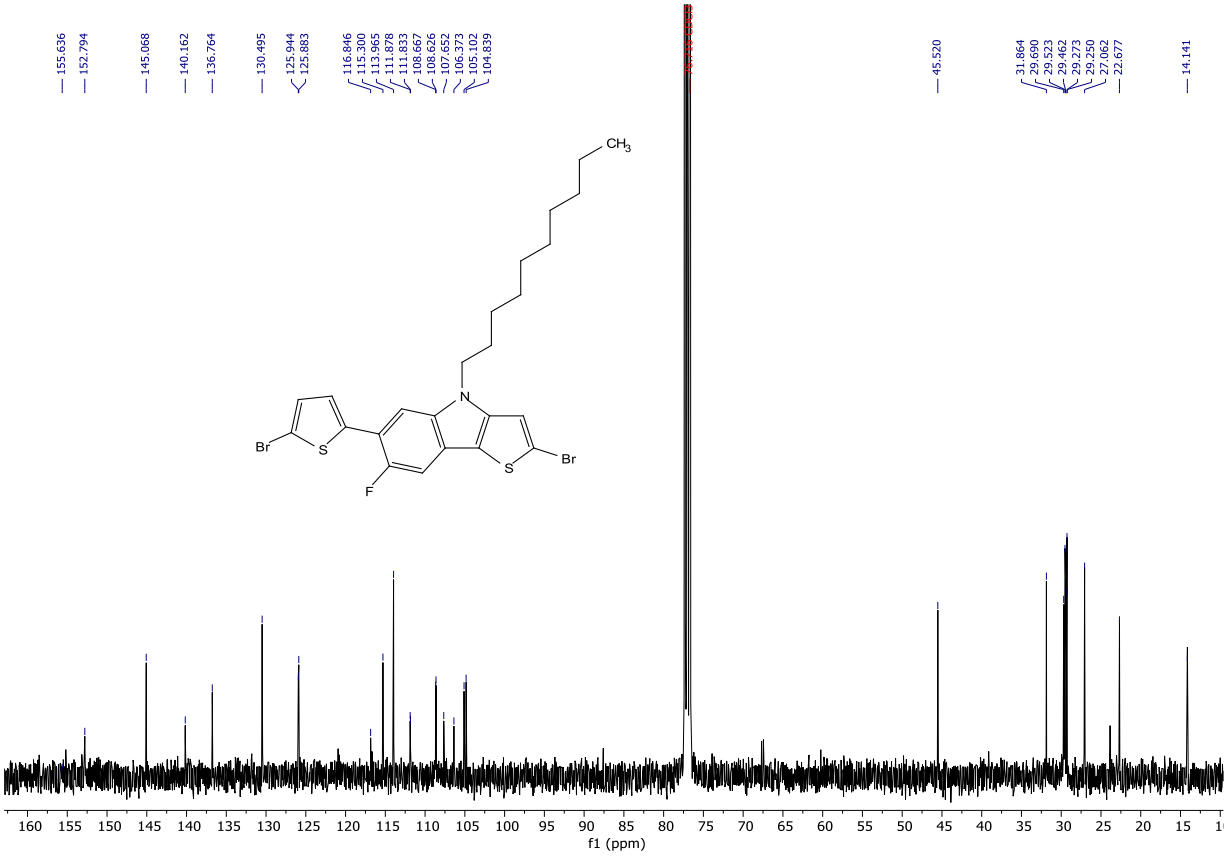

Appendix 26: The ^{13}C-NMR spectrum of 2-bromo-6-(5-bromothiophen-2-yl)-4-decyl-7-fluoro-*4H*-thieno[3,2-*b*]indole (**38**).

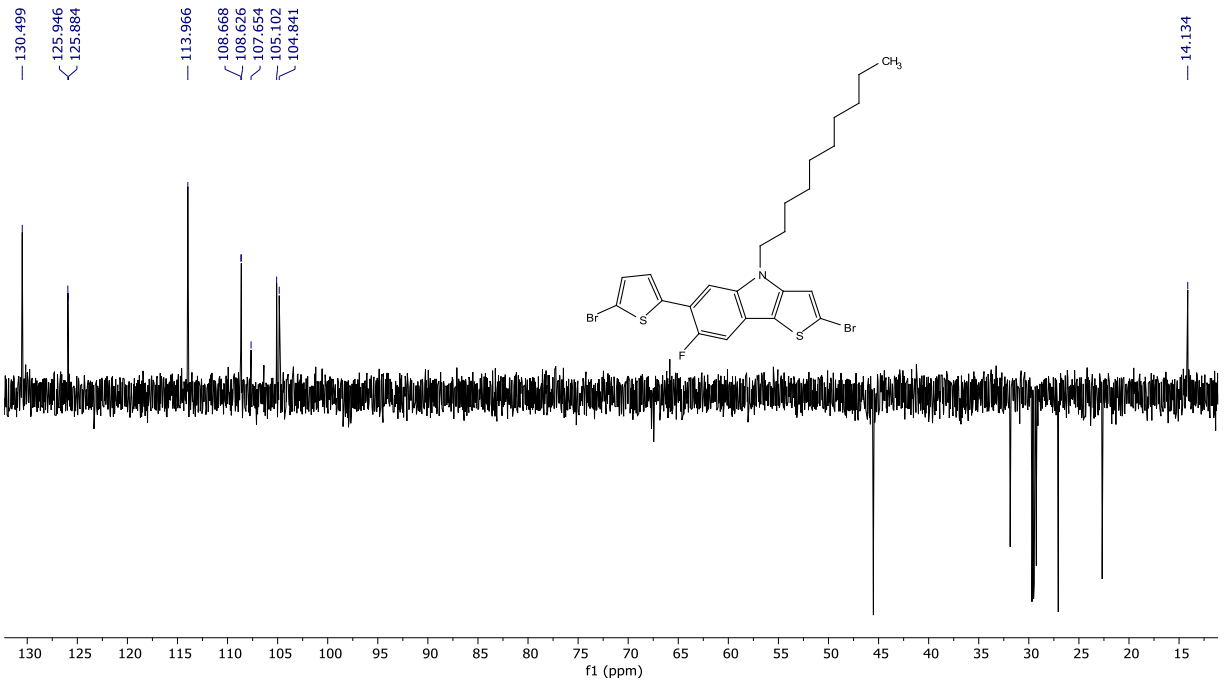

Appendix 27: The DEPT-135 spectrum of 2-bromo-6-(5-bromothiophen-2-yl)-4-decyl-7-fluoro-*4H*-thieno[3,2-*b*]indole (**38**).

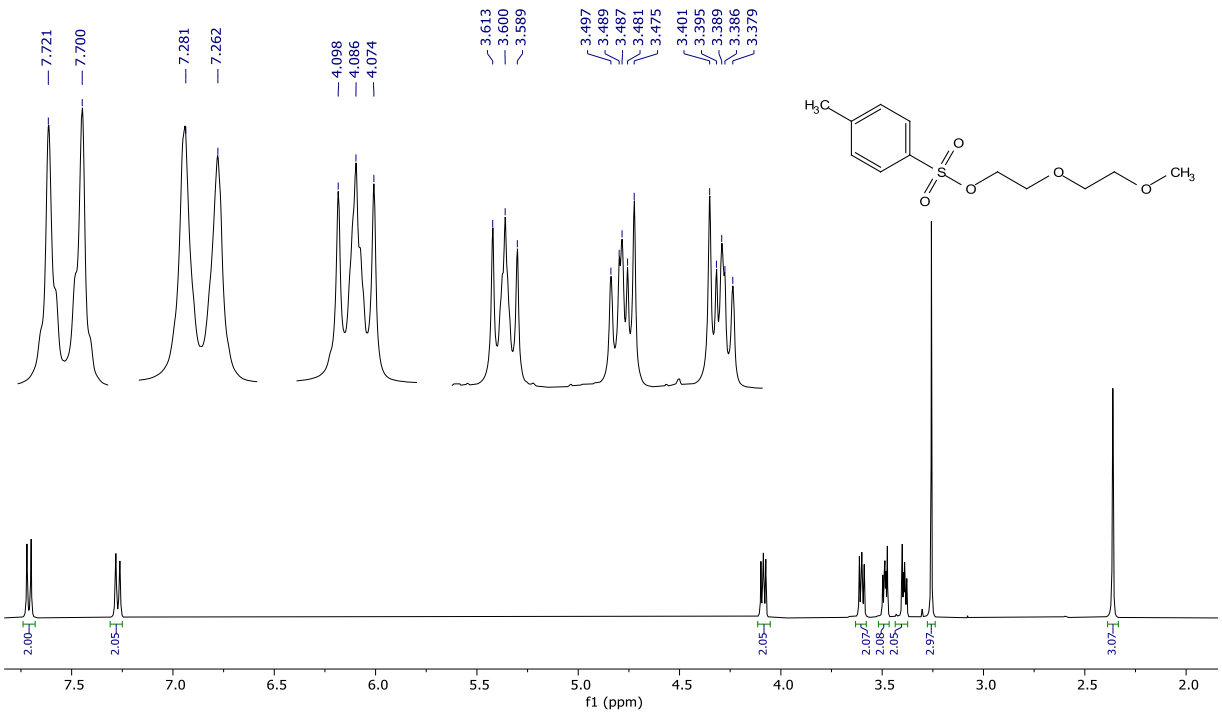

Appendix 28: The ^{1}H-NMR spectrum of 2-(2-methoxyethoxy)ethyl 4-methylbenzene-sulfonate (**41**).

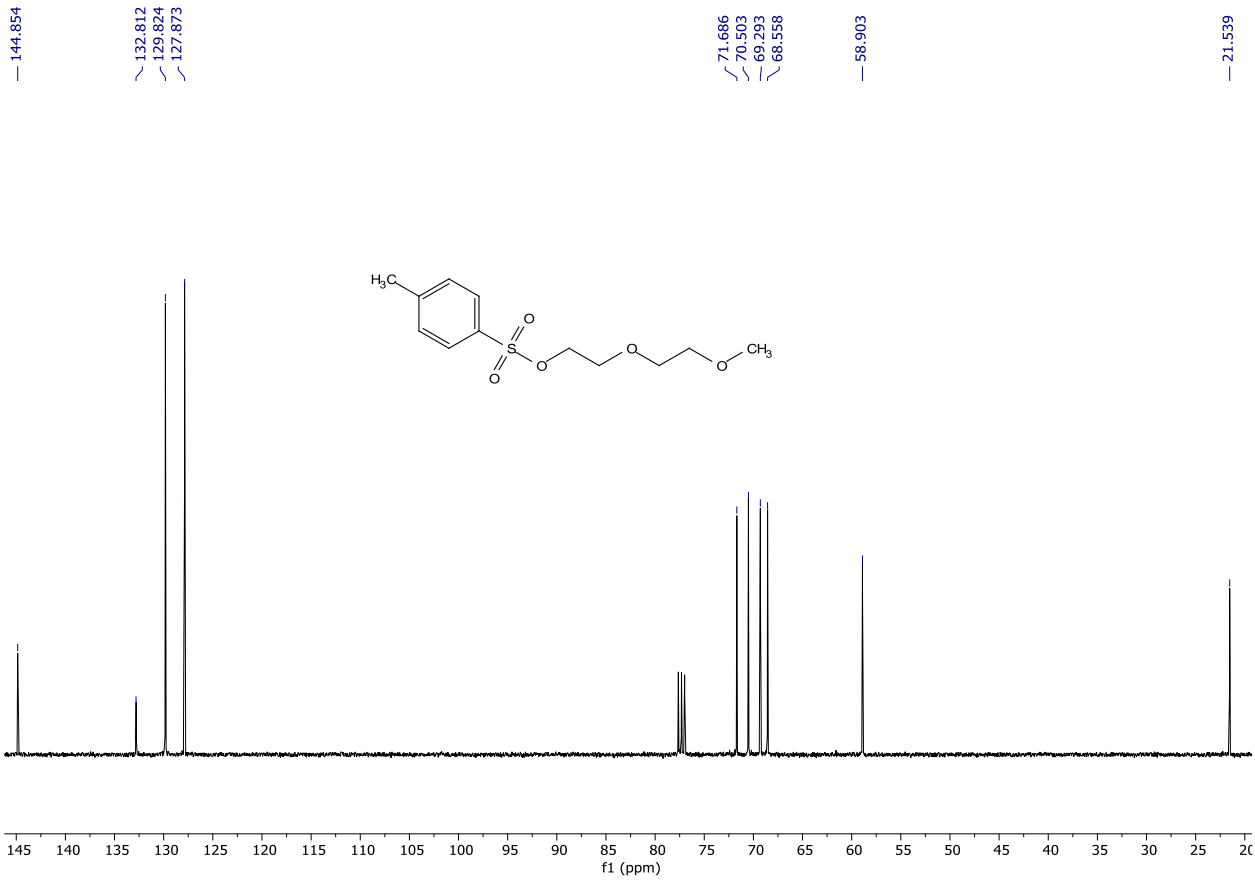

Appendix 29: The ^{13}C-NMR spectrum of 2-(2-methoxyethoxy)ethyl 4-methylbenzene-sulfonate (**41**).

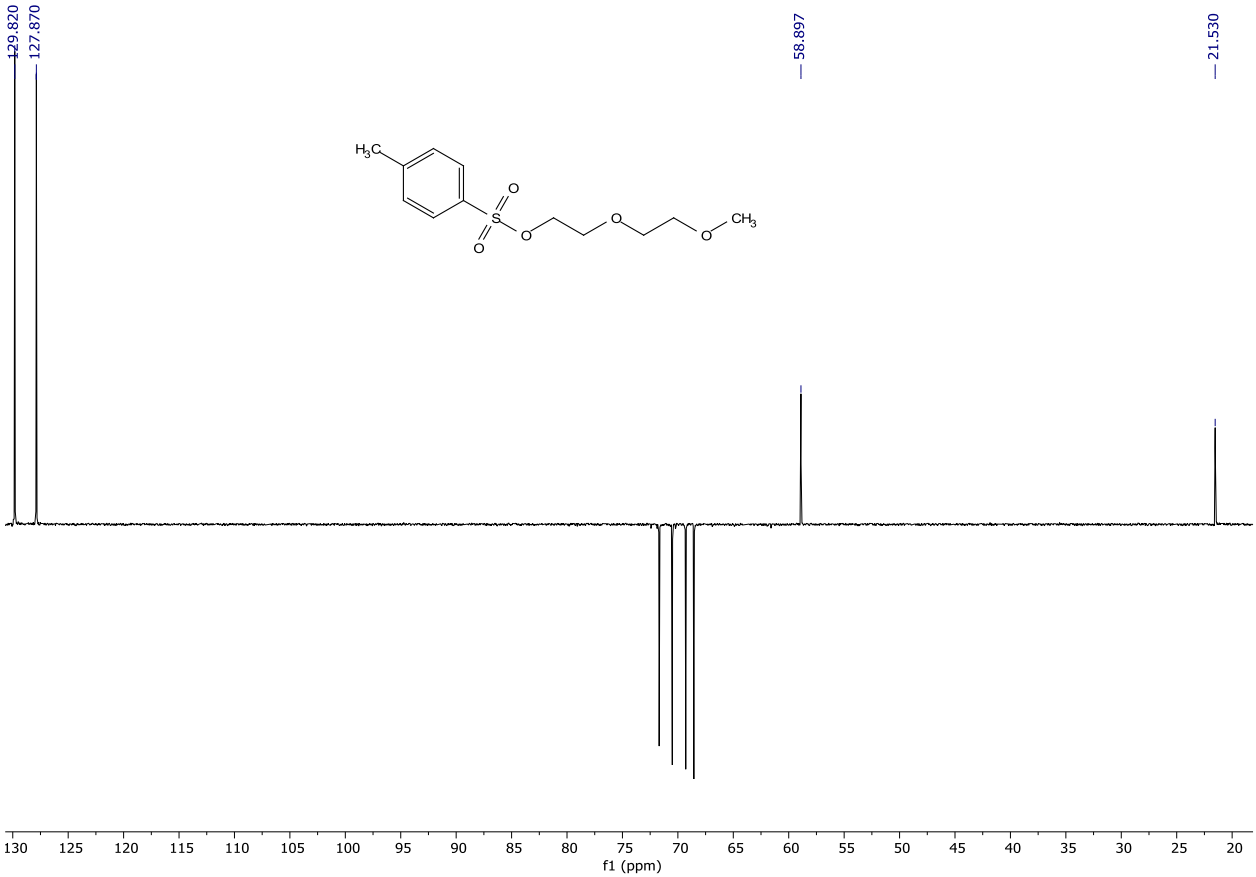

Appendix 30*:* The DEPT-135 spectrum of 2-(2-methoxyethoxy)ethyl 4-methylbenzene-sulfonate (**41**).

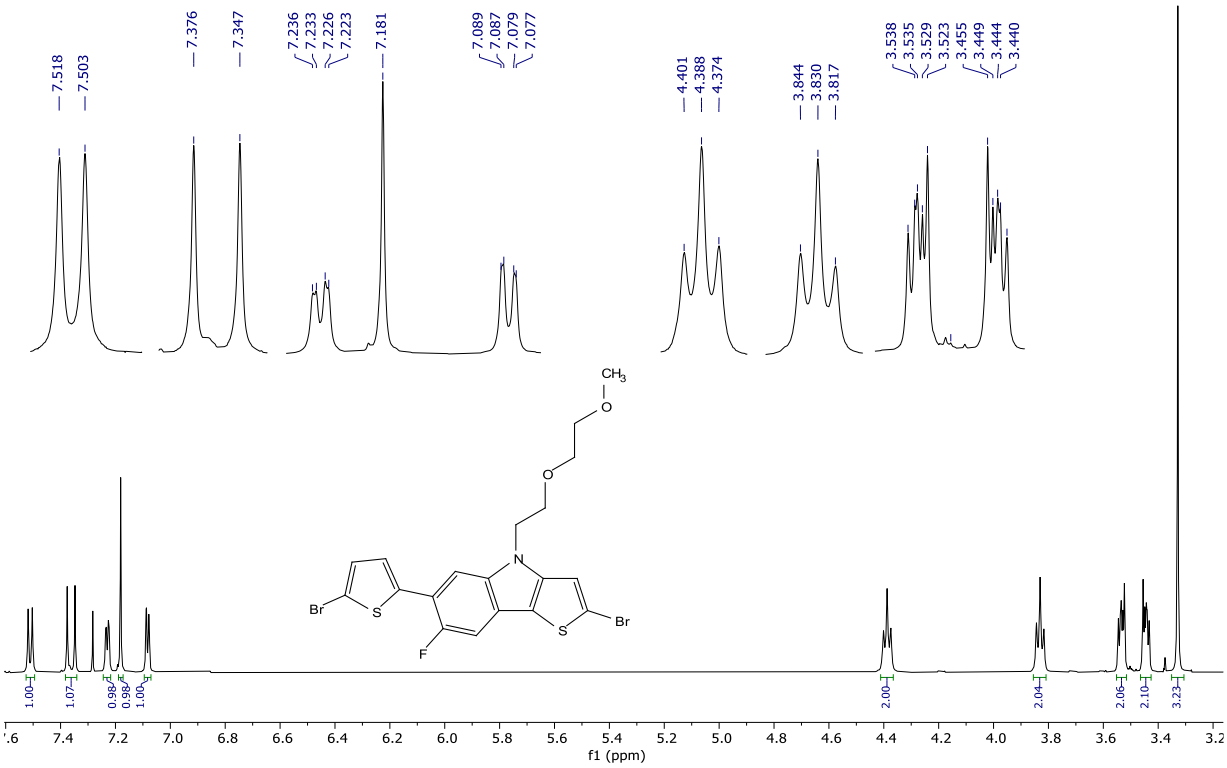

Appendix 31: The ^{1}H-NMR spectrum of 2-bromo-6-(5-bromothiophen-2-yl)-7-fluoro-4-(2-(2-methoxyethoxy)ethyl)-*4H*-thieno[3,2-*b*]indole (**43**).

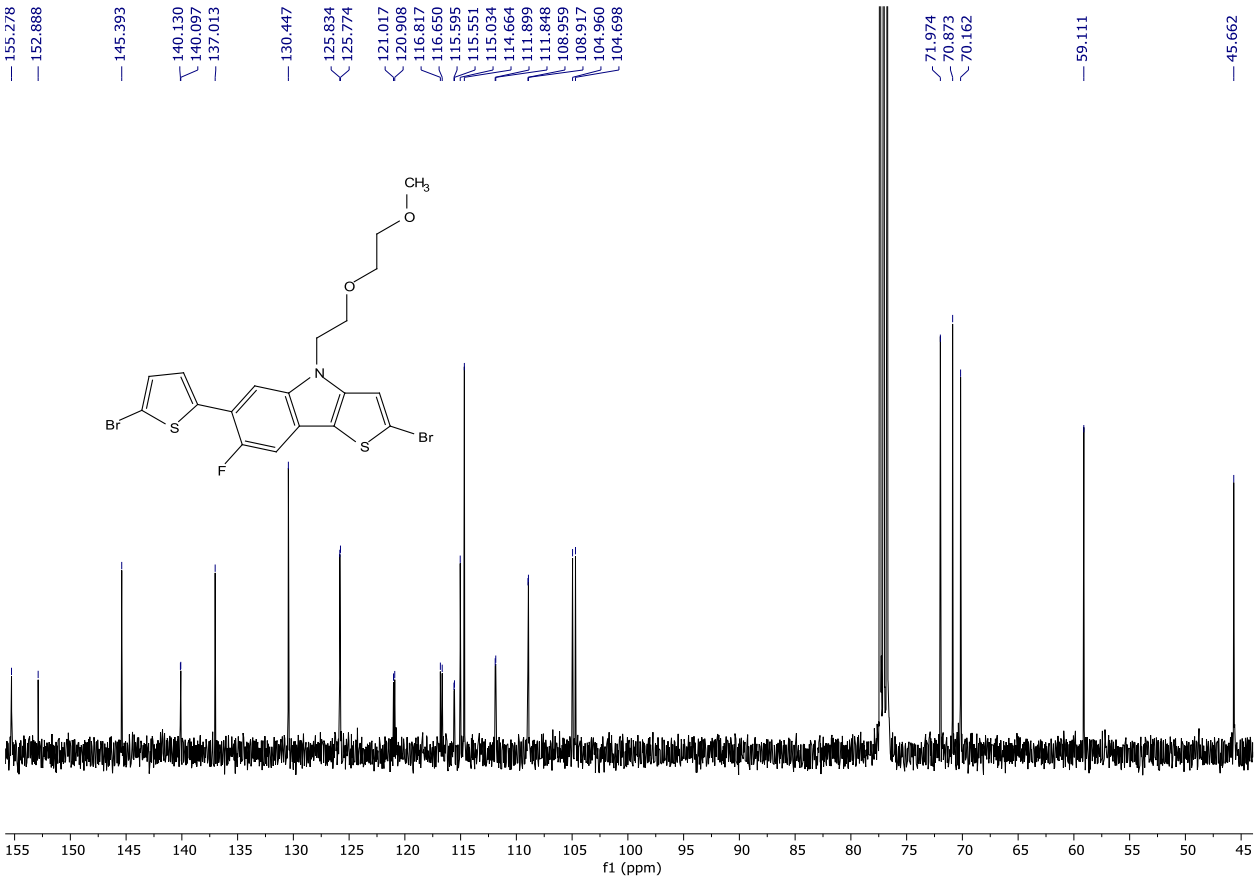

Appendix 32: The ^{13}C-NMR spectrum of 2-bromo-6-(5-bromothiophen-2-yl)-7-fluoro-4-(2-(2-methoxyethoxy)ethyl)-*4H*-thieno[3,2-*b*]indole (**43**).

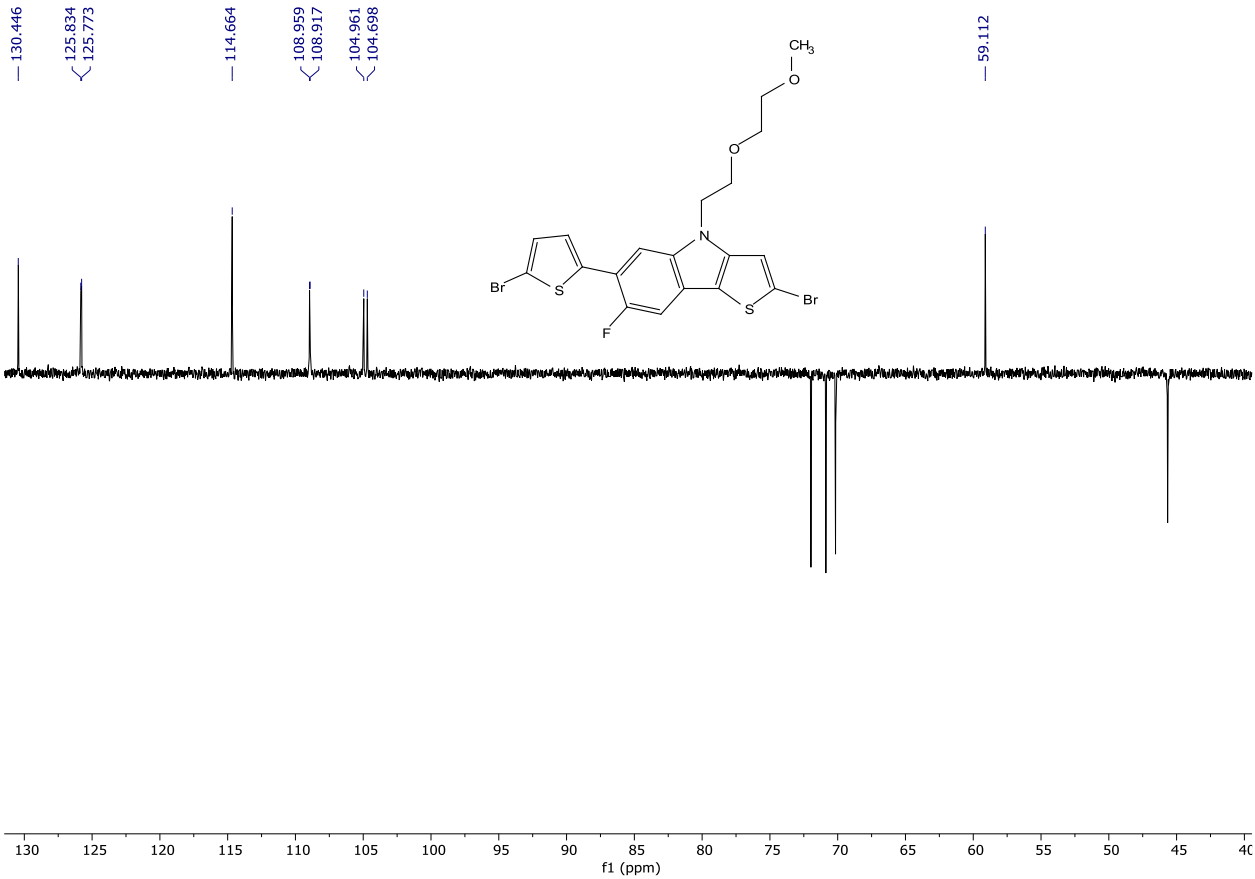

Appendix 33: The DEPT-135 spectrum of 2-bromo-6-(5-bromothiophen-2-yl)-7-fluoro-4-(2-(2-methoxyethoxy)ethyl)-4*H*-thieno[3,2-*b*]indole (**43**).